Functionalization of Silica Nanoparticle by Grafting of Antibacterial Polymers and Immobilization of Flame Retardant onto the Surface

TAKASHI KAWAHARA

Doctoral Program in Advanced Materials Science and Technology

Graduate School of Science and Technology

Niigata University

2013

Contents

Chapter 1

General Introduction

1.1 Properties of silica nanoparticle

Inorganic particles, such as silica (silicon dioxide), titanium dioxide, ferrite, and gold nanoparticle and so on, and carbon materials, such as carbon black, graphite, activated carbon, and carbon nanotubes, are widely used in various industrial fields. For example, silica and titanium dioxide are widely used industrially as fillers and pigments for polymer materials. Inorganic nanoparticles have excellent properties such as heat, chemical and weather resistance, lightweight, and low thermal expansion.

Today, silicas are firmly rooted in components or raw materials for a wide variety of high-technology products. Silica exists in the type of crystalline form, amorphous form, colloidal form, glassy form and dissolved form [1, 2]. These silicas have different physical property and particle size. Also, different production processes of synthetic silica result in silica products with different technical and applicational properties.

Silica of AEROSIL 200 used in this study is produced by the large-scale industrial synthesis of AEROSIL products, "AEROSIL Process" [3-7]. This process can be described essentially as a continuous flame hydrolysis of silicon tetrachloride ($SiCl_4$). During this process, silicon tetrachloride is converted to the gas phase and then reacts spontaneously and quantitatively in an oxyhydrogen flame with the intermediately-formed water to produce the desired silicon dioxide.

$$2\,H_2 + O_2 \longrightarrow 2\,H_2O$$
$$SiCl_4 + 2\,H_2O \longrightarrow SiO_2 + 4\,HCl$$
$$2\,H_2 + O_2 + SiCl_4 \longrightarrow SiO_2 + 4\,HCl$$

During this chemical reaction a considerable amount of heat is released, which is eliminated in a cooling line. The only by-product is gaseous hydrogen chloride, which is separated from the AEROSIL fumed silica solid matter.

Figure 1-1 shows a flow chart of the AEROSIL Process [8]. By varying the concentration of the co-reactants, the flame temperature, and the dwell time of the silica in the combustion chamber, it is possible to influence the particle size, the particle size

distribution, the specific surface, and the surface properties of the silicas within wide boundaries.

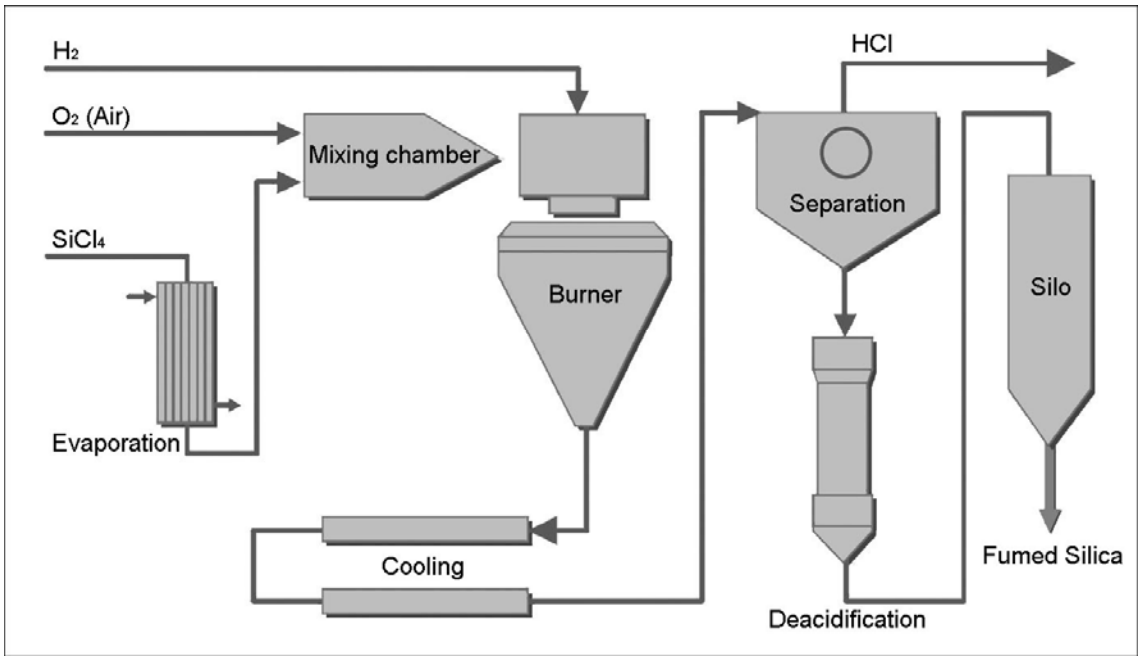

Figure 1-1. Flow chart of AEROSIL process.

1.2 Surface modification

In recent years, the surface modification and application of inorganic particles have become of major interest [9-11]. The surface modified inorganic particles are used in various fields such as optical, electrical, mechanical, chemical, and biochemical applications. The surface modification is very important to design the functional materials with high quality.

In general, dispersing nanoparticles, such as silica nanoparticle and carbon black, uniformly into a polymer or an organic solvent is very difficult because of aggregation of these particles. In addition, the mechanical properties of composite are considered to be depend on not only the mechanical properties of the polymer matrix, but also on the properties of interfacial regions between surface of nanoparticles and matrix polymer.

The chemical and physical modifications of silica nanoparticle and carbon black surfaces, therefore, have been extensively studied. The chemical modification of surfaces

is permanent, but physical modification is temporary.

In general, the surface treatment of inorganic particle is achieved by use of silane coupling agents, silicone oil, titanium coupling agents, and some reagents. For example, silane coupling agents can be introduced functional groups, such as amino, isocyanate, epoxy, mercapto, vinyl, or methacryl group, on the surface of inorganic particle. These surface treatment reagents are widely used in industrial fields [12]. On the other hand, carbon black has reactive functional groups, such as carboxyl and phenolic hydroxyl groups, on its surface [13].

Tsubokawa and his co-workers have pointed out that the dispersibility of silica nanoparticles and carbon black is extremely improved by surface grafting of polymers, namely, chemical binding of polymers, onto silica nanoparticle and carbon black surfaces [9-11]. In addition grafting of polymers onto these surfaces interests us for designing new functional organic-inorganic hybrid materials which have the excellent properties both of nanoparticles as mentioned above and of grafted polymers, such as photosensitivity, curing ability, bioactivity, and pharmacological activity [14-17].

Furthermore, many experimental attempts by other researchers also have been made to graft polymers onto silica nanoparticle and carbon black surfaces. For example, it has been reported that grafting of polymers from nanoparticles (polymer brush) was successfully achieved by atom transfer radical polymerization (ATRP) initiated by a system consisting of surface functional groups and transition metal complexes [18-22]. In situ radical transfer addition polymerization [23] and emulsion polymerization from silica nanoparticles has been also reported [24].

1.3 Methodology of surface grafting

Several methodologies of the surface grafting of polymers onto nanoparticles have been developed for the preparation of various kind of graft copolymers. These methodologies can be applied to the preparation of polymer-grafted nanoparticles. In general, one of the following principles may be applied to prepare polymer-grafted nanoparticles (Scheme 1-1) [9-11].

(1) Grafting onto process: the termination of growing polymer radical, cation, and anion, formed during the polymerization of various monomers initiated by conventional initiator in the presence of nanoparticles and the deactivation of living polymer radical, cation, and anion with functional groups on nanoparticle surface.
(2) Grafting from process: the initiation of graft polymerization of various monomers from radical, cationic and anionic initiating groups previously introduced onto nanoparticle surfaces.
(3) Polymer reaction process: the reaction of surface functional groups on nanoparticles with polymers having functional groups, such as hydroxyl, carboxyl, and amino groups.
(4) Stepwise growth process: the polymer chains are grown from surface functional groups on nanoparticles by repeated reaction of low molecular compounds by dendrimer synthesis methodology.

By process (1), although polymer-grafted nanoparticles can be obtained, the percentage of grafting onto nanoparticles is less than 10%, because of the preferential formation of ungrafted polymers. On the contrary, by the termination of living polymer, polymers with well-defined molecular weight and narrow molecular weight distribution can be grafted onto nanoparticle surfaces.

Process (2) is one the most favorable for the preparation of polymer-grafted nanoparticles with a high percentage of grafting. The molecular weight and number of grafted polymer chains can be controlled by use of surface initiated living polymerization.

An important characteristic of process (3) is that not only the molecular weight and the number of grafted chains on nanoparticle surfaces were easily controlled, but also commercially available polymers having a well-defined structure can be grafted. But the number of grafted polymer chains on nanoparticle surface decreases with increasing molecular weight of polymer, because of steric hindrance.

In addition, by process (4), although dendron with theoretical structure was not easily grafted, hyperbranched polymers having a large number of terminal functional groups can be grafted onto nanoparticle surfaces.

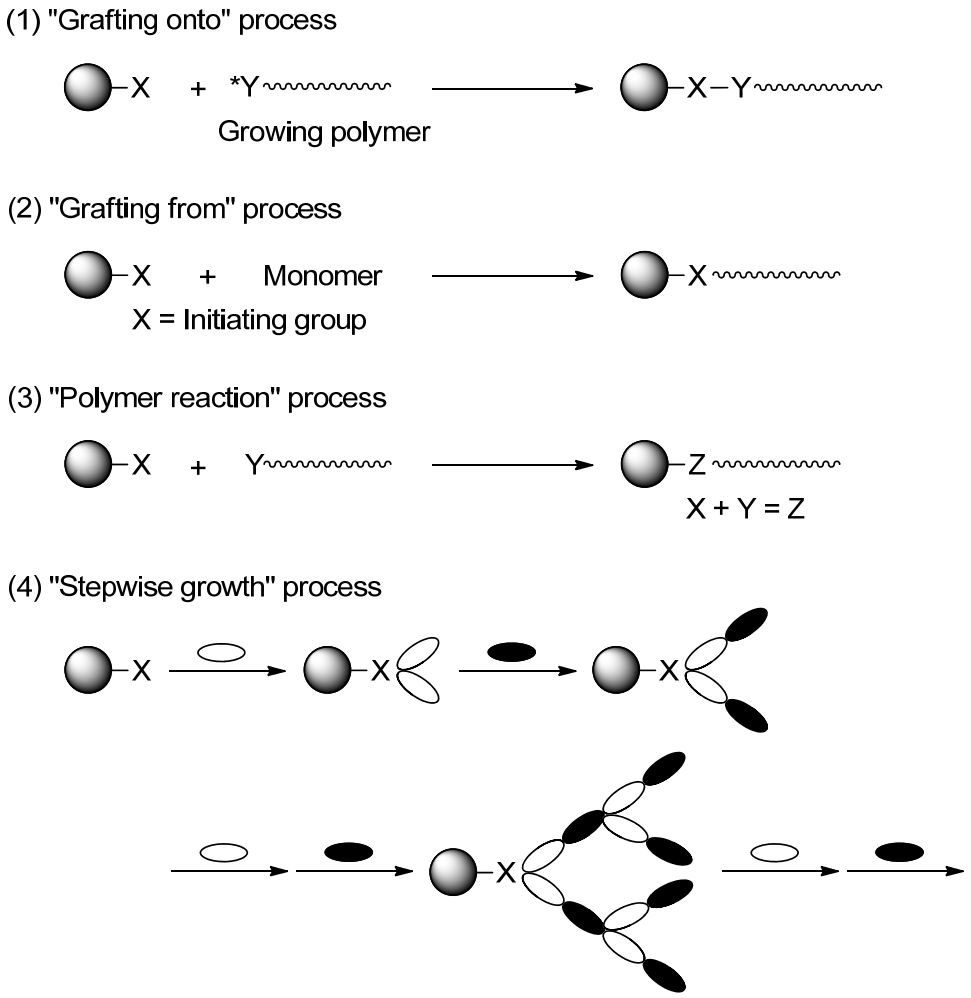

Scheme 1-1. Methodology of surface grafting of polymers onto silica nanoparticle and carbon black.

1.4 Surface grafting in a solvent-free dry-system

The surface grafting of polymers onto nanoparticles are generally achieved by wet-process using a solvent. However, scale-up synthesis of polymer-grafted nanoparticles was hardly achieved, because complicated reaction processes, such as centrifugation, filtration, and solvent extraction, are required for the synthesis of polymer-grafted nanoparticles, and a lot of waste solvent comes out.

Therefore, Murota et al. have designed the solvent-free dry-system to simplification of reaction process and scale-up synthesis and reported that synthesis of hyperbranched poly(amidoamine)-grafted silica in solvent-free dry-system [25]. It was achieved as

follow. Into the flask that contained silica having amino groups, methyl acrylate (MA) was sprayed and the silica was agitated at 50 °C under argon gas. After the reaction, unreacted MA was removed under vacuum. Then, ethylenediamine (EDA) was sprayed and the silica was reacted at 50 °C with agitation. After the reaction, unreacted EDA was removed under vacuum. Both these process were repeated to propagate the hyperbranched poly(amidoamine) from the silica surface (Scheme 1-2) [25].

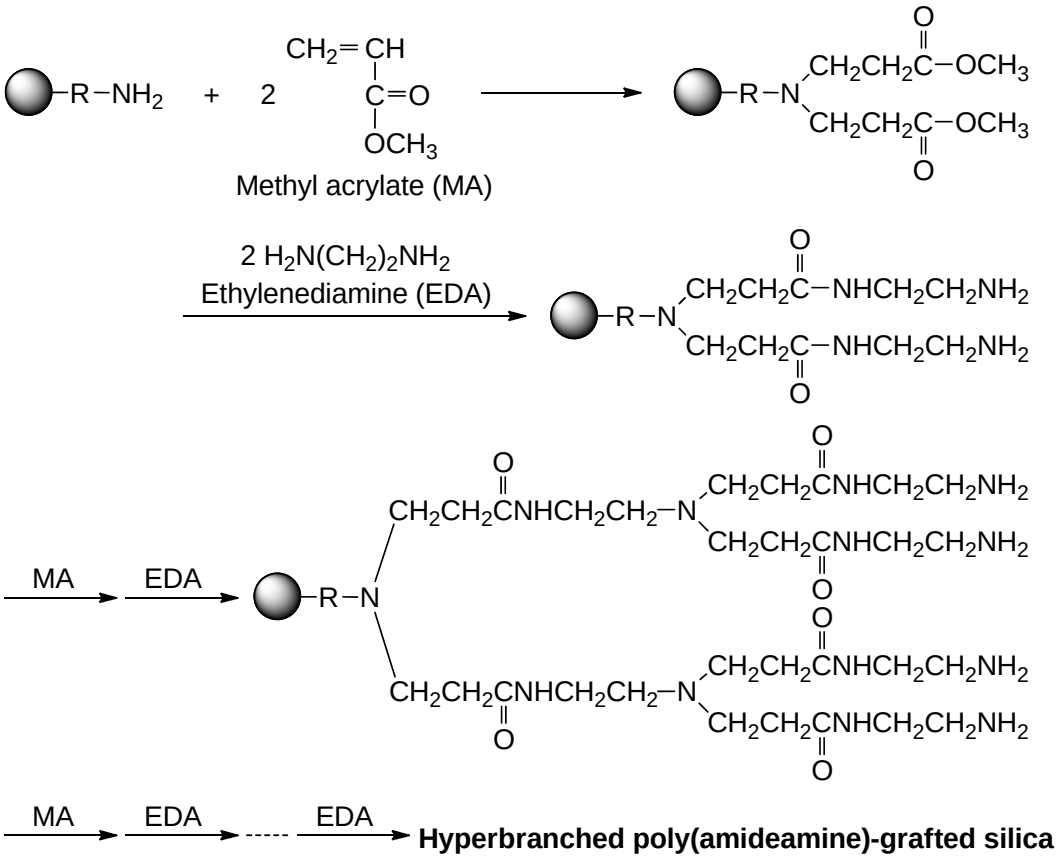

Scheme 1-2. Grafting of poly(amidoamine) onto silica nanoparticle surface by dendrimer synthesis methodology.

Figure 1-2 shows the comparison of the procedures of graft polymerization onto nanoparticles in solvent-free dry-system with those in solvent system. In solvent system, the purification and isolation of resulting nanoparticles was achieved by troublesome procedures, such as filtration and centrifugation. Therefore, the scale-up synthesis of polymer-grafted nanoparticles was hardly achieved and large quantities of waste solvent come out.

On the contrary, in solvent-free dry-system, the isolation and purification of nanoparticle was easily achieved, because untreated monomer can be removed under high vacuum. Therefore, it is considered that the solvent-free dry-system is environmentally friendly system and it is expected that graft polymerization onto nanoparticle surface in solvent-free dry-system enable us the scale-up synthesis of polymer-grafted nanoparticles.

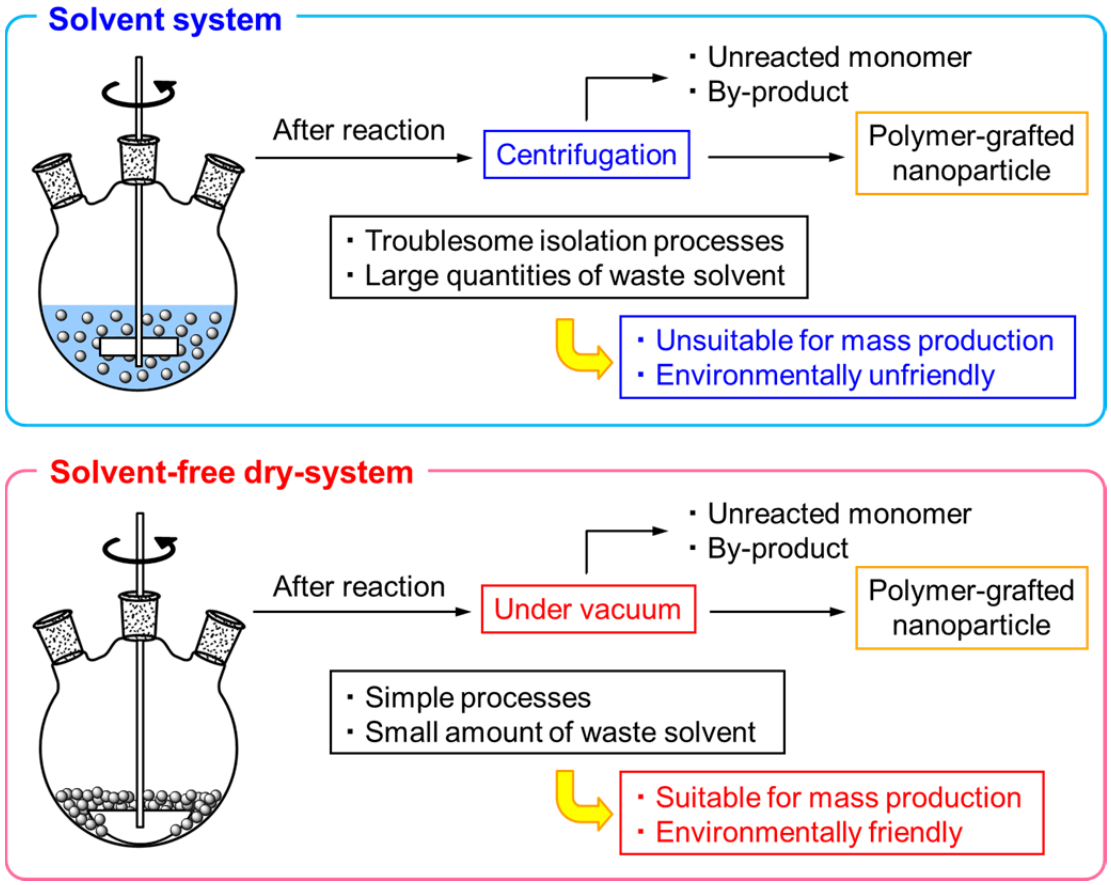

Figure 1-2. Difference between graft polymerization in solvent system and solvent-free dry-system.

1.5 Antibacterial agents

Infectious diseases by various pathogenic organisms, such as bacteria, viruses, and fungi, are great concern in many fields, particularly in medical devices, surgery equipment, hospital surfaces and furniture, dental restoration, health care products and

hygienic applications, food packaging and storage, home electric appliances, and so on [26]. Infectious diseases kill worldwide more people than any other single cause. These diseases are triggered by germs, such as bacteria, viruses, and fungi, which are found everywhere, in air, soil, and water. Mainly, the infections are caused by touching, eating, drinking or breathing something that contains a germ. Generally, these infections are combated with antimicrobial agents, which are susceptible to their action.

Nowadays, various kind of antibacterial agents against pathogenic bacteria were reported [26-29]. These antibacterial agents can be divided into inorganic, organic, and natural antibacterial agents. The general organic antibacterial agents, such as quaternary phosphonium salt and quaternary ammonium salt, were known for their strong antibacterial activity but they were almost unstable and often solved out from composite materials. To solve these problems, antibacterial agents were polymerized or immobilized onto another material [30]. For example, polymer hydrogels from copolymers containing quaternary phosphonium salt groups show high antibacterial activity [31]. Yamashita et al. have succeeded in the grafting of polymer having alkylphosphonium sulfate groups (poly(St-$SO_3^-P^+Bu_3R$)) onto the surface of silica nanoparticle [32]. In addition, they have pointed out that the surface of silicone rubber filled with the poly(St-$SO_3^-P^+Bu_3R$)-grafted silica shows strong antibacterial activity to *Staphylococcus aureus* and *Escherichia coli*.

1.6 Flame retardants

Most of organic polymers are combustible, because they contain hydrogen and carbon. For their various applications in the building, electrical, transportation, mining and other industries, they have to fulfill flame retardancy requirements. Thus the main objectives in development of flame retarding polymers are to increase ignition resistance and reduce of flame spread when incorporated in flammable polymers [33].

Several types of flame retardant additives are used to improve flame retarding properties to polymer materials. These flame retardants can be divided into halogen, inorganic, phosphorous, nitrogen and nitrogen-phosphorous flame retardant. Table 1-1

shows type and application of typical flame retardants come into practical use [34].

Table 1-1. Type and application of typical flame retardants.

Category	Type	Application
Halogen system	Decabromo diphenyl ethane	Commodity resin, engineering plastic, thermosetting resin, synthetic rubber, fiber
	Tetrabromo bisphenol A	Thermosetting resin, commodity resin
Phosphorous system	Triphenyl phosphine	Commodity resin, engineering plastic, thermosetting resin, synthetic rubber, fiber
	Red-phosphorous	Commodity resin, synthetic rubber
	Ammonium polyphosphate	Commodity resin, synthetic rubber
Inorganic system and other system	Aluminium and magnesium hydroxide	Commodity resin, synthetic rubber
	Nano-filler (clay, silica, carbon nanotube)	Commodity resin, synthetic rubber, fiber
	Nitrogen compound	Commodity resin, synthetic rubber, fiber

The bromine flame retardants are good flame retardant properties, but they have problems of bleeding phenomena and deterioration in mechanical properties, because they act as plasticizer.

Yuuki et al. have reported to prepare the silica having flame retardant, the immobilization of bromine flame retardant, poly(tetrabromobisphenol-A) diglycidyl ether (PTBBA), onto hyperbranched poly(amidoamine)-grafted silica (Silica-PAMAM) [35]. The immobilization of PTBBA onto Silica-PAMAM was successfully achieved by the reaction of terminal amino groups of Silica-PAMAM with epoxy groups of PTBBA. Silica-PAMAM-PTBBA was dispersed uniformly in an epoxy resin, and the epoxy resin was cured in the presence of hexamethylenediamine. Flame retardant activity of the epoxy resin filled with Silica-PAMAM-PTBBA was estimated by limiting oxygen index (LOI). The LOI of epoxy resin filled with Silica-PAMAM-PTBBA was higher than that filled with untreated silica and free PTBBA. It was confirmed that the flame retardant activity of epoxy resin was improved by the addition of the Silica-PAMAM-PTBBA. In addition, the elimination of PTBBA from the epoxy resin filled with

Silica-PAMAM-PTBBA into boiling water was hardly observed by immobilization of PTBBA onto silica surface.

However, along with this undoubted advantage, halogen containing compounds could produce corrosive and obscuring smoke and might give toxic gases with deleterious effects on environmental impact and human health, when they burned [36]. In this respect, environmentally friendly halogen-free flame retardant systems are currently being developed to substitute halogen based flame retardant systems.

Recently, flame retardants based on phosphorous-containing compound has great demand, because these are low toxicity, available in solid state, high efficiency. Among various phosphorus-based flame retardants, triphenyl phosphate and its analogues are widely known to be the most effective for many polymers [37, 38]. In addition, cyclophosphazene is known as halogen-free flame retardant which was suitable for electronic materials because of comparatively low dielectric constant, hydrolysis resistant and flame retardant ability [39-41].

However, thermal stability of these phosphorous flame retardants is low and they have bleeding phenomena. In particular, cyclophosphazene is poor compatibility with polymers which leads to reduce mechanical properties of composites and limit their application [42].

1.7 Objectives of this work

Figure 1-3 shows the difference between using alone functional materials and using functional silicas when added to matrix. The functional materials, such as antibacterial agents and flame retardants, are low dispersibility, solved out from the polymer matrices, and decreased of mechanical properties of the polymer matrices, when the functional material was added to the polymer matrices.

To improve the above problems and prepare the silica having functionality, the present research has been carried out for investigating the functionalization of silica nanoparticle by surface modification.

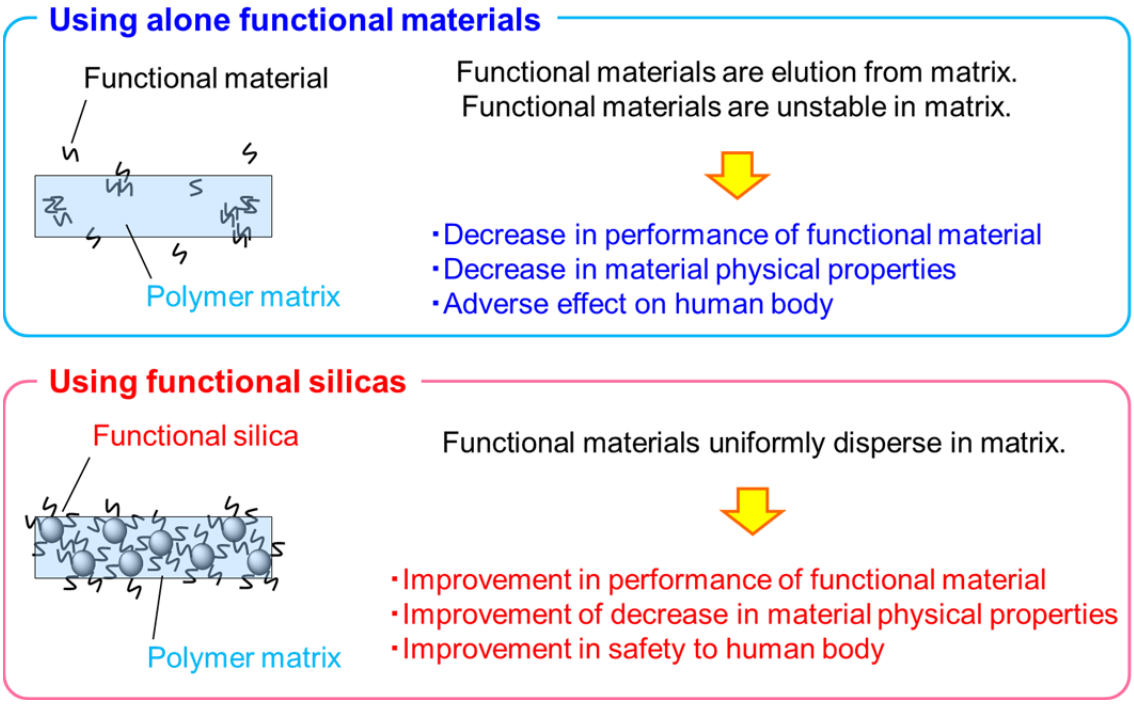

Figure 1-3. Difference between using functional materials and using functional silicas when added to the matrix.

In Chapter 2, the radical grafting of poly(vinylbenzyl tributylphosphonium chloride) (poly(St-$CH_2P^+(Bu)_3Cl^-$)) onto silica nanoparticle surface was investigated. The grafting of poly(St-$CH_2P^+(Bu)_3Cl^-$) was achieved by two methods: one is treatment of poly(vinylbenzyl chloride)-grafted silica with tributylphosphine and the other is direct grafting of poly(St-$CH_2P^+(Bu)_3Cl^-$) by radical graft polymerization of the corresponding monomer. In addition, the antibacterial activity of the surfaces of composites prepared from the poly(St-$CH_2P^+(Bu)_3Cl^-$)-grafted silica was discussed.

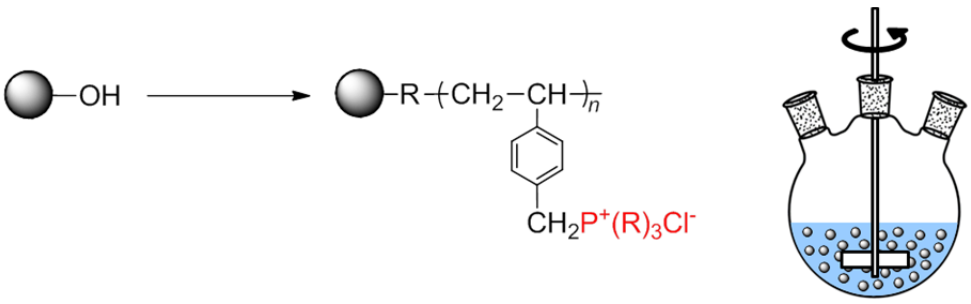

Scheme 1-3. Preparation of antibacterial polymer-grafted silica nanoparticle in solvent system.

In Chapter 3, we investigated the radical graft polymerization of antibacterial monomer, vinylbenzyl tributylphosphonium chloride (St-$CH_2P^+(Bu)_3Cl^-$), onto silica nanoparticle surface in a solvent-free dry-system. The method of graft polymerization was achieved by azo groups introduced onto the silica nanoparticle surface and by atom transfer radical polymerization (ATRP). In addition, the antibacterial activities of the surfaces of composites prepared from the antibacterial polymer-grafted silica were discussed.

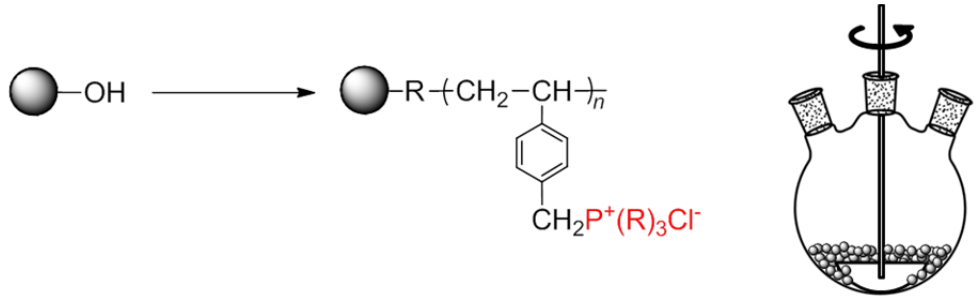

Scheme 1-4. Preparation of antibacterial polymer-grafted silica nanoparticle in solvent-free dry-system.

In Chapter 4, immobilization of phosphorous flame retardant, bis(4-aminophenoxy) phenyl phosphine oxide (BAPPO), onto silica nanoparticle surface was investigated. In addition, thermal property, glass-transition temperature and flame-retardant activity of epoxy resin filled with the BAPPO-immobilized silica were discussed.

Conclusions are presented in Chapter 5.

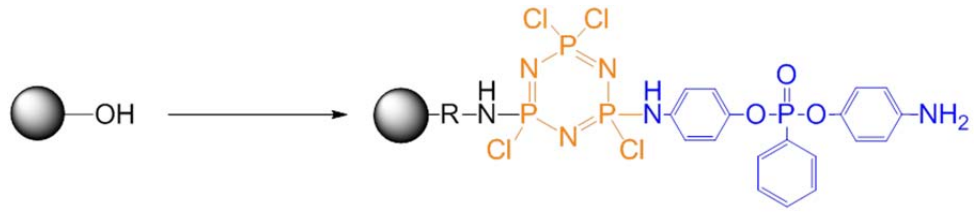

Scheme 1-5. Preparation of flame retardant-immobilized silica nanoparticle.

References

[1] R. B. Sosman, “The Properties of Silica”, Chemical Catalog, New York (1927).

[2] R. K. Iler, “The Chemistry of Silica”, *J. Wiley*, New York (1979).

[3] DBP 762 723, Degussa AG (1942).

[4] C. H. Love and F. H. MC Berty, *Fiat Rep*. No. 743 (1946).

[5] H. Brünner, *Dtsch. Apoth. Ztg.* **98**, 1005 (1985).

[6] L. J. White and G. J. Duffy, *Ind. Eng. Chem.* **51**, 232 (1959).

[7] E. Wagner and H. Brünner, *Angew. Chem.* **72**, 744 (1960).

[8] Technical Bulletin Fine Particles 11, Degussa AG (2004).

[9] N. Tsubokawa, *Prog. Polym. Sci.* **17**, 417 (1992).

[10] N. Tsubokawa, *Nippon Gomu Kyoukaishi* **70**, 378 (1997).

[11] N. Tsubokawa, *Sikizai Kyoukaishi* **71**, 656 (1998).

[12] R. Laible and K. Hamann, *Adv. Colloid Interface Sci.* **13**, 65 (1980).

[13] The Carbon Black Society ed., “The Carbon Black Handbook”, The Carbon Black Society, 157 (1995).

[14] N. Tsubokawa, *Prog. Polym. Sci.* **17**, 417 (1992).

[15] N. Tsubokawa, In: Blits JP, Little CB (eds) Fundamental and Applied Aspects of Chemically Modified Surface. The Royal Soc Chem, London, pp. 36-51 (1999).

[16] N. Tsubokawa, *Bull. Chem. Soc. Japan* **75**, 2115 (2002).

[17] N. Tsubokawa, *Sikizai Kyoukaishi* **80**, 174, 215, 267 (2007).

[18] J. Pyun and K. Matyjaszewski, *Chem. Matter* **13**, 3436 (2001).

[19] K. Ohno, K. Koh, Y. Tsuji, and T. Fukuda, *Macromolecules* **35**, 8989 (2002).

[20] T. Lui, S. Jia, T. Kowalewski, K. Matyjaszewski, R. Casadio-Portilla, and J. Belmont, *Langmuir* **19**, 6342 (2003).

[21] A. E. Harrak, G. Carrot, J. Oberdisse, J. Jestin, and F. Bou, *Polymer* **46**, 1095 (2005).

[22] T. Lui, R. Casadio-Portilla, J. Belmont, and K. Matyjaszewski, *J. Polym. Sci.: Part A: Polym. Chem.* **43**, 4695 (2005).

[23] P. Liu, WM. Liu, and QJ. Xue, *Eur. Polym. J.* **40**, 267 (2004).

[24] X. Ding, J. Zhao, Y. Liu, H. Zhang, and Z. Wang, *Mater. Lett.* **58**, 3126 (2004).

[25] M. Murota, S. Sato, and N. Tsubokawa, *Polym. Adv. Technol.* **13**, 144 (2002).

[26] A. Mũnoz-Bonilla and M. Fernández-García, *Prog. Polym. Sci.* **37**, 281-339 (2012).

[27] Y. Nakagawa, N. Dohi, T. Tawaratani, and I. Shibasaki, *J. Antibact. Antifung. Agents* **11**, 263 (1983).

[28] T. Ikeda, H. Yamaguchi, and S. Tazuke, *J. Bioact. Compat. Polym*. **1**, 301-308 (1986).

[29] A. Kanazawa, T. Ikeda, and T. Endo, *J. Polm. Sci., Part A: Polym. Chem*. **31**, 335-343, 1441-1447, 1467-1472, 2873-2876, 3003-3011, 3031-3038 (1993).

[30] Y. Inaba, M. Sugiya, and H. Sawada, Technical Report of Nippon Chemical Industrial Co., Ltd. No.1 (2000).

[31] T. Watanabe and T. Nonaka, Technical Report of Nippon Chemical Industrial Co., Ltd. No.4 (2000).

[32] R. Yamashita, Y. Takeuchi, H. Kikuchi, K. Shirai, T. Yamauchi, and N. Tsubokawa, *Polym. J.* **38**, 844-851 (2006).

[33] H. Nishizawa, in Flame-Retardant Technology of Polymeric Materials, CMC press, Tokyo, p. 113 (2002).

[34] H. Nishizawa, *J. Soc. Rubber Ind. Jpn.* **79**, 316-322 (2006).

[35] T. Yamauchi, A. Yuuki, G. Wei, K. Shirai, K. Fujiki, and N. Tsubokawa, *J. Polym. Sci.: Part A: Polym. Chem.* **47**, 6145-6152 (2009).

[36] A. Sen, B. Mukharjee, A. Bhattacharya, L. Sanghi, and K. Bhowmik, *J. Appl. Polym. Sci.* **43**, 1673 (1991).

[37] J. Kim, K. Lee, J. Bae, J. Yang, and S. Hong, *Polym. Deg. Stab.* **79**, 201 (2003).

[38] H. Kakiuchi, in Epoxy resin, *Jpn. Soc. Epoxy Res. Technol.*, Tokyo, p. 28 (2003).

[39] M. Sato, Y. Kanbayashi, K. Kobayashi, and Y. Shima, *J. Catalysi*. **7**, 342 (1976).

[40] W. A. Christopher, *Chem. Rev.* **91**. 119 (1991).

[41] M. Witt and H. W. Roesky, *Chem. Rev.* **94**, 1163 (1994).

[42] Y. Liu and G. Zhao, *Chin. J. Chem. Eng*. **15**, 429 (2007).

Chapter 2

Preparation and Properties of Antibacterial Polymer-grafted Silica Nanoparticles

Abstract

Antibacterial polymer was grafted onto silica nanoparticle and the surface properties of various composites filled with the silica were investigated. The grafting of antibacterial polymer, poly(vinylbenzyl tributylphosphonium chloride) (poly(St-$CH_2P^+(Bu)_3Cl^-$)), onto silica surface was achieved by two methods: one is treatment of poly(vinylbenzyl chloride) (poly(St-CH_2Cl))-grafted silica with tributylphosphine and the other is direct grafting of poly(St-$CH_2P^+(Bu)_3Cl^-$) by radical graft polymerization of the corresponding monomer. The grafting of poly(St-CH_2Cl) and poly(St-$CH_2P^+(Bu)_3Cl^-$) onto silica surface were initiated by the system consisting of trichloroacetyl groups on the silica surface and $Mo(CO)_6$. Trichloroacetyl groups were introduced onto the silica surface by the reaction of amino groups on the silica surface with trichloroacetyl isocyanate. The percentage of poly(St-CH_2Cl) grafting during the graft polymerization initiated by the system increased with progress of the polymerization reached 116%. The grafting of poly(St-$CH_2P^+(Bu)_3Cl^-$) onto silica surfaces was confirmed by FT-IR spectra, thermal decomposition GC-MS, and ^{13}C-CP/MAS-NMR. The surfaces of silicone rubber, polystyrene film, and paints filled with the poly(St-$CH_2P^+(Bu)_3Cl^-$)-grafted silica shows strong antibacterial activity. In addition, the silicone rubber filled with poly(St-$CH_2P^+(Bu)_3Cl^-$)-grafted silica retained the antibacterial activity even after the boiling in water for 24 h.

2.1 Introduction

Many researchers have extensively studied the chemical and physical modifications of nanoparticle surfaces. Among the permanent chemical modifications, the surface grafting of polymers, namely, chemical binding of polymers onto silica nanoparticles interests us for use in designing new functional inorganic/organic hybrid materials, which have excellent properties both of inorganic materials, such as heat-resistance and chemical-resistance, and of grafted polymers, such as photosensitivity, curing ability, bioactivity, biocompatibility, and pharmacological activities [1-6].

The purpose of this chapter is to prepare antibacterial polymer-grafted silica and to make the antibacterial composites filled with the silica. Various kinds of antibacterial polymers were reported [7-10]. For example, alkylphosphonium polymers show extremely strong antibacterial activity to *Staphylococcus aureus* and *Escherichia coli*. Yamashita et al. have succeeded in the grafting of polymer having alkylphosphonium sulfate groups (poly(St-$SO_3^-P^+Bu_3R$)) onto the surface of silica nanoparticle [11]. Yamashita et al. have pointed out that the surface of silicone rubber filled with the poly(St-$SO_3^-P^+Bu_3R$)-grafted silica shows strong antibacterial activity to *Staphylococcus aureus* and *Escherichia coli*.

On the other hand, Tsubokawa and his co-workers have reported that the system consisting of $Mo(CO)_6$ and surface trichloroacetyl groups on nanoparticles, such as silica and vapor grown carbon fiber (VGCF), has an ability to initiate the radical polymerization of various vinyl monomers to give the corresponding polymer-grafted silica and VGCF as shown in Scheme 2-1 [12, 13]. They pointed out that the effective radical grafting was achieved in the initiating system consisting of trichloroacetyl groups and $Mo(CO)_6$, and percentage of grafting exceeded 200% because of no formation of fragment radicals.

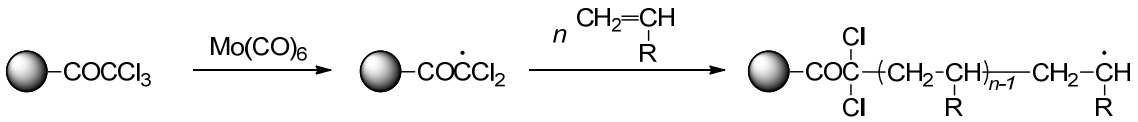

Scheme 2-1. Graft polymerization of vinyl monomer initiated by the system consisting of trichloroacetyl groups on the surface and $Mo(CO)_6$.

In this chapter, the radical grafting of antibacterial polymer, poly(vinylbenzyl tributylphosphonium chloride) (poly(St-$CH_2P^+(Bu)_3Cl^-$)), onto silica surface initiated by the system consisting of trichloroacetyl groups on the silica surface and $Mo(CO)_6$ was investigated. The grafting of poly(St-$CH_2P^+(Bu)_3Cl^-$) was achieved by two methods: one is treatment of poly(vinylbenzyl chloride) (poly(St-CH_2Cl))-grafted silica with tributylphosphine (Scheme 2-2) and the other is direct grafting of poly(St-$CH_2P^+(Bu)_3Cl^-$) by radical graft polymerization of the corresponding monomer (Scheme 2-3). In addition, the antibacterial activity of the surfaces of composites prepared from the poly(St-$CH_2P^+(Bu)_3Cl^-$)-grafted silica were also discussed.

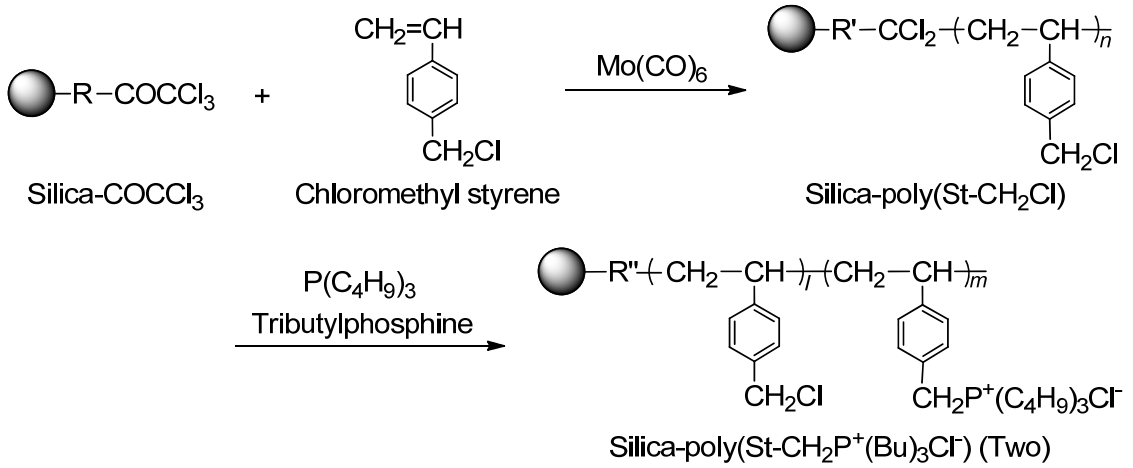

Scheme 2-2. Preparation of Silica-poly(St-$CH_2P^+(Bu)_3Cl^-$) (Two) by two-step reaction.

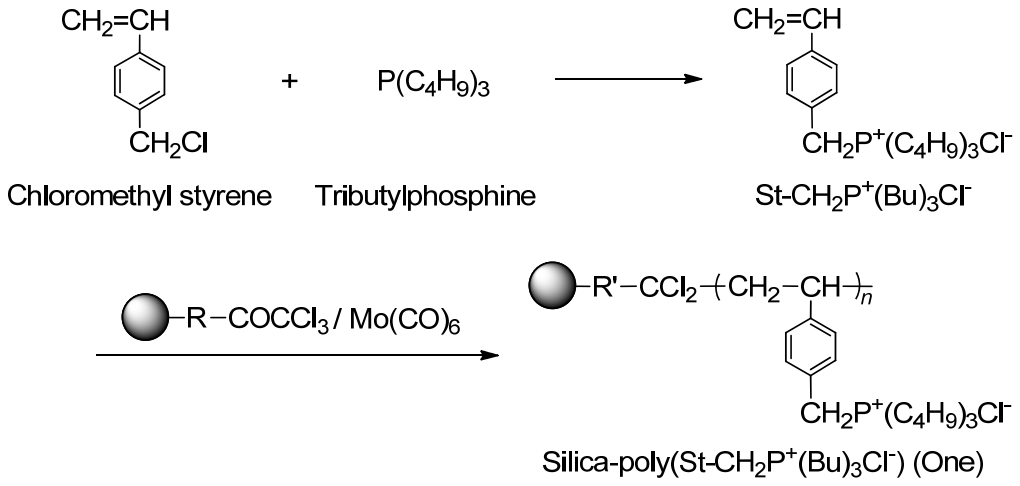

Scheme 2-3. Preparation of Silica-poly(St-$CH_2P^+(Bu)_3Cl^-$) (One) by direct graft polymerization of St-$CH_2P^+(Bu)_3Cl^-$.

2.2 Experimental

2.2.1 Materials and reagents

Silica nanoparticle used was Aerosil 200 and it was obtained from Nippon Aerosil Co., Ltd., Japan. The specific surface area, average particle size, and silanol group content were 200 m^2/g, 12 nm, and 1.37 mmol/g, respectively. The content of silanol groups was determined by measuring volumetrically the amount of ethane evolved by the reaction with triethylaluminum [14, 15]. The silica was dried *in vacuo* at room temperature for 24 h before use.

γ-Aminopropyltriethoxysilane (γ-APS) was used without further purification. 4-(Chloromethyl)styrene (St-CH_2Cl) obtained from Sigma-Aldrich Co. was used without further purification. Trichloroacetyl isocyanate, molybdenum hexacarbonyl ($Mo(CO)_6$), and tributylphosphine obtained from Kanto Chemical Co., Inc. were used without further purification. Dimethyl sulfoxide (DMSO) obtained from Kanto Chemical Co., Inc. was distilled before use. Dehydrated toluene and tetrahydrofuran (THF) were obtained from Kanto Chemical Co., Inc. and used without further purification.

2.2.2 Silicone rubber, polystyrene, and paints

Silicone rubber, poly(dimethylsiloxane), (two-component type) was obtained from Shin-Etsu Chemical Co., Ltd. Polystyrene was obtained from Wako Pure Chemical Industries, Ltd. and used without further purification. Water paint (Neogloss G-80; acrylic emulsion type) and oil paint (Neopaint urethane #5500AB; two-component acrylic urethane type) were obtained from Asia Industry Co., Ltd.

2.2.3 Synthesis of antibacterial monomer

Antibacterial monomer, vinylbenzyl tributylphosphonium chloride

(St-$CH_2P^+(Bu)_3Cl^-$), was prepared by the reaction of chlorometyl styrene (St-CH_2Cl) with tributylphosphine according to the method of literature as shown in Scheme 2-4 [9].

A typical example was as follows: Into a 500 mL four-necked flask, 120 mL of chlorometyl styrene and 300 mL of hexane were added and the atmosphere was exchanged for nitrogen. Then, 97 mL of tributylphosphine was added. The mixture was stirred at 30 °C for 72 h under nitrogen. After the reaction, the synthesized monomer was dispersed in hexane and the monomer was centrifuged. The monomer was washed with hexane until no more chlorometyl styrene and tributylphosphine were detected. The purified monomer was stored *in vacuo* at room temperature.

The structure of St-$CH_2P^+(Bu)_3Cl^-$ was confirmed by ^{1}H-NMR.

2.2.4 Introduction of trichloroacetyl groups onto silica nanoparticle surface

Introduction of amino groups onto the silica was also achieved by the treatment of surface silanol groups with γ-APS in a solvent-free dry-system according to the methods of the literature [16]. The silica having amino groups was abbreviated as Silica-NH_2.

The introduction of trichloroacetyl groups onto silica nanoparticle surface was achieved by the reaction of trichloroacetyl isocyanate with amino groups on the silica surface [12]. The treated silica was abbreviated as Silica-$COCCl_3$.

2.2.5 Preparation of Silica-poly(St-$CH_2P^+(Bu)_3Cl^-$)

2.2.5.1 Preparation of Silica-poly(St-$CH_2P^+(Bu)_3Cl^-$) by two-step reaction

The grafting of poly(St-$CH_2P^+(Bu)_3Cl^-$) was achieved by the treatment of poly(St-CH_2Cl)-grafted silica with tributylphosphine as shown in Scheme 2-2. The radical graft polymerization of St-CH_2Cl initiated by the system consisting of Silica-$COCCl_3$ and $Mo(CO)_6$ was carried out in a sealed tube under high vacuum. A

typical example was as follows. Into a polymerization tube, 0.20 g of Silica-$COCCl_3$, 0.01 g of $Mo(CO)_6$, 5.0 mL of St-CH_2Cl, and a stirrer bar were charged. The mixture was frozen in a liquid nitrogen bath, degassed with a high vacuum pump, and then thawed. After this operation was repeated three times, the tube was heated at 100 °C with stirring. After the reaction, the product was dispersed in THF and centrifuged. The supernatant solution was removed and precipitated silica was dispersed again in THF. The procedures were repeated until no more ungrafted polymer could be detected in the supernatant solution. The resulting silica was abbreviated as Silica-poly(St-CH_2Cl).

The Silica-poly(St-CH_2Cl) was treated with tributylphosphine to convert the benzyl chloride groups to tributylphosphonium groups [9]. A typical example was as follows. 1.0 g of Silica-poly(St-CH_2Cl) was charged into a three-necked flask attached with a reflux condenser, and then a mixture of 50.0 mL of toluene and 5.0 mL of tributylphosphine was dropped by a syringe into the flask under nitrogen. The reaction mixture was refluxed at 110 °C with stirring for 24 h. After the reaction, the product was dispersed in THF and centrifuged. The supernatant solution was removed and precipitated silica was dispersed again in THF. The procedures were repeated until no more tributylphosphine could be detected in the supernatant solution. The resulting silica was abbreviated as Silica-poly(St-$CH_2P^+(Bu)_3Cl^-$) (Two).

2.2.5.2 Preparation of Silica-poly(St-$CH_2P^+(Bu)_3Cl^-$) by direct graft polymerization of St-$CH_2P^+(Bu)_3Cl^-$

The direct graft polymerization of St-$CH_2P^+(Bu)_3Cl^-$ initiated by the system consisting of Silica-$COCCl_3$ and $Mo(CO)_6$ was carried out in a sealed tube under high vacuum as shown in Scheme 2-3. The graft polymerization was carried out by the same manner as grafting of poly(St-CH_2Cl) onto silica as mentioned above. The resulting silica was abbreviated as Silica-poly(St-$CH_2P^+(Bu)_3Cl^-$) (One).

2.2.6 Determination of percentage of grafting

The grafting of poly(St-CH_2Cl) and poly(St-$CH_2P^+(Bu)_3Cl^-$) onto silica surface was determined by the following equation:

$$\text{Grafting (\%)} = (A / B) \times 100$$

where A is weight of poly(St-CH_2Cl) or poly(St-$CH_2P^+(Bu)_3Cl^-$) grafted onto silica surface and B is weight of silica used. A was determined by measuring the weight loss when these polymer-grafted silica was heated at 800 °C using a thermogravimetric analyzer (TGA) under nitrogen.

2.2.7 Tributylphosphonium group content of Silica-poly(St-$CH_2P^+(Bu)_3Cl^-$)

Tributylphosphonium group content of Silica-poly(St-$CH_2P^+(Bu)_3Cl^-$) was calculated from the weight increment of Silica-poly(St-CH_2Cl) after the treatment with tributylphosphine determined by TGA as mentioned above.

2.2.8 Measurements

Thermogravimetric analysis (TGA) was performed under a nitrogen flow using a thermogravimetric analyzer (Shimadzu Co., TGA-50) at a heating rate of 10 °C/min. Infrared spectrum was recorded on a FT-IR spectrophotometer (Shimadzu Co., FTIR-8200A). Thermal decomposition gas chromatograms and mass spectra were recorded on a gas chromatograph mass spectrometer (Shimadzu Co., GCMS-QP2010) equipped with a double shot pyrolyzer (Frontier Laboratories Ltd., PY-2020D). The column was programmed from 70 to 320 °C at a heating rate of 20 °C/min and then held at 320 °C for 5 min. ^{13}C-CP/MAS-NMR was recorded on a Bruker MSL-300.

2.2.9 Preparation of composites filled with Silica-poly(St-$CH_2P^+(Bu)_3Cl^-$)

Silica-poly(St-$CH_2P^+(Bu)_3Cl^-$) was uniformly dispersed in poly(dimethylsiloxane) containing a curing agent using a planetary centrifugal mixer (Thinky Co., AR-100) at room temperature. The mixture was poured into a Teflon mold. By heating the mixture at 70 °C for 20 min, silicone rubber filled with Silica-poly(St-$CH_2P^+(Bu)_3Cl^-$) was obtained.

Polystyrene film filled with Silica-poly(St-$CH_2P^+(Bu)_3Cl^-$) was prepared as follows. 10.0 g of polystyrene was dissolved in toluene. Then, 0.10 g of Silica-poly(St-$CH_2P^+(Bu)_3Cl^-$) was added into the solution and the mixture was stirred under irradiation of ultrasonic wave. The mixture was casted in a Petri dish and toluene was evaporated at room temperature.

Paints filled with Silica-poly(St-$CH_2P^+(Bu)_3Cl^-$) were prepared as follows. 0.1% of Silica-poly(St-$CH_2P^+(Bu)_3Cl^-$) was mixed with a commercially available paint and curing agent using a planetary centrifugal mixer. The mixture was painted on a Petri dish and dried at 50 °C for 24 h.

Size of all samples was 50 mm × 50 mm.

2.2.10 Assessment of antibacterial activity of the composite surfaces

The surface antibacterial activity of the composites filled with antibacterial polymer-grafted silica was estimated according to the method of the Japanese Industrial Standards (JIS Z 2801) [17].

2.2.10.1 Bacteria

Staphylococcus aureus NBRC 12732, *Escherichia coli* NBRC 3972, and *Pseudomonas aeruginosa* NBRC 13275 were obtained from National Institute of Technology and Evaluation. These bacteria were grown on slant culture medium at 37 °C.

2.2.10.2 Culture medium

(a) Nutrient broth

A typical example was as follows. Into a beaker, 0.3 g of fish extract, 1.0 g of polypeptone, and 0.5 g of sodium chloride, and 100 mL of purified water were charged and dissolved completely. The mixture were adjusted the pH 7.0 using NaOH aqueous solution or HCl aqueous solution. The mixture was taken a part into a culture medium bottle, and sterilized it with high pressure steam.

(b) Slant culture medium

A typical example was as follows. Into a beaker, 0.5 g of fish extract, 1.0 g of polypeptone, 0.5 g of sodium chloride, 1.5 g of agar powder, and 100 mL of purified water were charged and dissolved completely. The mixture were adjusted the pH 7.0 using NaOH aqueous solution or HCl aqueous solution. 6.0 mL of the mixture was poured into test tubes, and put silicone stoppers, and sterilized them with high pressure steam. After sterilization, test tubes were slanted in the clean room.

(c) Plate count agar

A typical example was as follows. Into a beaker, 2.5 g of yeast extract, 5.0 g of trypticase peptone, 1.0 g of glucose, 15.0 g of agar powder, and 1000 mL of purified water were charged and dissolved completely. The mixture were adjusted the pH 7.0 using NaOH aqueous solution or HCl aqueous solution. The mixture was taken a part into a culture medium bottles, and sterilized them with high pressure steam. After sterilization, culture medium bottles were heated in a water bath at 50 °C.

(d) SCDLP broth

A typical example was as follows. Into a beaker, 2.0 g of polypeptone, 0.5 g of sodium chloride, 0.25 g of K_2HPO_4, 0.25 g of glucose, 0.1 g of lecithin, 0.7 g of nonionic surfactant, and 100 mL of purified water were charged and dissolved completely. The mixture were adjusted the pH 7.0 using NaOH aqueous solution or HCl

aqueous solution. The mixture was taken a part into a culture medium bottles, and sterilized them with high pressure steam. Polypeptone was substituted for soybean peptone and casein peptone.

(e) Phosphate buffer solution

A typical example was as follows. Into a beaker, 3.4 g of KH_2PO_4, and 100 mL of purified water were charged and dissolved completely. The mixture were adjusted the pH 7.0 using NaOH aqueous solution or HCl aqueous solution. The solution was taken a part into test tubes, and sterilized them with high pressure steam.

(f) Phosphate buffered physiological saline

A typical example was as follows. Phosphate buffer solution was diluted with physiological saline (0.85% sodium chloride aqueous solution) into an 800-fold volume. The solution was taken a part into a culture medium bottles, and sterilized them with high pressure steam.

2.2.10.3 Antibacterial test

A typical example is as follows. Culture contains virus was prepared by ordinary method and used for antibacterial test.

The test pieces (50 mm × 50 mm × 1 mm, obtained at section 2.2.9) was wiped with absorbent cotton immersed ethanol and dry it completely and placed in sterilized Petri dish making the test surface up. The above test inoculum was instilled with a pipet onto each test piece in the Petri dish: the number of bacteria was about 1.0×10^4-1.3×10^7 per test piece. The instilled test inoculum was covered with a film. The Petri dishes containing the test piece inoculated with the test inoculum (3 untreated test pieces and 3 test pieces) were incubated at 37 °C and a relative humidity of 90% for 24 h. After the incubation, the covering film was removed, and 10 mL of SCDLP broth was added into the Petri dish and mixed with the test inoculum on the test piece to wash out the test bacteria. Exactly 1.0 mL of the washings was added into a test tube containing 9.0 mL

of phosphate buffered physiological saline. Then, 1.0 mL of mixture in the test tube was added into another test tube containing 9.0 mL of phosphate buffered physiological saline. By repeating the procedures, 10-fold serial dilutions were prepared. From these dilutions, the surviving bacteria were counted by the agar plate culture method. After the inoculation, the agar plates were incubated at 37 °C and a relative humidity of 90% for 48 h. After the incubation, the colonies were counted.

The concentration of living cells of test piece surface was determined by the following equation.

$$\text{Concentration of living cells (CFU/mL)} = N \times n \times V$$

N: Number of colonies

n: Dilution multiple

V: Volume of SCDLP broth

2.2.11 Stability of antibacterial activity

The stability of antibacterial activity of silicone rubber filled with Silica-poly(St-$CH_2P^+(Bu)_3Cl^-$) was researched as follows. The test piece (50 mm × 50 mm × 1 mm, obtained at section 2.2.9) and 50 mL of ion-exchanged water were charged into a flask equipped with a reflux condenser. The test piece was heated under reflux for 24 h. After the boiling, the test piece was carried out antibacterial test.

In addition, silicone rubber filled with free poly(St-$CH_2P^+(Bu)_3Cl^-$) was also carried out. The amount of filled with free poly(St-$CH_2P^+(Bu)_3Cl^-$) was adjusted as exactly same that of grafted chain onto silica surface.

2.3 Results and Discussion

2.3.1 Synthesis of antibacterial monomer

The synthesis of antibacterial monomer, vinylbenzyl tributylphosphonium chloride (St-$CH_2P^+(Bu)_3Cl^-$), was carried out by the reaction of chlorometyl styrene (St-CH_2Cl) with tributylphosphine according to the method of literature as shown in Scheme 2-4 [9].

Figure 2-1 shows ^{1}H-NMR spectrum of St-$CH_2P^+(Bu)_3Cl^-$. The spectrum was conformed to the literature data of St-$CH_2P^+(Bu)_3Cl^-$ [34]. Yield: 58.0 %. Melting point: 125.6 °C. ^{1}H-NMR ($CDCl_3$): 0.94 (9H, t, P-CH_2-$(CH_2)_2$-$\underline{CH_3}$), 1.46-1.75 (12H, m, P-CH_2-$(\underline{CH_2})_2$-CH_3), 2.41 (6H, m, P-$\underline{CH_2}$-$(CH_2)_2$-CH_3), 4.29 (2H, d, -$\underline{CH_2}$-P), 5.32 (1H, d, vinyl proton), 5.79 (1H, d, vinyl proton), 6.70 (1H, dd, vinyl proton), 7.40 (4H, s, aromatic protons).

This result suggests that antibacterial monomer, St-$CH_2P^+(Bu)_3Cl^-$, was successfully synthesized.

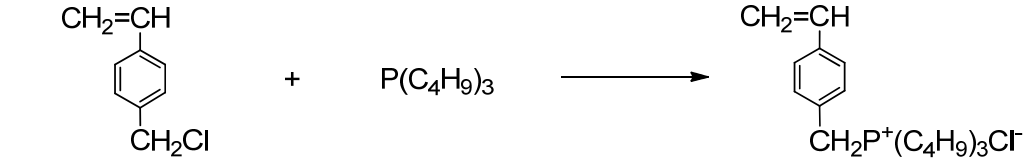

Scheme 2-4. Synthesis of antibacterial monomer.

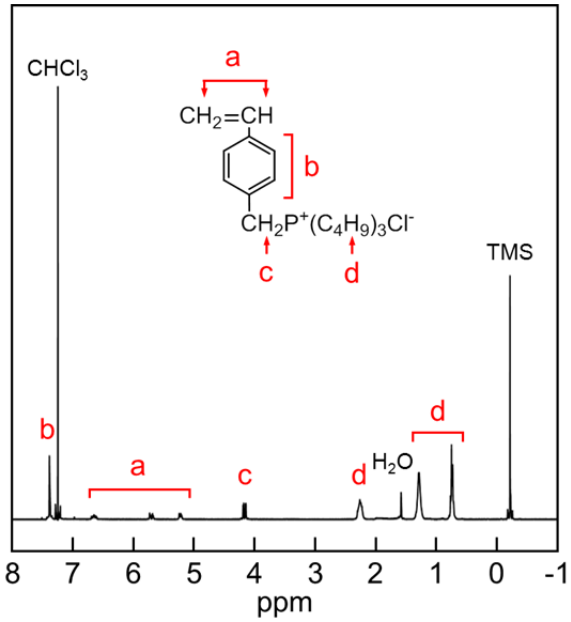

Figure 2-1. ^{1}H-NMR spectrum of St-$CH_2P^+(Bu)_3Cl^-$.

2.3.2 Introduction of trichloroacetyl groups onto silica nanoparticle surface

Introduction of amino groups onto the silica surface as immobilizing sites for trichloroacetyl groups was achieved by the treatment of the silica surface with γ-APS in the solvent-free dry-system (Scheme 2-5) [16]. The amino group content introduced onto the silica surface was determined by titration to be 0.29 mmol/g.

The introduction of trichloroacetyl groups onto silica surface by the reaction of trichloroacetyl isocyanate with amino groups on the silica surface was successfully achieved (Scheme 2-5). The content of trichloroacetyl groups introduced onto silica surface, which was determined from the unreacted amino groups, was 0.26 mmol/g. The result suggests that about 90% of amino groups were successfully converter to trichloroacetyl groups.

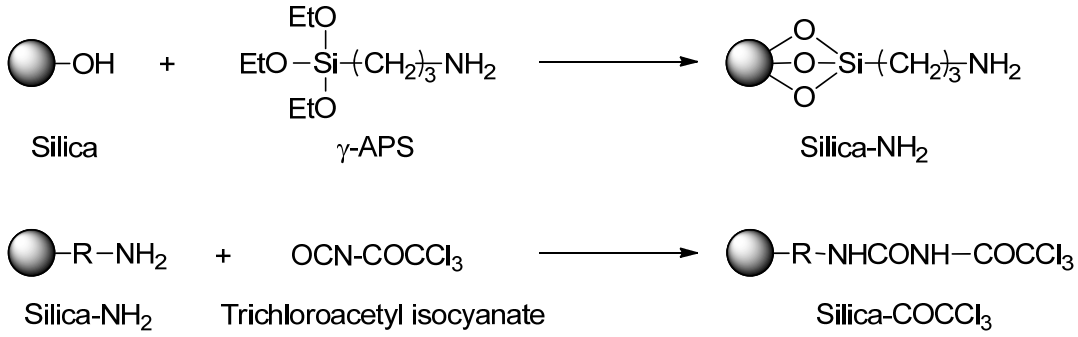

Scheme 2-5. Introduction of trichloroacetyl groups onto silica nanoparticle surface.

2.3.3 Preparation of Silica-poly(St-$CH_2P^+(Bu)_3Cl^-$)

2.3.3.1 Preparation of Silica-poly(St-$CH_2P^+(Bu)_3Cl^-$) by two-step reaction

Figure 2-2 shows the result of the grafting of poly(St-CH_2Cl) onto silica nanoparticle surface during the graft polymerization of St-CH_2Cl initiated by the system consisting of Silica-$COCCl_3$ and $Mo(CO)_6$. No polymerization of St-CH_2Cl was initiated by the system consisting of untreated silica and $Mo(CO)_6$. On the contrary, the graft polymerization of St-CH_2Cl was successfully initiated by the system consisting of Silica-$COCCl_3$ and $Mo(CO)_6$. The percentage of poly(St-CH_2Cl) grafting onto the silica surface increased with progress of the polymerization and reached 116% after 6 h.

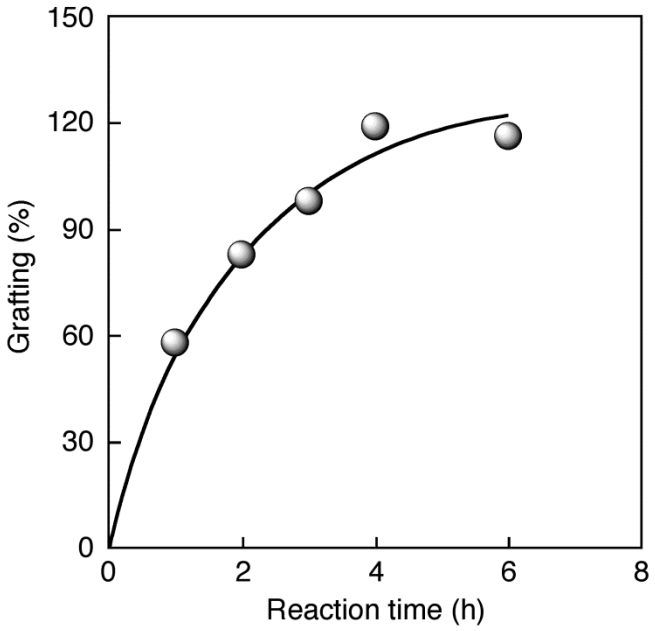

Figure 2-2. Grafting of poly(St-CH_2Cl) onto silica nanoparticle surface during the polymerization of St-CH_2Cl initiated by the system consisting of Silica-$COCCl_3$ and $Mo(CO)_6$.
Silica-$COCCl_3$, 0.20 g; $Mo(CO)_6$, 0.01 g; St-CH_2Cl, 5.0 mL; 100 °C.

To convert the benzyl chloride groups of grafted chains on the silica to tributylphosphonium groups, Silica-poly(St-CH_2Cl) was treated with tributylphosphine as shown in Scheme 2-2. Figure 2-3 shows FT-IR spectra of (a) Silica-$COCCl_3$, (b) Silica-poly(St-CH_2Cl), and (c) Silica-poly(St-$CH_2P^+(Bu)_3Cl^-$) (Two). FT-IR spectra of Silica-poly(St-CH_2Cl) show a new absorption at 2930 cm^{-1}, which is characteristic of methylene groups of poly(St-CH_2Cl). FT-IR spectra of Silica-poly(St-$CH_2P^+(Bu)_3Cl^-$) (Two) show strong absorptions at 2959-2872 cm^{-1}, which are characteristic of alkyl chains of tributylphosphonium groups. Therefore, the results suggest that poly(St-CH_2Cl) grafted onto silica surface was successfully converted to poly(St-$CH_2P^+(Bu)_3Cl^-$).

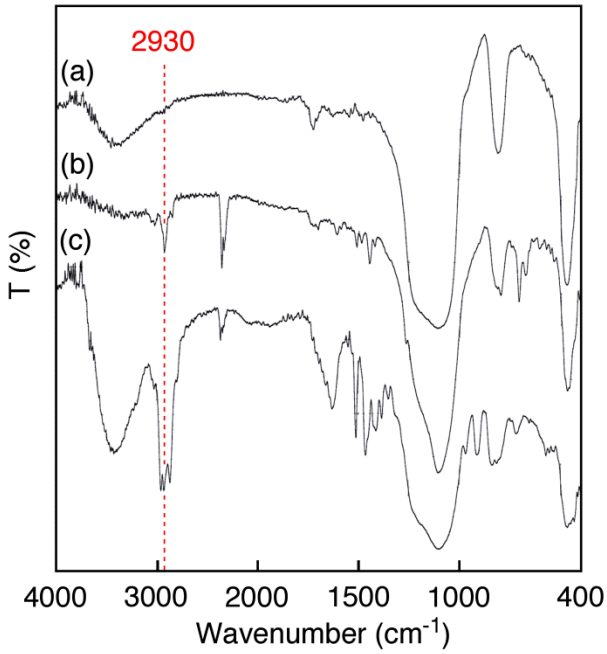

Figure 2-3. FT-IR spectra of (a) Silica-$COCCl_3$, (b) Silica-poly(St-CH_2Cl), and (c) Silica-poly(St-$CH_2P^+(Bu)_3Cl^-$) (Two).

Figure 2-4 shows the thermal decomposition gas chromatograms and mass spectra (GC-MS) of (a) tributylphosphine and (b) Silica-poly(St-$CH_2P^+(Bu)_3Cl^-$) (Two). Mass spectra of decomposed gas of Silica-poly(St-$CH_2P^+(Bu)_3Cl^-$) (Two) at retention time 5.2 min was in agreement with those of tributylphosphine. Therefore, the result also shows that tributylphosphonium groups were introduced onto Silica-poly(St-CH_2Cl).

Figure 2-5 shows ^{13}C-CP/MAS-NMR spectrum of Silica-poly(St-$CH_2P^+(Bu)_3Cl^-$) (Two). The signals of carbon atoms based on poly(St-$CH_2P^+(Bu)_3Cl^-$) were observed. The signal of carbon atoms based on benzyl chloride groups, which did not reacted with tributylphosphine, were observed at 50 ppm.

Based on the above results, it is concluded that poly(St-$CH_2P^+(Bu)_3Cl^-$) was successfully grafted onto silica surface. The percentage of benzyl chloride groups reacted with tributylphosphine was determined to be about 70% by thermogravimetric analysis.

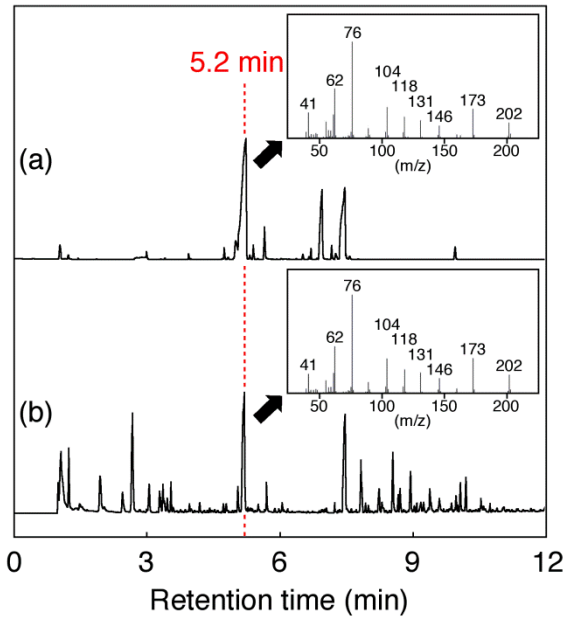

Figure 2-4. Thermal decomposition gas chromatograms and mass spectra (GC-MS) of (a) tributylphosphine and (b) Silica-poly(St-$CH_2P^+(Bu)_3Cl^-$) (Two).

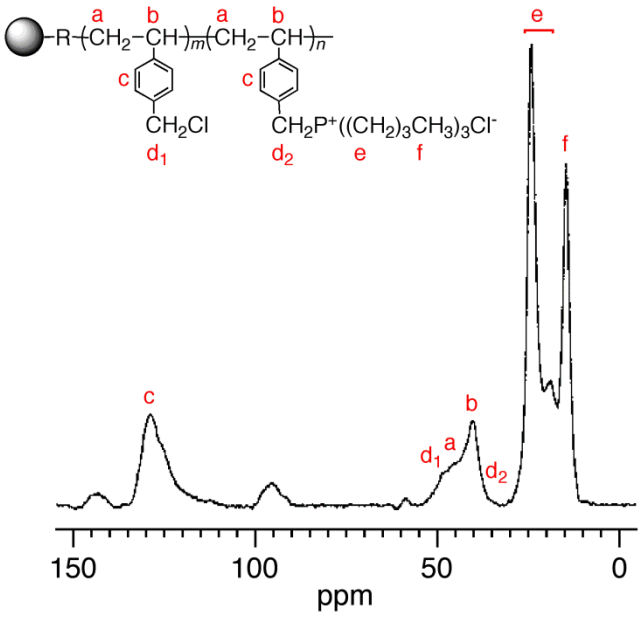

Figure 2-5. ^{13}C-CP/MAS-NMR spectrum of Silica-poly(St-$CH_2P^+(Bu)_3Cl^-$) (Two).

Figure 2-6 shows the relationship between the percentage of poly(St-CH_2Cl) grafting onto silica surface and tributylphosphonium group content. The tributylphosphonium group content on silica surface increased with an increase in percentage of poly(St-CH_2Cl) grafting.

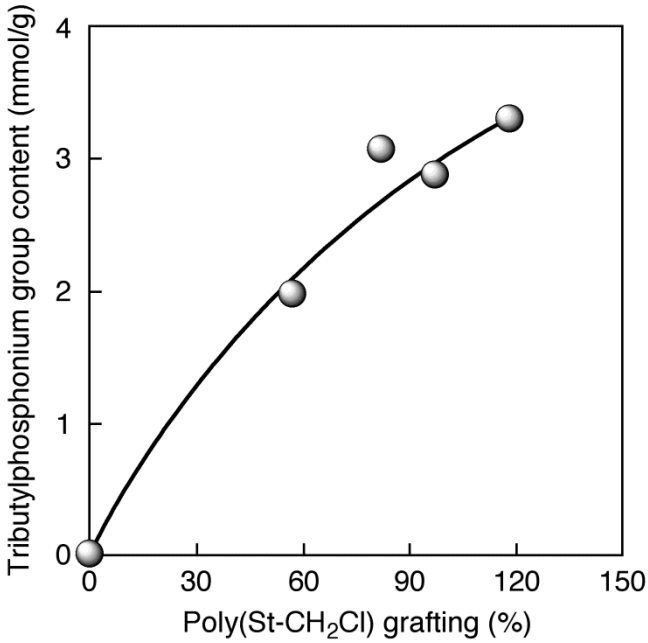

Figure 2-6. Relationship between the percentage of poly(St-CH_2Cl) grafting onto silica nanoparticle surface and tributylphosphonium group content introduced onto the surface by the treatment with tributylphosphine.

2.3.3.2 Preparation of Silica-poly(St-$CH_2P^+(Bu)_3Cl^-$) by direct grafting

Silica-poly(St-$CH_2P^+(Bu)_3Cl^-$) was prepared by the direct graft polymerization of the corresponding monomer initiated by the system consisting of Silica-$COCCl_3$ and $Mo(CO)_6$ as shown in Scheme 2-3. Figure 2-7 shows the relationship between percentage of poly(St-$CH_2P^+(Bu)_3Cl^-$) grafting and reaction time. The percentage grafting of poly(St-$CH_2P^+(Bu)_3Cl^-$) onto silica surface increased with progress of the polymerization and reached 22.6% after 60 min. But the percentage of grafting was smaller than that of Silica-poly(St-$CH_2P^+(Bu)_3Cl^-$) (Two). This may be due to the fact that antibacterial monomer, St-$CH_2P^+(Bu)_3Cl^-$, has bulky side group.

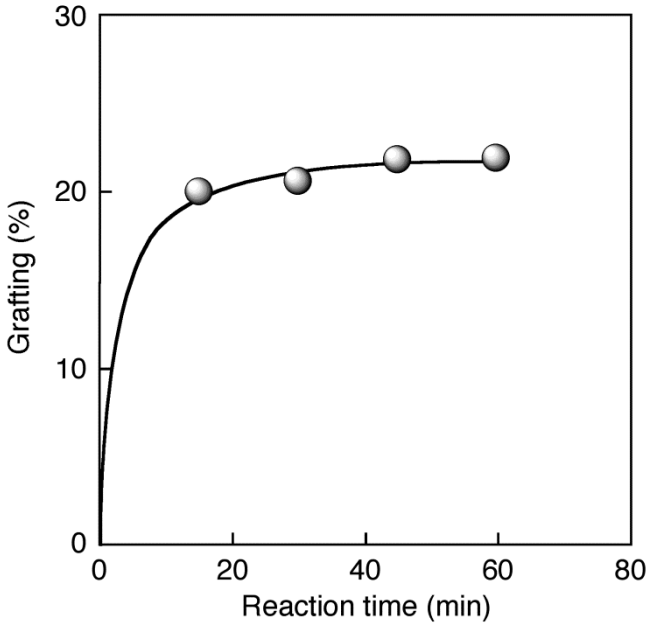

Figure 2-7. Grafting of poly(St-$CH_2P^+(Bu)_3Cl^-$) onto silica nanoparticle surface during the polymerization of St-$CH_2P^+(Bu)_3Cl^-$ initiated by the system consisting of Silica-$COCCl_3$ and $Mo(CO)_6$.
Silica-$COCCl_3$, 0.20 g; $Mo(CO)_6$, 0.01 g; St-$CH_2P^+(Bu)_3Cl^-$, 0.9 g; DMSO, 10 mL; 70 °C.

Mass spectra of decomposed gas of Silica-poly(St-$CH_2P^+(Bu)_3Cl^-$) (One) at retention time 5.2 min was in agreement with those of tributylphosphine.

Figure 2-8 shows ^{13}C-CP/MAS-NMR spectrum of Silica-poly(St-$CH_2P^+(Bu)_3Cl^-$) (One). The signals of carbon atoms based on poly(St-$CH_2P^+(Bu)_3Cl^-$) were observed. Based on the above results, it is concluded that poly(St-$CH_2P^+(Bu)_3Cl^-$) was also successfully grafted onto silica surface.

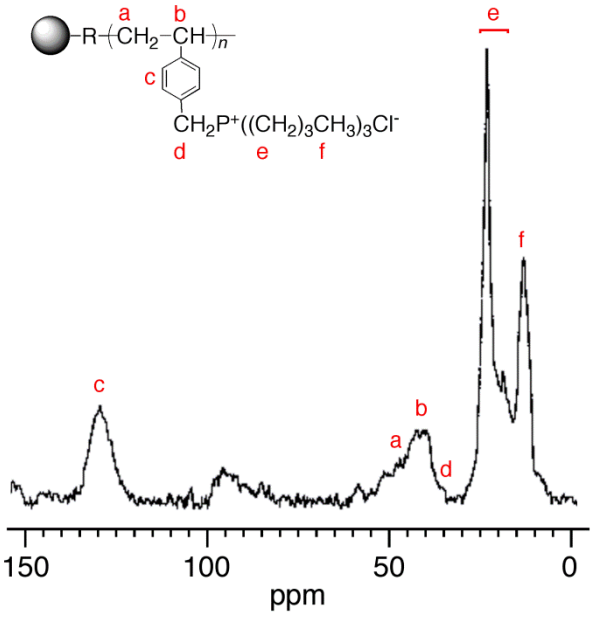

Figure 2-8. ^{13}C-CP/MAS-NMR spectrum of Silica-poly(St-$CH_2P^+(Bu)_3Cl^-$) (One).

2.3.4 Estimation of antibacterial activity of Silica-poly(St-$CH_2P^+(Bu)_3Cl^-$)

Figure 2-9 shows the effect of Silica-poly(St-$CH_2P^+(Bu)_3Cl^-$) (Two) (Grafting = 142%) on the antibacterial activity against *Staphylococcus aureus*. It was found that the surface of silicone rubber filled with untreated silica shows no antibacterial activity. On the contrary, cells of *Staphylococcus aureus* decreased from 2.4×10^5 to less than 10 CFU/mL on silicone rubber filled with 1.0 wt% of Silica-poly(St-$CH_2P^+(Bu)_3Cl^-$) (Two). Even the surface of silicone rubber filled with 0.1 wt% of Silica-poly(St-$CH_2P^+(Bu)_3Cl^-$) (Two) shows antibacterial activity.

Based on the above results, it was concluded that the surface of silicone rubber filled with Silica-poly(St-$CH_2P^+(Bu)_3Cl^-$) (Two) shows strong antibacterial activity to *Staphylococcus aureus*.

Figure 2-10 shows the effect of Silica-poly(St-$CH_2P^+(Bu)_3Cl^-$) (One) (Grafting = 22.6%) on the antibacterial activity to *Staphylococcus aureus*. Figure 2-10 clearly shows that the surface of silicone rubber filled with 1.0 wt% of Silica-poly(St-$CH_2P^+(Bu)_3Cl^-$) (One) also shows antibacterial activity to *Staphylococcus aureus*.

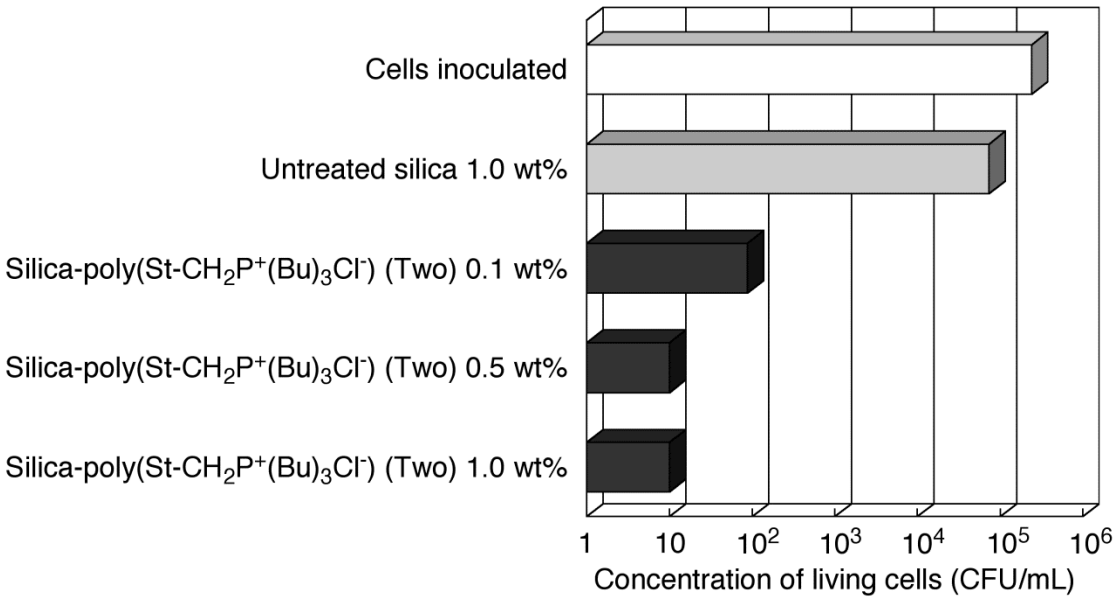

Figure 2-9. Antibacterial activity of the surface of silicone rubber filled with Silica-poly(St-$CH_2P^+(Bu)_3Cl^-$) (Two) (Grafting = 142%) against *Staphylococcus aureus.*

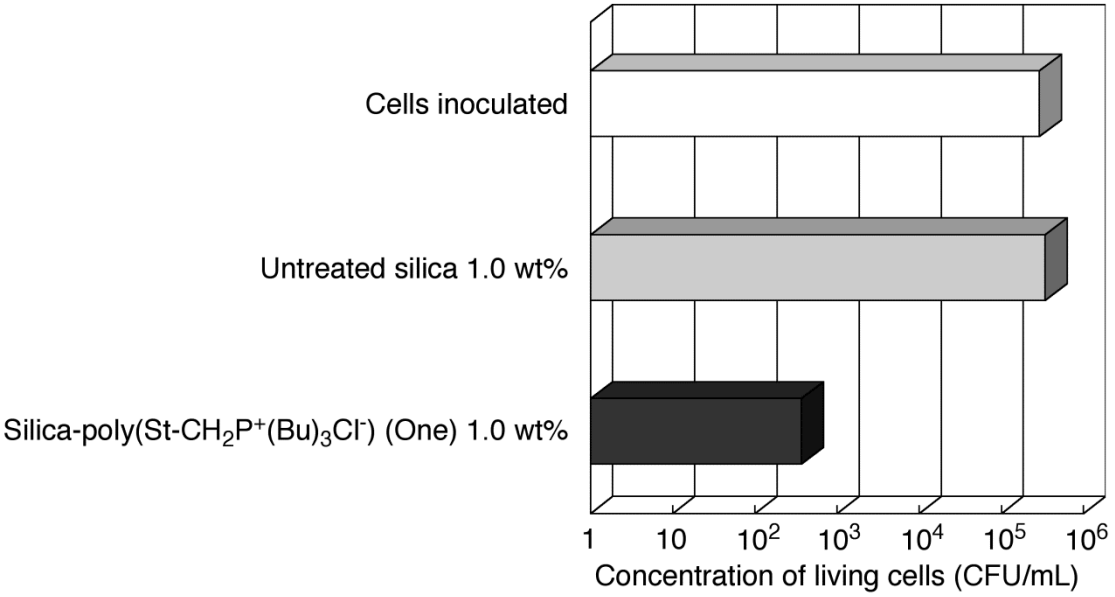

Figure 2-10. Antibacterial activity of the surface of silicone rubber filled with Silica-poly(St-$CH_2P^+(Bu)_3Cl^-$) (One) (Grafting = 22.6%) against *Staphylococcus aureus.*

2.3.5 Antibacterial activity of the surface of silicone rubber filled with Silica-poly(St-$CH_2P^+(Bu)_3Cl^-$) against several bacteria

Figure 2-11 shows the antibacterial activity of the surface of silicone rubber filled with Silica-poly(St-$CH_2P^+(Bu)_3Cl^-$) (Two) (Grafting = 142%) against (A) *Escherichia coli* and (B) *Pseudomonas aeruginosa*. It was found that the surface of silicone rubber filled with 1.0 wt% of Silica-poly(St-$CH_2P^+(Bu)_3Cl^-$) (Two) also shows strong antibacterial activity against *Escherichia coli* and *Pseudomonas aeruginosa*.

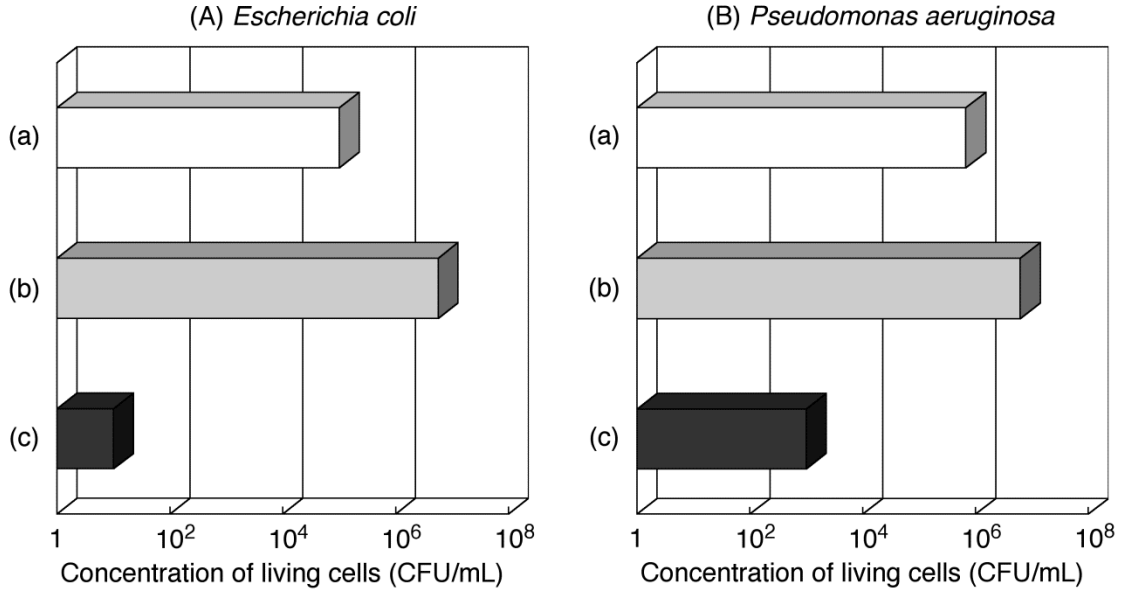

Figure 2-11. Antibacterial activity of the surface of silicone rubber filled with Silica-poly(St-$CH_2P^+(Bu)_3Cl^-$) (Two) (Grafting = 142%) against (A) *Escherichia coli* and (B) *Pseudomonas aeruginosa*. (a) cells inoculated, (b) untreated silica 1.0 wt%, and (c) Silica-poly(St-$CH_2P^+(Bu)_3Cl^-$) (Two) 1.0 wt%.

Figure 2-12 shows the relationship between contacting time and concentration of living cells of *Staphylococcus aureus* on silicone rubber filled with 1.0 wt% of Silica-poly(St-$CH_2P^+(Bu)_3Cl^-$) (Two) (Grafting = 142%). It was found that the concentration of living cells decreased from 1.4×10^5 to less than 10 CFU/mL even after 3 h. The result suggests that the surface of silicone rubber filled with 1.0% of Silica-poly(St-$CH_2P^+(Bu)_3Cl^-$) (Two) effectively inhibited the proliferation of bacteria.

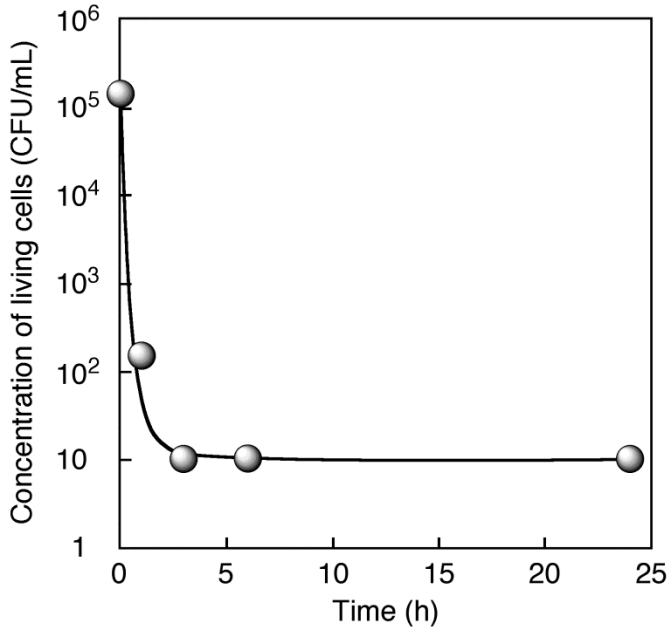

Figure 2-12. Relationship between contacting time and concentration of living cells of *Staphylococcus aureus* on the surface of silicone rubber filled with 1.0 wt% of Silica-poly(St-$CH_2P^+(Bu)_3Cl^-$) (Two) (Grafting = 142%).

2.3.6 Antibacterial activity of the surface of polystyrene film filled with Silica-poly(St-$CH_2P^+(Bu)_3Cl^-$)

Figure 2-13 shows the antibacterial activity of the surface of polystyrene film filled with 1.0 wt% of Silica-poly(St-$CH_2P^+(Bu)_3Cl^-$) (Two) (Grafting = 91%) against *Staphylococcus aureus*. It was found that the surface of polystyrene filled with Silica-poly(St-$CH_2P^+(Bu)_3Cl^-$) (Two) inhibited the proliferation of *Staphylococcus aureus*, and the living cells decreased from 4.3×10^4 to 3.3×10^2 CFU/mL. It is concluded that Silica-poly(St-$CH_2P^+(Bu)_3Cl^-$) (Two) can be applied as an antibacterial filler not only silicone rubber but also polystyrene.

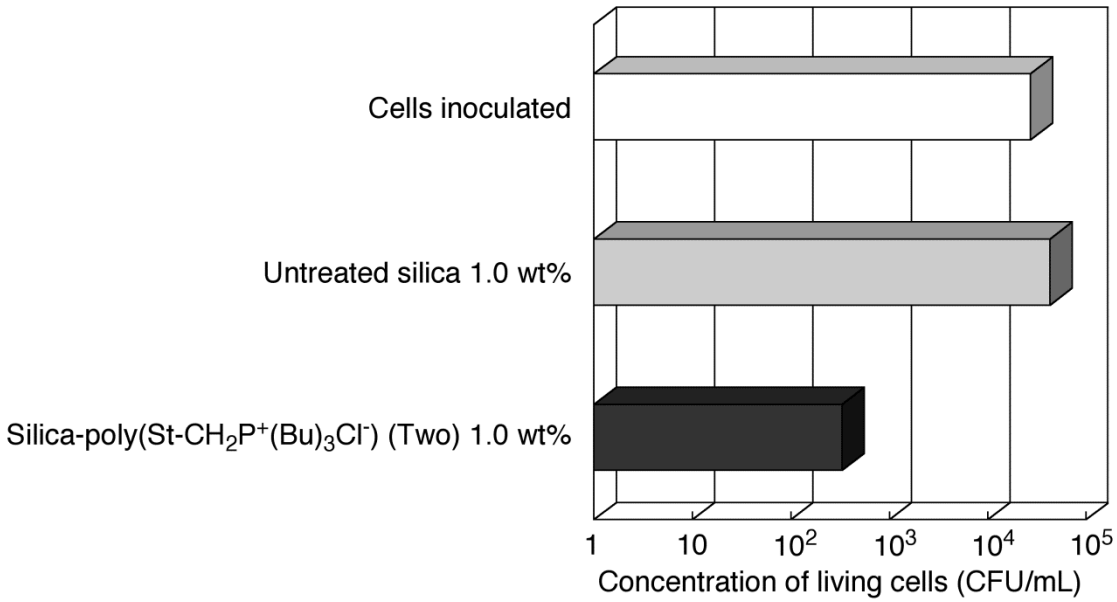

Figure 2-13. Antibacterial activity of the surface of polystyrene filled with Silica-poly(St-$CH_2P^+(Bu)_3Cl^-$) (Two) (Grafting = 91%) against *Staphylococcus aureus.*

2.3.7 Antibacterial activity of the surface of paints filled with Silica-poly(St-$CH_2P^+(Bu)_3Cl^-$)

Figure 2-14 shows the antibacterial activity of the surface of (A) water paint (acrylic emulsion type) and (B) oil paint (acrylic urethane type) filled with 2.0 wt% of Silica-poly(St-$CH_2P^+(Bu)_3Cl^-$) (Two) (Grafting = 145%) against *Escherichia coli*. It was found that the surface of water paint filled with Silica-poly(St-$CH_2P^+(Bu)_3Cl^-$) (Two) inhibited the proliferation of *Escherichia coli*, and the living cells decreased from 1.6×10^7 to 8.9×10^3 CFU/mL. In addition, it became apparent that the surface of oil paint filled with Silica-poly(St-$CH_2P^+(Bu)_3Cl^-$) (Two) also inhibited the proliferation of *Escherichia coli*.

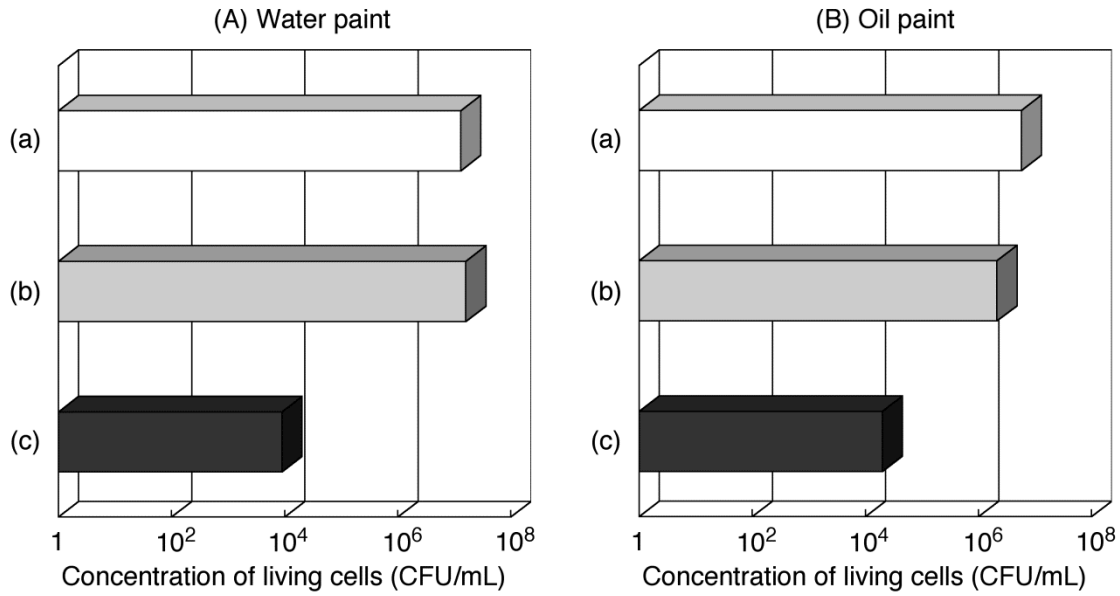

Figure 2-14. Antibacterial activity of (A) water paint (acrylic emulsion type) and (B) oil paint (acrylic urethane type) filled with Silica-poly(St-$CH_2P^+(Bu)_3Cl^-$) (Two) (Grafting = 145%) against *Escherichia coli*.
(a) cells inoculated, (b) untreated silica 2.0 wt%, and
(c) Silica-poly(St-$CH_2P^+(Bu)_3Cl^-$) (Two) 2.0 wt%.

2.3.8 Stability of antibacterial activity of the surface of silicone rubber filled with Silica-poly(St-$CH_2P^+(Bu)_3Cl^-$)

The decrease of antibacterial activity based on the elimination from silicone rubber filled with Silica-poly(St-$CH_2P^+(Bu)_3Cl^-$) (Two) by boiling in water was estimated. Figure 2-15 shows the antibacterial activity of the surface of silicone rubber filled with free poly(St-$CH_2P^+(Bu)_3Cl^-$) and Silica-poly(St-$CH_2P^+(Bu)_3Cl^-$) (Two) (Grafting = 142%) against *Escherichia coli* after boiling in water. The amount of free poly(St-$CH_2P^+(Bu)_3Cl^-$) filled into silicone rubber is exactly equal to that of grafted poly(St-$CH_2P^+(Bu)_3Cl^-$) on the silica surface.

Before the boiling in water (boiling for 0 h), the surface of silicone rubbers filled with free poly(St-$CH_2P^+(Bu)_3Cl^-$) and filled with Silica-poly(St-$CH_2P^+(Bu)_3Cl^-$) (Two) shows strong antibacterial activity. However, the antibacterial activity of the surface of silicone rubber filled with free poly(St-$CH_2P^+(Bu)_3Cl^-$) dramatically decreased even

after boiling for 1 h and lost the antibacterial activity after boiling for 24 h because of elimination of poly(St-$CH_2P^+(Bu)_3Cl^-$) from silicone rubber surface. On the contrary, the surface of silicone rubber filled with Silica-poly(St-$CH_2P^+(Bu)_3Cl^-$) (Two) was maintained antibacterial activity even after boiling for 24 h.

The results clearly show that by grafting of poly(St-$CH_2P^+(Bu)_3Cl^-$) onto silica surface, the elution of poly(St-$CH_2P^+(Bu)_3Cl^-$) from silicone rubber was completely inhibited because of an anchor effect of silica nanoparticle.

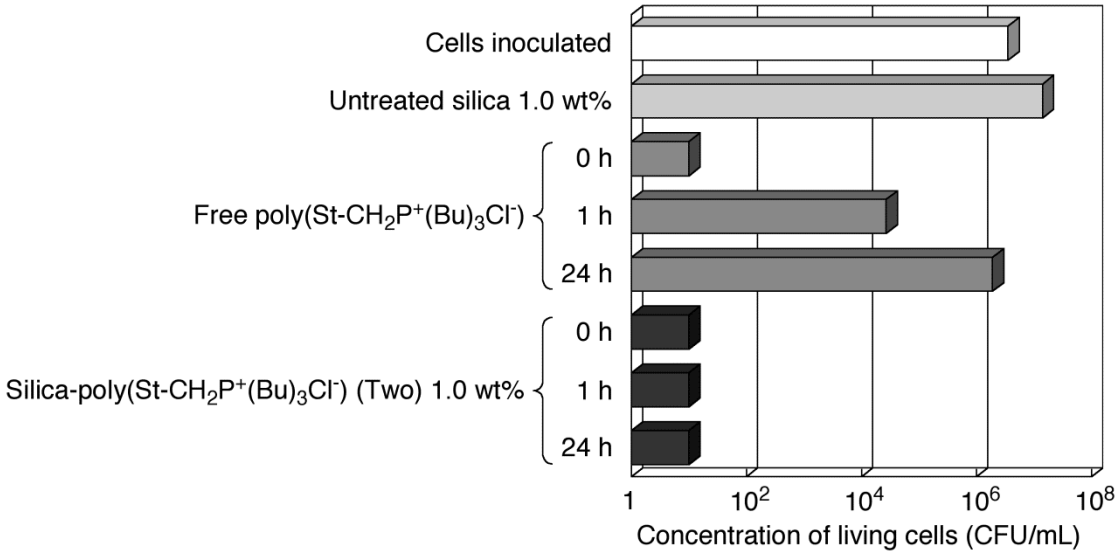

Figure 2-15. Antibacterial activity of the surface of silicone rubber filled with free poly(St-$CH_2P^+(Bu)_3Cl^-$) and Silica-poly(St-$CH_2P^+(Bu)_3Cl^-$) (Two) (Grafting = 142%) against *Escherichia coli* after boiling in water.

2.4 Conclusions

1. Antibacterial polymer, poly(St-$CH_2P^+(Bu)_3Cl^-$), was successfully grafted by two methods: one is treatment of poly(St-CH_2Cl)-grafted silica with tributylphosphine and the other is direct grafting of poly(St-$CH_2P^+(Bu)_3Cl^-$) by radical graft polymerization of the corresponding monomer.

2. The surfaces of silicone rubber, polystyrene film, and paints, filled with Silica-poly(St-$CH_2P^+(Bu)_3Cl^-$) showed strong antibacterial activity against various bacteria.

3. The surface of silicone rubber filled with Silica-poly(St-$CH_2P^+(Bu)_3Cl^-$) was maintained antibacterial activity even after boiling for 24 h in water because of an anchor effect of silica nanoparticle.

References

[1] N. Tsubokawa, Eds. J. P. Blits and C. B. Little, “Fundamental and Applied Aspects of Chemically Modified Surfaces”, The Royal Soc. Chem., CRC Press, London, p.36 (1999).

[2] N. Tsubokawa, *Bull. Chem. Soc. Jpn.* **75**, 2115-2136 (2002).

[3] N. Tsubokawa, *Polym. J.* **37**, 637-655 (2005).

[4] R. Yokoyama, S. Suzuki, K. Shirai, T. Yamauchi, N. Tsubokawa, and M. Tsuchimochi, *Eur. Polym. J.* **42**, 3221-3229 (2006).

[5] M. Ukaji, M. Takamura, K. Shirai, W. Gang, T. Yamauchi, and N. Tsubokawa, *Polym. J.* **40**, 607-613 (2008).

[6] N. Tsubokawa, *Polym. J.* **39**, 983-1000 (2007).

[7] Y. Nakagawa, N. Dohi, T. Tawaratani, and I. Shibasaki, *J. Antibact. Antifung. Agents* **11**, 263 (1983).

[8] T. Ikeda, H. Yamaguchi, and S. Tazuke, *J. Bioact. Compat. Polym*. **1**, 301-308 (1986).

[9] A. Kanazawa, T. Ikeda, and T. Endo, *J. Polm. Sci., Part A: Polym. Chem*. **31**, 335-343, 1441-1447, 1467-1472, 2873-2876, 3003-3011, 3031-3038 (1993).

[10] A. Mũnoz-Bonilla and M. Fernández-García, *Prog. Polym. Sci.* **37**, 281-339 (2012).

[11] R. Yamashita, Y. Takeuchi, H. Kikuchi, K. Shirai, T. Yamauchi, and N. Tsubokawa, *Polym. J.* **38**, 844-851 (2006).

[12] Y. Shirai and N. Tsubokawa, *React. Funct. Polym*. **32**, 153-160 (1997).

[13] G. Wei, K. Shirai, K. Fujiki, H. Saitoh, T. Yamauchi, and Norio Tsubokawa, *Carbon* **42**, 1923-1929 (2004).

[14] S. Matsuda and S. Okazaki, *Nippon Kagaku Kaishi* 1287 (1986).

[15] E. H. Brown and C. A. Krans, *J. Am. Chem. Soc.* **51**, 2690-2696 (1929).

[16] M. Murota, S. Sato, and N. Tsubokawa, *Polym. Adv. Technol.* **13**, 144-150 (2002).

[17] Japanese Industrial Standards (JIS), Antibacterial products - Test for antibacterial activity and efficacy, JIS Z 2801.

Chapter 3

Preparation and Properties of Antibacterial Polymer-grafted Silica Nanoparticles in a Solvent-free Dry-system

Abstract

The grafting of antibacterial polymer onto silica nanoparticle surface by azo-initiated radical polymerization and atom transfer radical polymerization (ATRP) in a solvent-free dry-system were investigated. Vinylbenzyl tributylphosphonium chloride (St-$CH_2P^+(Bu)_3Cl^-$) was used as antibacterial monomer. In azo-initiated radical polymerization, antibacterial polymer, poly(St-$CH_2P^+(Bu)_3Cl^-$), was successfully grafted onto silica surface by the drop-wise addition of a small amount of antibacterial monomer mixture solution onto silica nanoparticle having azo groups in solvent-free dry-system. In ATRP, antibacterial polymer was successfully grafted onto silica surface by the drop-wise addition of a small amount of mixture solution, in which antibacterial monomer and copper complex were dissolved, onto silica nanoparticle having chlorosulfonyl groups in solvent-free dry-system. In both polymerizations, it was found that the nearly equal amounts of antibacterial polymers were grafted onto silica nanoparticle surface in solvent-free dry-system and solvent system: the percentage of grafting was around 26%. The antibacterial properties of silicone rubber composites surface filled with antibacterial polymer-grafted silica against *Staphylococcus aureus* and *Escherichia coli* were also investigated. It was found that the silicone rubber composites filled with antibacterial polymer-grafted silica inhibited the proliferation of *Staphylococcus aureus* and *Escherichia coli*.

3.1 Introduction

In Chapter 2, it was described that the grafting of antibacterial polymers onto silica nanoparticle surface [1, 2]. In addition, it was described that the surface of polymer matrices filled with the antibacterial polymer-grafted silica shows strong antibacterial activity against various bacteria. The surface of silicone rubber filled with antibacterial polymer-grafted silica was maintained antibacterial activity even after boiling for 24 h in water because of an anchor effect of silica nanoparticle [2].

However, the large-scale synthesis of polymer-grafted nanoparticle was hardly achieved in solvent system, due to complicated reaction procedures, such as centrifugation, filtration, and solvent extraction, were needed for the production of polymer-grafted nanoparticle, and large amount of waste solvent comes out. In contrast, the large-scale synthesis of polymer-grafted nanoparticle can be succeeded in a solvent-free dry-system by simple reaction processes and a small amount of waste solvent.

Therefore, Murota et al. have reported the scale-up synthesis of hyperbranched poly(amidoamine)-grafted silica nanoparticle in a solvent-free dry-system by using dendrimer synthesis methodology [3]. That is, hyperbranched poly(amidoamine) was allowed to grow from silica surface by repeating two steps: (1) Michael addition of methyl acrylate to amino groups on the surface and (2) amidation of terminal ester groups with ethylenediamine. Methyl acrylate was sprayed onto silica having amino groups and the silica was agitated. After the reaction, unreacted methyl acrylate was removed under vacuum. Then, ethylenediamine was sprayed and the reaction was conducted with agitation. After the reaction, unreacted ethylenediamine was also removed under vacuum. Both these process were repeated to propagate the hyperbranched poly(amidoamine) from the silica surface in the solvent-free dry-system.

In addition, Ueda et al. have reported the radical graft polymerization of vinyl monomers onto silica nanoparticle surface initiated by azo groups on the surface in a solvent-free dry-system for the purpose of the prevention of the environmental pollution and the simplification of reaction process [4].

In recent years, surface-initiated living radical polymerization (LRP), such as atom transfer radical polymerization (ATRP), reversible addition-fragmentation chain transfer polymerization (RAFT), and nitroxide-mediated polymerization (NMP), has been rapidly developing for its excellent controllability over the molecular weight and polydispersity of the graft polymers and its capability of affording an exceptionally high graft density with the robustness and versatility of LRP retained [5-17].

The atom transfer radical polymerization (ATRP) is a powerful variant of living radical polymerization, which can be applied to a large variety of monomers [18]. ATRP relies on creation of a dynamic equilibrium between a large amount of a dormant species and a small amount of propagating radicals (Scheme 3-1) [19]. It has been reported that grafting of polymers from nanoparticles was successfully achieved by ATRP initiated by a system consisting of surface functional groups and transition metal complexes [20-24]. ATRP has been demonstrated to provide controlled polymerizations of styrenes, acrylates, and acrylonitrile with variations in composition and architecture found in block, graft, star, and hyperbranched structures [19, 25, 26].

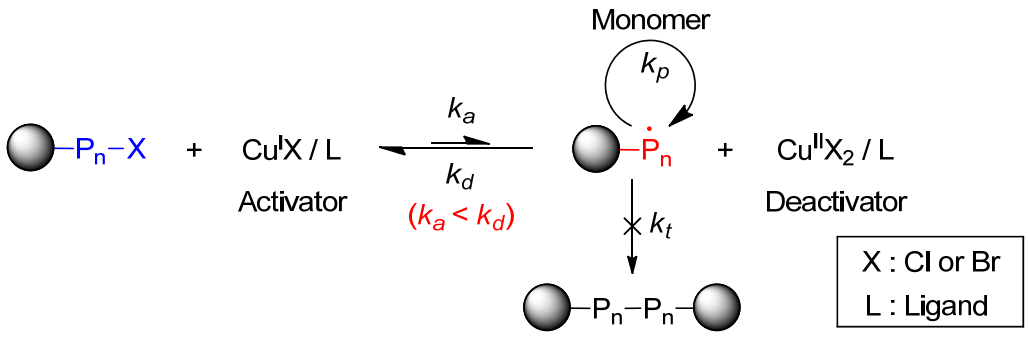

Scheme 3-1. Mechanism of ATRP.

In this chapter, for large-scale synthesis of antibacterial polymer-grafted silica, the grafting of antibacterial polymer onto silica nanoparticle surface by azo-initiated radical polymerization (Scheme 3-2) and ATRP (Scheme 3-3) in a solvent-free dry-system was investigated. Vinylbenzyl tributylphosphonium chloride (St-$CH_2P^+(Bu)_3Cl^-$) was used as antibacterial monomer. In addition, the antibacterial activity of the surfaces of silicone rubber filled with antibacterial polymer-grafted silica was evaluated.

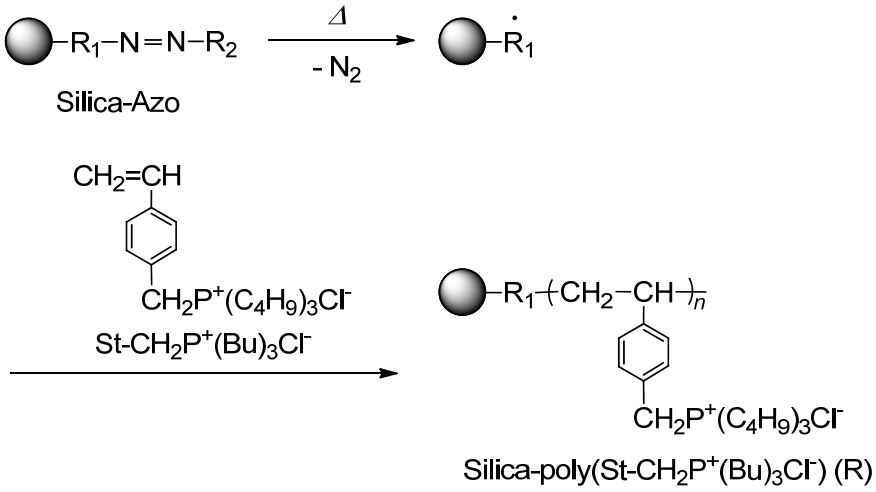

Scheme 3-2. Graft polymerization of antibacterial monomer onto silica nanoparticle surface by azo-initiated radical polymerization.

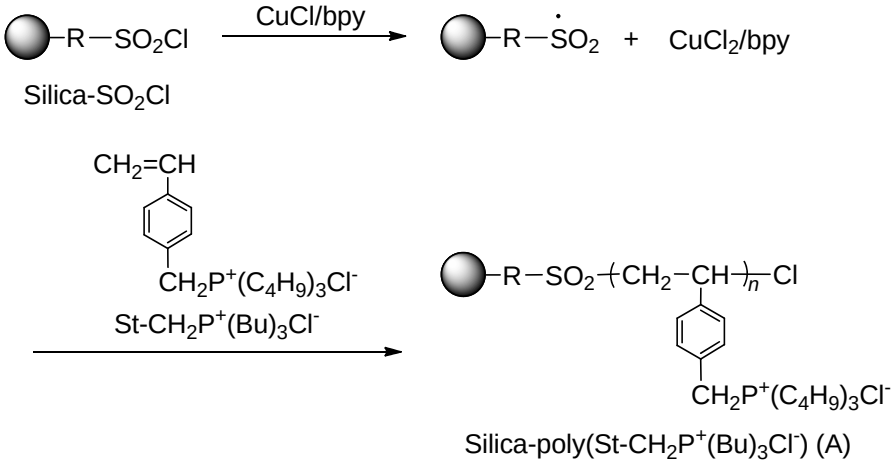

Scheme 3-3. Graft polymerization of antibacterial monomer onto silica nanoparticle surface by atom transfer radical polymerization (ATRP).

3.2 Experimental

3.2.1 Materials and reagents

Silica nanoparticle used was Aerosil 200 and it was obtained from Nippon Aerosil Co., Ltd., Japan. The specific surface area, average particle size, and silanol group content were 200 m^2/g, 12 nm, and 1.37 mmol/g, respectively. The content of silanol groups was determined by measuring volumetrically the amount of ethane evolved by the reaction with triethylaluminum [27, 28]. The silica was dried *in vacuo* at room temperature for 24 h before use.

(3-Isocyanatopropyl)triethoxysilane (IPTES) obtained from Momentive Performance Materials Inc. was used without further purification. 4,4'-Azobis(4-cyanovaleric acid) (ACVA) obtained from Wako Pure Chemical Industries, Ltd. was dried *in vacuo* at room temperature before use. 2-(4-Chlorosulfonylphenyl)ethyltrichlorosilane (CTCS), 50% in methylene chloride obtained from Gelest, Inc. was used without further purification.

4-(Chloromethyl)styrene and tributylphosphine obtained from Tokyo Chemical Industry Co., Ltd. were used without further purification. Copper(I) chloride (CuCl) obtained from Wako Pure Chemical Industries, Ltd. was purified by stirring in acetic acid, filtered and washed with ethanol and dried *in vacuo* at room temperature. 2,2’-Bipyridine (bpy) obtained from Kanto Chemical Co., Inc. was used without further purification. 1-Propanol, 2-butanone, dehydrated toluene, and dehydrated tetrahydrofuran (THF) were obtained from Kanto Chemical Co., Inc. and used without further purification.

Silicone rubber (two-component type) was obtained from Shin-Etsu Chemical Co., Ltd.

3.2.2 Synthesis of antibacterial monomer

Antibacterial monomer, vinylbenzyl tributylphosphonium chloride ($St\text{-}CH_2P^+(Bu)_3Cl^-$), was prepared by the reaction of chlorometyl styrene ($St\text{-}CH_2Cl$) with tributylphosphine according to the method of literature [29]. Detailed methods are shown in the Chapter 2 (Section 2.2.3).

3.2.3 Radical graft polymerization of antibacterial monomer initiated by azo groups introduced onto silica nanoparticle surface in a solvent-free dry-system

3.2.3.1 Introduction of azo groups onto silica nanoparticle surface

The introduction of azo groups onto silica nanoparticle surface was achieved by the two-step reaction in a solvent-free dry-system as shown in Scheme 3-5. The first is introduction of isocyanate groups onto the silica surface by the treatment of surface silanol groups with IPTES. The second is introduction of azo groups onto the silica surface by the reaction of surface isocyanate groups with ACVA. A typical example was as follows. Into a 200 mL four-necked flask, 10.0 g of silica nanoparticle was added and the atmosphere was exchanged for argon. 3.4 mL of IPTES and 10 mL of toluene mixture solution was dropped by a syringe into the flask under argon. The mixture was agitated at 75 rpm at 110 °C for 20 h under argon. After the reaction, unreacted IPTES and toluene were removed under high vacuum at 30 °C for 4 h. Then, 1.9 g of ACVA and 7.0 mL of THF mixture solution was dropped by a syringe into the flask under argon. The mixture was agitated at 75 rpm at 30 °C for 20 h under argon. After the reaction, THF was removed under high vacuum at 30 °C for 4 h. The resulting silica was dispersed in methanol and the dispersion was centrifuged. The silica was washed three times with methanol and three times with acetone. Then, the resulting silica was stored in cold dark place. The silica having azo groups was abbreviated as Silica-Azo.

3.2.3.2 Radical graft polymerization of antibacterial monomer initiated by azo groups introduced onto silica nanoparticle surface in a solvent-free dry-system

The radical graft polymerization of antibacterial monomer, St-$CH_2P^+(Bu)_3Cl^-$, initiated by azo groups introduced onto silica surface was carried out in a solvent-free dry-system as shown in Scheme 3-2. A typical example was as follows. Into a 200 mL four-necked flask, 2.0 g of unpurified Silica-Azo was added and the atmosphere was exchanged for argon. 1.0 g of St-$CH_2P^+(Bu)_3Cl^-$ and 2.0 mL of 1-propanol mixture solution was dropped by a syringe into the flask under argon. The mixture was agitated at 75 rpm at 70 °C for 20 h under argon. After the reaction, the resulting silica was dispersed in acetone and the dispersion was centrifuged. The silica was washed three times with methanol and three times with acetone. Then, the purified silica was stored *in vacuo* at room temperature. The resulting silica was abbreviated as Silica-poly(St-$CH_2P^+(Bu)_3Cl^-$) (R).

3.2.4 Graft polymerization of antibacterial monomer onto silica nanoparticle surface by ATRP in a solvent-free dry-system

3.2.4.1 Introduction of chlorosulfonyl groups onto silica nanoparticle surface

The introduction of chlorosulfonyl groups onto silica nanoparticle surface was achieved by the treatment of surface silanol groups with CTCS in a solvent-free dry-system as shown in Scheme 3-6. A typical example was as follows. Into a 200 mL four-necked flask, 5.0 g of silica nanoparticle was added and the atmosphere was exchanged for argon. 5.0 mL of CTCS solution was dropped by a syringe into the flask under argon. The mixture was agitated at 75 rpm at 110 °C for 20 h under argon. After the reaction, unreacted CTCS was removed under high vacuum at 50 °C for 4 h. The resulting silica was dispersed in THF and the dispersion was centrifuged. The silica was washed four times with THF. Then, the resulting silica was stored *in vacuo* at room temperature. The silica having chlorosulfonyl groups was abbreviated as Silica-SO_2Cl.

3.2.4.2 Graft polymerization of antibacterial monomer onto silica nanoparticle surface by ATRP in a solvent-free dry-system

The graft polymerization of antibacterial monomer onto silica surface was carried out by ATRP in a solvent-free dry-system as shown in Scheme 3-3. A typical example was as follows. Into a 200 mL four-necked flask, unpurified Silica-SO_2Cl was added and the atmosphere was exchanged for argon. 1.0 g of St-$CH_2P^+(Bu)_3Cl^-$, 0.395 g (4.0 mmol) of CuCl, and 1.874 g (12.0 mmol) of 2,2'-bipyridine (bpy), and 2.0 mL of 2-butanone mixture solution was dropped by a syringe into the flask under argon ([SO_2Cl group]:[CuCl]:[bpy] = 1:1:3). The mixture was agitated at 75 rpm at 50 °C for 20 h under argon. After the reaction, the resulting silica was dispersed in EDTA-2Na aqueous solution: acetic acid buffer solution (pH 4.0) (1:1, v/v) and the dispersion was centrifuged. The silica was washed once with EDTA-2Na aqueous solution: acetic acid buffer solution (pH 4.0) (1:1, v/v), twice with water, once with 3.0 mol/L HCl aqueous solution, twice with water, twice with methanol, and twice with THF. Then, the purified silica was stored *in vacuo* at room temperature. The resulting silica was abbreviated as Silica-poly(St-$CH_2P^+(Bu)_3Cl^-$) (A).

3.2.5 Determination of percentage of grafting

The percentage of antibacterial polymer grafting was determined by the following equations:

$$\text{Grafting (\%)} = (A / B) \times 100$$

where A is weight of polymer grafted onto silica surface and B is weight of silica used. The former value was determined by measuring the weight loss when polymer-grafted silica was heated at 900 °C by use of a thermogravimetric analyzer (TGA) under air.

3.2.6 Measurements

Thermogravimetric analysis (TGA) was performed under air flow using a thermogravimetric analyzer (Shimadzu Co., TGA-50) at a heating rate of 10 °C/min. Infrared spectrum was recorded on a FT-IR spectrophotometer (Shimadzu Co., FTIR-8400S). Thermal decomposition gas chromatograms and mass spectra (GC-MS) were recorded on a gas chromatograph mass spectrometer (Shimadzu Co., GCMS-QP2010) equipped with a double shot pyrolyzer (Frontier Laboratories Ltd., PY-2020D). The column was programmed from 70 to 320 °C at a heating rate of 20 °C/min and then held at 320 °C for 5 min. Elemental analysis was recorded on an Organic Elemental Analyzer (PerkinElmer Co., Ltd., 2400II Automatic elemental analyzer (CHNS/O)).

3.2.7 Preparation of composites filled with antibacterial polymer-grafted silica

Silicone rubber filled with antibacterial polymer-grafted silica was prepared by a two-component type silicone rubber. Antibacterial polymer-grafted silica was uniformly dispersed in poly(dimethylsiloxane) using a planetary centrifugal mixer (Thinky Co., AR-100) at room temperature. Then, containing a curing agent was added into the mixture, and the mixture was uniformly mixed by the mixer. After the mixing, the mixture was poured into a Teflon mold. By heating the mixture at 70 °C for 6 h, silicone rubber filled with antibacterial polymer-grafted silica was obtained. Size of sample was 50 mm × 50 mm × 1 mm.

3.2.8 Assessment of antibacterial activity of the composite surfaces

The surface antibacterial activity of the silicone rubber filled with antibacterial polymer-grafted silica was estimated according to the method of the Japanese Industrial Standards (JIS Z 2801) [30]. Detailed methods are shown in the Chapter 2 (Section 2.2.10).

3.3 Results and Discussion

3.3.1 Synthesis of antibacterial monomer

The synthesis of antibacterial monomer, vinylbenzyl tributylphosphonium chloride (St-$CH_2P^+(Bu)_3Cl^-$), was carried out by the reaction of chlorometyl styrene (St-CH_2Cl) with tributylphosphine according to the Chapter 2 (Section 2.3.1).

3.3.2 Radical graft polymerization of antibacterial monomer initiated by azo groups introduced onto silica nanoparticle surface in a solvent-free dry-system

3.3.2.1 Introduction of azo groups onto silica nanoparticle surface

The introduction of azo groups onto silica surface as initiating sites for radical graft polymerization was successfully achieved by the reaction of ACVA with isocyanate groups introduced silica, which was prepared by the treatment of IPTES with silanol groups on the silica surface in a solvent-free dry-system (Scheme 3-4). The content of azo groups introduced onto silica surface was determined to be 0.21 mmol/g by elemental analysis.

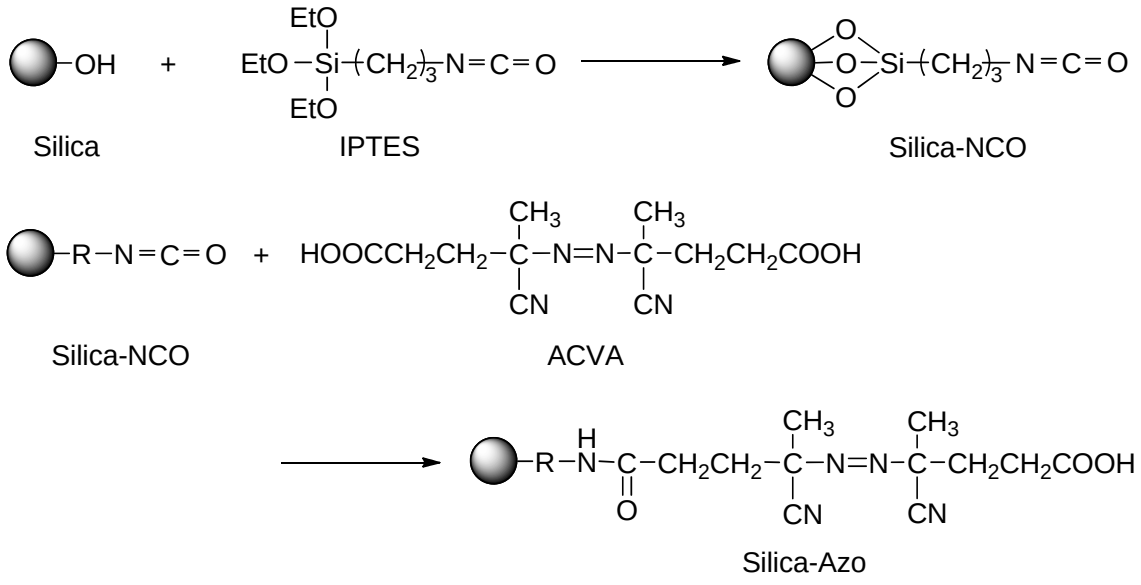

Scheme 3-4. Introduction of azo groups onto silica nanoparticle surface.

3.3.2.2 Radical graft polymerization of antibacterial monomer initiated by azo groups introduced onto silica nanoparticle surface in a solvent-free dry-system

The radical graft polymerization of antibacterial monomer, St-$CH_2P^+(Bu)_3Cl^-$, initiated by azo groups introduced onto the silica nanoparticle surface in a solvent-free dry-system was investigated as shown in Scheme 3-2. The radical graft polymerization of St-$CH_2P^+(Bu)_3Cl^-$ was successfully initiated by azo groups introduced onto the silica surface in a solvent-free dry-system. The St-$CH_2P^+(Bu)_3Cl^-$ grafting reached to 26.4% at 70 °C after 20 h.

Figure 3-1 shows FT-IR spectra of (a) Silica-Azo, (b) Silica-poly(St-$CH_2P^+(Bu)_3Cl^-$) (R), and (c) St-$CH_2P^+(Bu)_3Cl^-$ monomer. The spectrum of Silica-poly(St-$CH_2P^+(Bu)_3Cl^-$) (R) show a new absorption at 1460 cm^{-1}, which is characteristic of phosphonium salt attached to the butyl group [31]. In addition, absorption at 2930 cm^{-1} is characteristic of methylene groups of St-$CH_2P^+(Bu)_3Cl^-$. Therefore, it is confirmed that poly(St-$CH_2P^+(Bu)_3Cl^-$) was successfully grafted onto the silica surface.

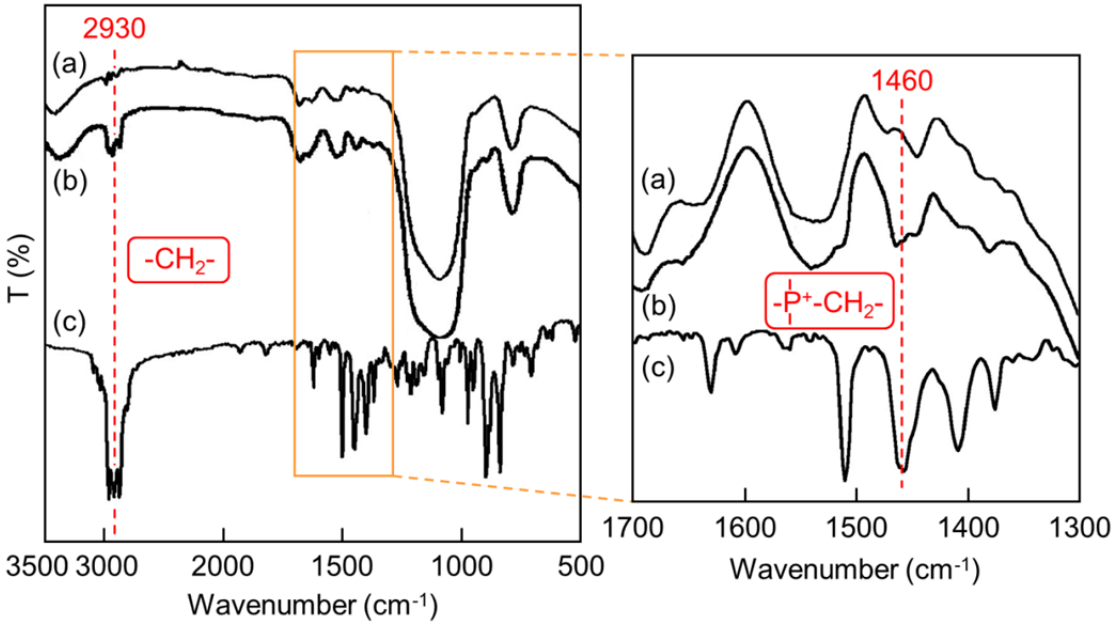

Figure 3-1. FT-IR spectra of (a) Silica-Azo, (b) Silica-poly(St-$CH_2P^+(Bu)_3Cl^-$) (R), and (c) St-$CH_2P^+(Bu)_3Cl^-$.

Gas chromatograms of thermal decomposed gas of (a) St-$CH_2P^+(Bu)_3Cl^-$ monomer and (b) Silica-poly(St-$CH_2P^+(Bu)_3Cl^-$) (R) are shown in Figure 3-2. In comparison with these chromatograms, the thermal decomposition gas of Silica-poly(St-$CH_2P^+(Bu)_3Cl^-$) (R) at retention time 5.1 min was similar to that of St-$CH_2P^+(Bu)_3Cl^-$. In addition, as shown in Figure 3-3, the mass spectrum of decomposed gas of Silica-poly(St-$CH_2P^+(Bu)_3Cl^-$) (R) at retention time 5.1 min was in agreement with that of St-$CH_2P^+(Bu)_3Cl^-$. Figure 3-3 also shows that Silica-poly(St-$CH_2P^+(Bu)_3Cl^-$) (R) was decomposed to produce fragments of tributylphosphine. These results clearly show that poly(St-$CH_2P^+(Bu)_3Cl^-$) was successfully grafted onto the silica surface initiated by azo groups introduced onto the silica surface in a solvent-free dry-system.

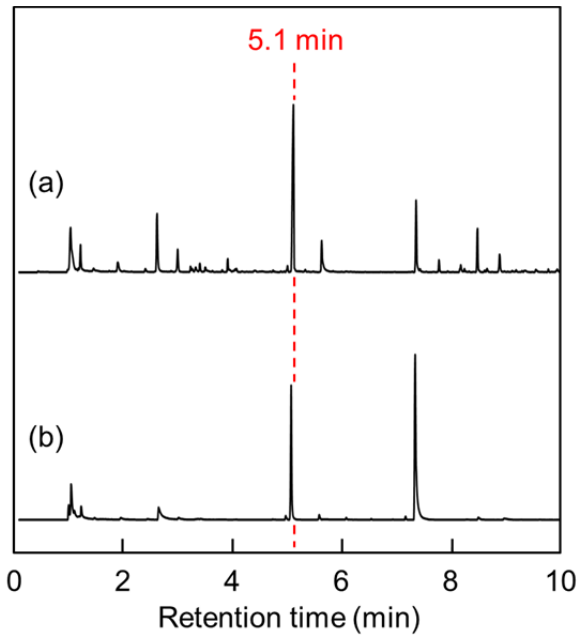

Figure 3-2. Gas chromatograms of thermal decomposed gas of (a) St-$CH_2P^+(Bu)_3Cl^-$ and (b) Silica-poly(St-$CH_2P^+(Bu)_3Cl^-$) (R).

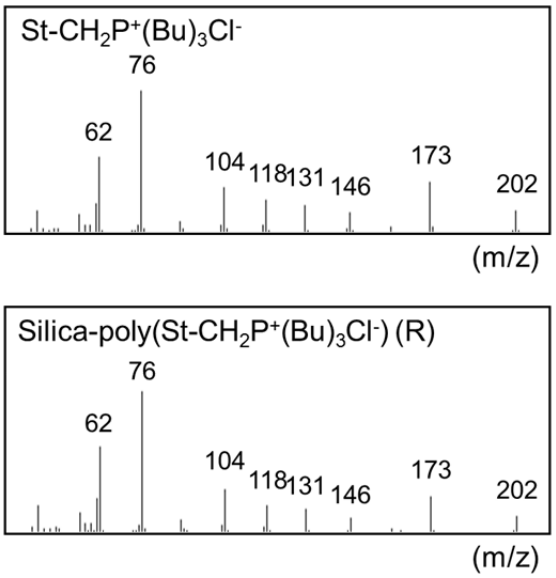

Figure 3-3. Mass spectra of thermal decomposed gas of St-$CH_2P^+(Bu)_3Cl^-$ and Silica-poly(St-$CH_2P^+(Bu)_3Cl^-$) (R) of retention time at 5.1 min.

To investigate the effect of the feed amount of monomer on the grafting of antibacterial polymer onto silica nanoparticle surface, feed amount of antibacterial monomers were changed. Figure 3-4 shows the relationship between monomer in feed and the grafting of antibacterial polymer onto the silica surface. It was found that the grafting of poly(St-$CH_2P^+(Bu)_3Cl^-$) was increased with increasing St-$CH_2P^+(Bu)_3Cl^-$ in feed.

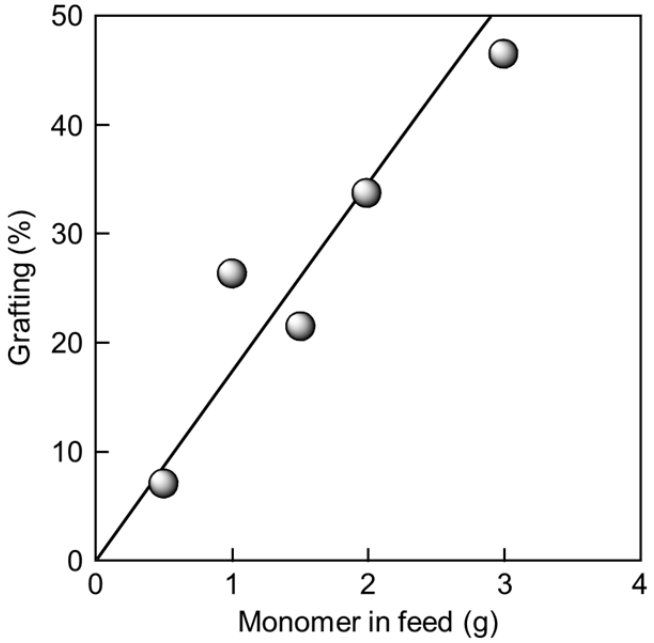

Figure 3-4. Relationship between monomer in feed and the grafting of antibacterial polymer onto silica nanoparticle surface.
Silica-Azo, 2.66 g; 1-propanol, 2.0 mL; 70 °C, 20 h.

3.3.2.3 Comparison of grafting in a solvent-free dry-system with that in a solvent system

To investigate the effect of solvent-free dry-system on the grafting of antibacterial polymer onto silica nanoparticle surface, the grafting percentage of antibacterial polymer-grafted silica prepared in a solvent-free dry-system were compared with that in a solvent system.

Table 3-1 shows the comparison of solvent-free dry-system with solvent system on

grafting of antibacterial polymer onto silica nanoparticle surface by azo-initiated radical polymerization. It was found that nearly equal amount of antibacterial polymer was grafted onto the silica surface in the both system. The result suggests that the preparation of antibacterial polymer-grafted silica initiated by azo groups introduced onto the silica surface in a solvent-free dry-system was more efficient than that in a solvent system.

Table 3-1. Comparison of solvent-free dry-system with solvent system on grafting of antibacterial polymers onto silica nanoparticle surface.

	Grafting (%)
Solvent-free dry-system [1)]	26.4
Solvent system [2)]	26.2

[1)] Silica, 2.0 g; azo group, 0.21 mmol/g; antibacterial monomer, 1.0 g; 1-propanol, 2.0 mL; 70 ºC, 20 h.
[2)] Silica, 0.1 g; azo group, 0.21 mmol/g; antibacterial monomer, 2.0 g; 1-propanol, 20 mL; 70 ºC, 20 h.

3.3.3 Graft polymerization of antibacterial monomer onto silica nanoparticle surface by ATRP in a solvent-free dry-system

3.3.3.1 Introduction of chlorosulfonyl groups onto silica nanoparticle surface

The introduction of chlorosulfonyl groups onto silica surface as initiating sites for ATRP was achieved by the treatment of CTCS with silanol groups on the silica surface as shown in Scheme 3-5. The content of chlorosulfonyl groups introduced onto silica surface was 0.84 mmol/g by thermogravimetric analysis.

Figure 3-5 shows FT-IR spectra of Silica-SO_2Cl and untreated silica. The spectrum of Silica-SO_2Cl shows a new absorption at 1380 cm^{-1}, which is characteristic of S=O stretching of CTCS [8]. This result suggests that chlorosulfonyl groups were introduced onto silica nanoparticle surface.

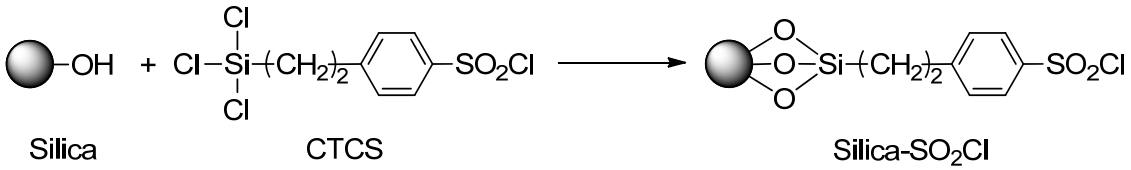

Scheme 3-5. Introduction of chlorosulfonyl groups onto silica nanoparticle surface.

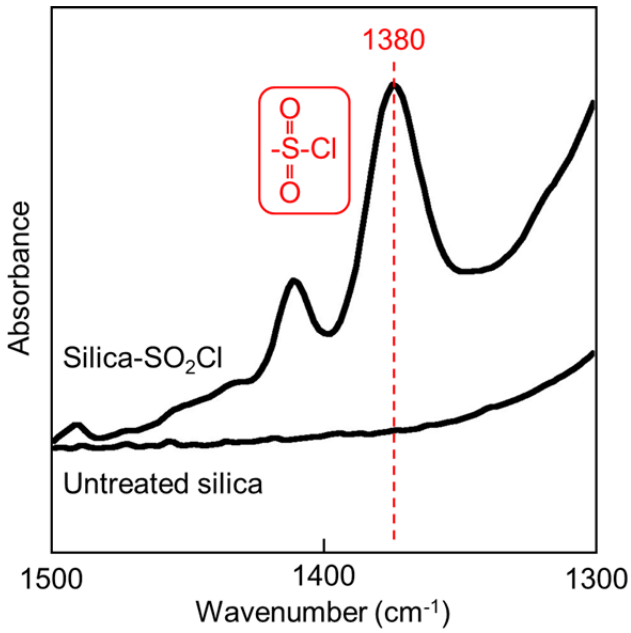

Figure 3-5. FT-IR spectra of Silica-SO_2Cl and untreated silica.

3.3.3.2 Graft polymerization of antibacterial monomer onto silica nanoparticle surface by ATRP in a solvent-free dry-system

The surface initiated ATRP of antibacterial monomer, St-$CH_2P^+(Bu)_3Cl^-$, onto silica nanoparticle surface was achieved by use of the initiating system consisting of Silica-SO_2Cl and CuCl/bpy as shown in Scheme 3-3.

Figure 3-6 shows FT-IR spectra of (a) Silica-SO_2Cl, (b) Silica-poly(St-$CH_2P^+(Bu)_3Cl^-$) (A), and (c) St-$CH_2P^+(Bu)_3Cl^-$ monomer. The spectrum of Silica-poly(St-$CH_2P^+(Bu)_3Cl^-$) (A) shows a new absorption at 1460 cm^{-1}, which is characteristic of phosphonium salt attached to the butyl group [31]. In addition, absorption at 2930 cm^{-1} is characteristic of methylene groups of St-$CH_2P^+(Bu)_3Cl^-$.

Therefore, it is confirmed that poly(St-$CH_2P^+(Bu)_3Cl^-$) was successfully grafted onto the silica surface.

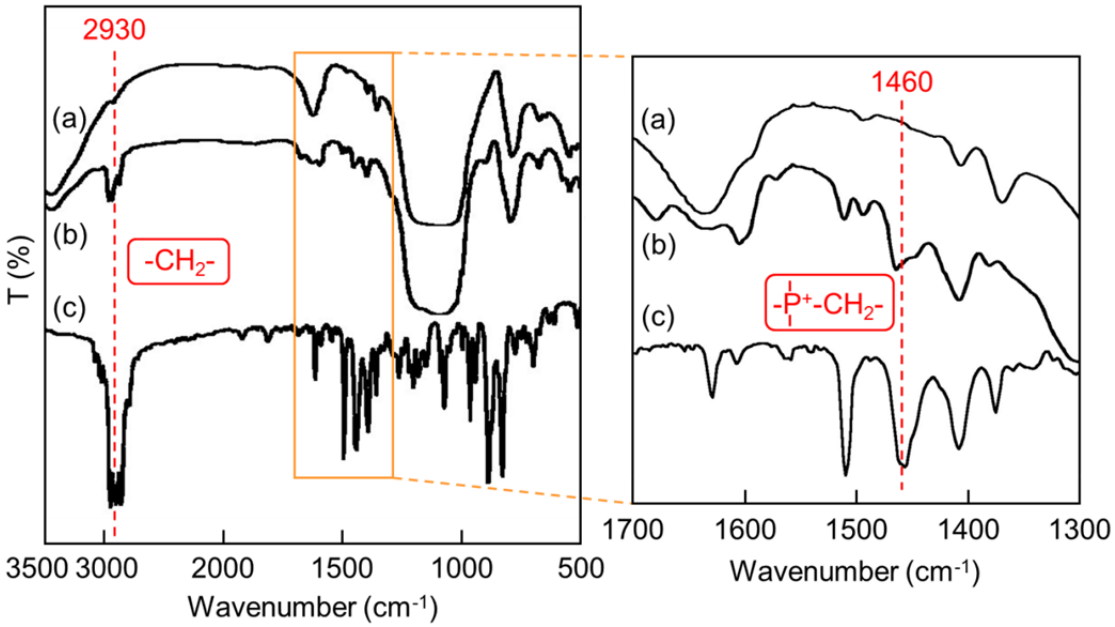

Figure 3-6. FT-IR spectra of (a) Silica-SO_2Cl, (b) Silica-poly(St-$CH_2P^+(Bu)_3Cl^-$) (A), and (c) St-$CH_2P^+(Bu)_3Cl^-$.

Gas chromatograms of thermal decomposed gas of (a) St-$CH_2P^+(Bu)_3Cl^-$ monomer and (b) Silica-poly(St-$CH_2P^+(Bu)_3Cl^-$) (A) are shown in Figure 3-7. In comparison with these chromatograms, the thermal decomposition gas of Silica-poly(St-$CH_2P^+(Bu)_3Cl^-$) (A) at retention time 5.1 min was similar to that of St-$CH_2P^+(Bu)_3Cl^-$. In addition, as shown in Figure 3-8, the mass spectrum of decomposed gas of Silica-poly(St-$CH_2P^+(Bu)_3Cl^-$) (A) at retention time 5.1 min was in agreement with that of St-$CH_2P^+(Bu)_3Cl^-$. Figure 3-8 also shows that Silica-poly(St-$CH_2P^+(Bu)_3Cl^-$) (A) was decomposed to produce fragments of tributylphosphine. Based on the above results, it is concluded that poly(St-$CH_2P^+(Bu)_3Cl^-$) was successfully grafted onto the silica surface by ATRP in a solvent-free dry-system.

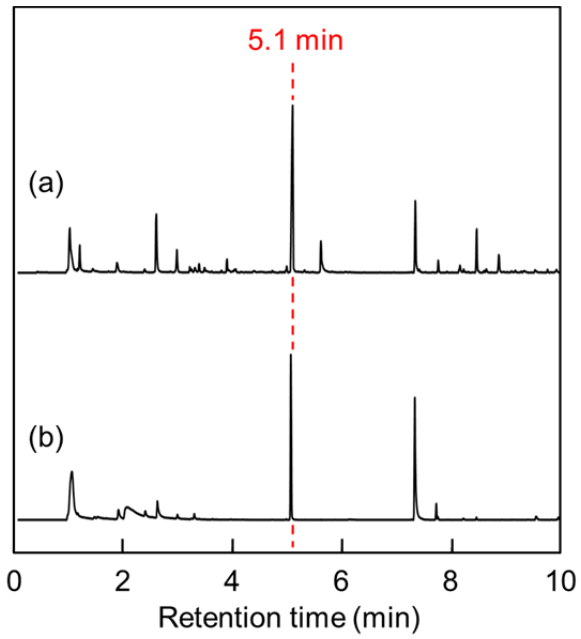

Figure 3-7. Gas chromatograms of thermal decomposed gas of (a) St-$CH_2P^+(Bu)_3Cl^-$ and (b) Silica-poly(St-$CH_2P^+(Bu)_3Cl^-$) (A).

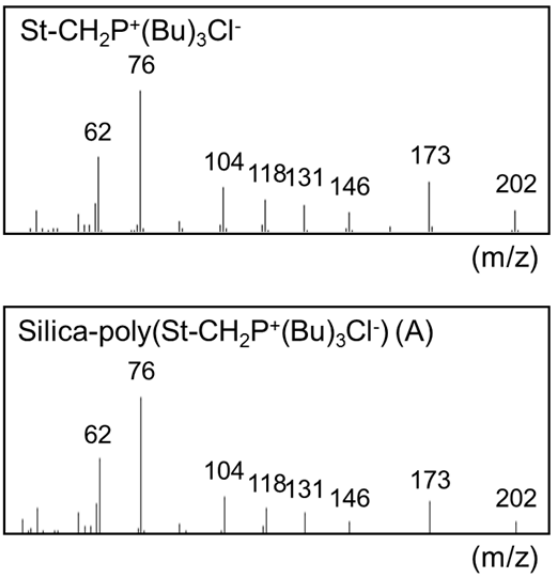

Figure 3-8. Mass spectra of thermal decomposed gas of St-$CH_2P^+(Bu)_3Cl^-$ and Silica-poly(St-$CH_2P^+(Bu)_3Cl^-$) (A) of retention time at 5.1 min.

To investigate the effect of reaction conditions on the grafting of antibacterial polymer onto silica nanoparticle surface, CuCl in feed, temperature, amount of SO_2Cl group content of silica nanoparticle, and monomer in feed were changed.

Figure 3-9 shows the effect of molar ratio of CuCl to initiating groups, chlorosulfonyl groups, on the graft polymerization of St-$CH_2P^+(Bu)_3Cl^-$ onto silica nanoparticle surface during the ATRP of St-$CH_2P^+(Bu)_3Cl^-$ initiated by the system consisting of Silica-SO_2Cl and copper complex in solvent-free dry-system. The molar ratio of CuCl to SO_2Cl groups (CuCl / SO_2Cl) was changed from 0 to 1.5. No polymerization of St-$CH_2P^+(Bu)_3Cl^-$ was initiated by the system consisting of only Silica-SO_2Cl. On the contrary, the graft polymerization of St-$CH_2P^+(Bu)_3Cl^-$ was successfully initiated by the system consisting of Silica-SO_2Cl and copper complex. As shown in Figure 3-9, the percentage of poly(St-$CH_2P^+(Bu)_3Cl^-$) grafting onto the silica surface increased with increasing in molar ratio and reached to 22% at molar ratio CuCl / SO_2Cl = 1 (mol/mol).

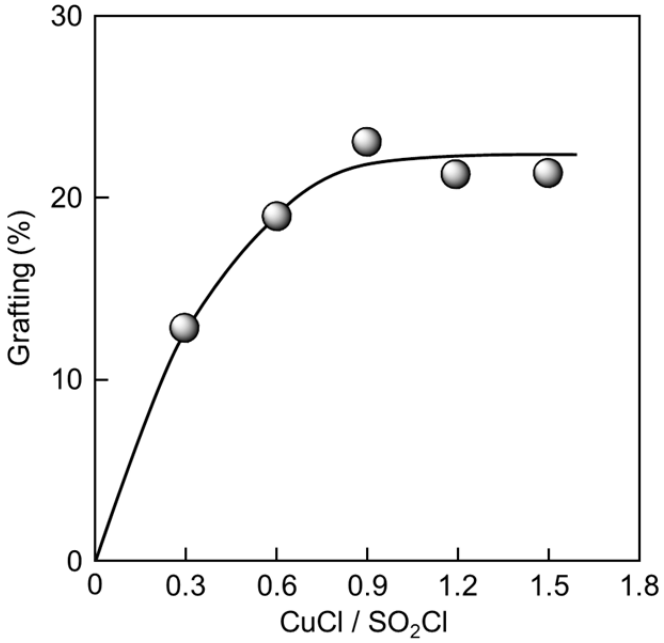

Figure 3-9. Relationship between the amount of CuCl and the grafting of antibacterial polymer onto silica nanoparticle surface.
Silica-SO_2Cl, 2.66 g; St-$CH_2P^+(Bu)_3Cl^-$, 1.0 g; 2-butanone, 2 mL;
[CuCl]:[bpy] = 1:3; 40 °C, 20 h.

Figure 3-10 shows the relationship between reaction temperature and percentage of grafting of poly(St-$CH_2P^+(Bu)_3Cl^-$) onto the silica surface. The percentage of poly(St-$CH_2P^+(Bu)_3Cl^-$) grafting onto the silica surface increased with increasing reaction temperature and reached to 31% at 50 °C.

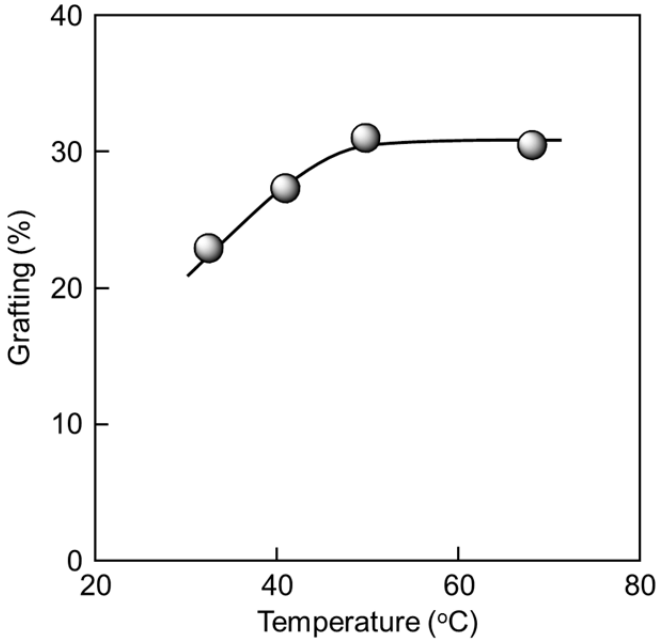

Figure 3-10. Relationship between reaction temperature and the grafting of antibacterial polymer onto silica nanoparticle surface.
Silica-SO_2Cl, 2.66 g; St-$CH_2P^+(Bu)_3Cl^-$, 1.0 g; 2-butanone, 2 mL; [SO_2Cl group]:[CuCl]:[bpy] = 1:1:3; 20 h.

Figure 3-11 shows the relationship between chlorosulfonyl group content on the silica and percentage of grafting of poly(St-$CH_2P^+(Bu)_3Cl^-$) onto the silica surface. It was found that the grafting of poly(St-$CH_2P^+(Bu)_3Cl^-$) was increased with increasing chlorosulfonyl group content of silica nanoparticle.

Figure 3-12 shows the relationship between monomer in feed and the grafting of poly(St-$CH_2P^+(Bu)_3Cl^-$) onto the silica surface. It was found that the grafting of poly(St-$CH_2P^+(Bu)_3Cl^-$) was no longer increased when monomer in feed exceeded 1.0 g.

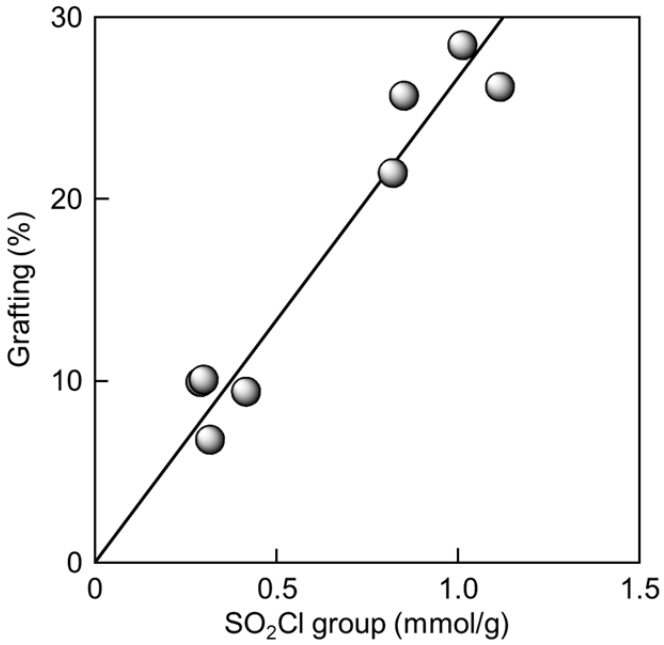

Figure 3-11. Relationship between chlorosulfonyl group content on the silica and the grafting of antibacterial polymer onto silica nanoparticle surface.
Silica, 2.0 g; St-$CH_2P^+(Bu)_3Cl^-$, 1.0 g; 2-butanone, 2.0 mL;
[SO_2Cl group]:[CuCl]:[bpy] = 1:1:3; 50 °C, 20 h.

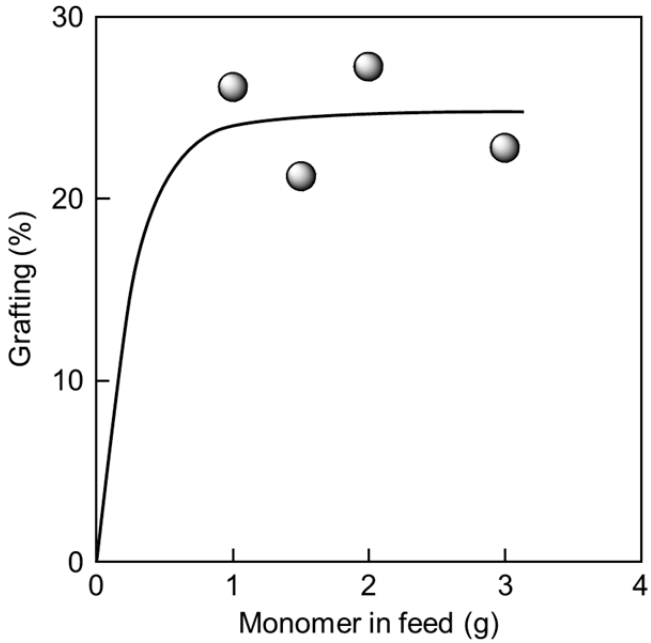

Figure 3-12. Relationship between monomer in feed and the grafting of antibacterial polymer onto silica nanoparticle surface.
Silica-SO_2Cl, 2.7 g; 2-butanone, 2.0 mL;
[SO_2Cl group]:[CuCl]:[bpy] = 1:1:3; 50 °C, 20 h.

3.3.3.3 Comparison of grafting in a solvent-free dry-system with that in a solvent system

To investigate the effect of solvent-free dry-system on the grafting of antibacterial polymer onto silica nanoparticle surface, the grafting percentage of antibacterial polymer-grafted silica prepared in a solvent-free dry-system were compared with that in a solvent system.

Table 3-2 shows the comparison of solvent-free dry-system with solvent system on grafting of antibacterial polymer onto silica nanoparticle surface by ATRP. It was found that nearly equal amount of antibacterial polymer was grafted onto the silica surface in the both system. The result suggests that the preparation of antibacterial polymer-grafted silica initiated by ATRP in a solvent-free dry-system was more efficient than that in a solvent system.

Table 3-2. Comparison of solvent-free dry-system with solvent system on grafting of antibacterial polymers onto silica nanoparticle surface.

	Grafting (%)
Solvent-free dry-system [1)]	26.2
Solvent system [2)]	25.1

[1)] Silica, 2.0 g; SO_2Cl group, 1.12 mmol/g; antibacterial monomer, 1.0 g; 2-butanone, 2.0 mL; [SO_2Cl]:[CuCl]:[bpy] = 1:1:3; 50 ºC, 20 h.
[2)] Silica, 0.2 g; SO_2Cl group, 1.12 mmol/g; antibacterial monomer, 1.0 g; 2-butanone, 10 mL; [SO_2Cl]:[CuCl]:[bpy] = 1:1:3; 50 ºC, 20 h.

3.3.3.4 Chain-extension graft polymerization of antibacterial polymer-grafted silica prepared by ATRP in a solvent-free dry-system

The chain-extension graft polymerization by ATRP in a solvent-free dry-system was investigated.

The chain-extension graft polymerization of Antibacterial polymer-grafted silica prepared by ATRP was carried out in a solvent-free dry-system by use of the initiating

system consisting of Silica-poly(St-$CH_2P^+(Bu)_3Cl^-$) (A) and CuCl/bpy as shown in Scheme 3-6.

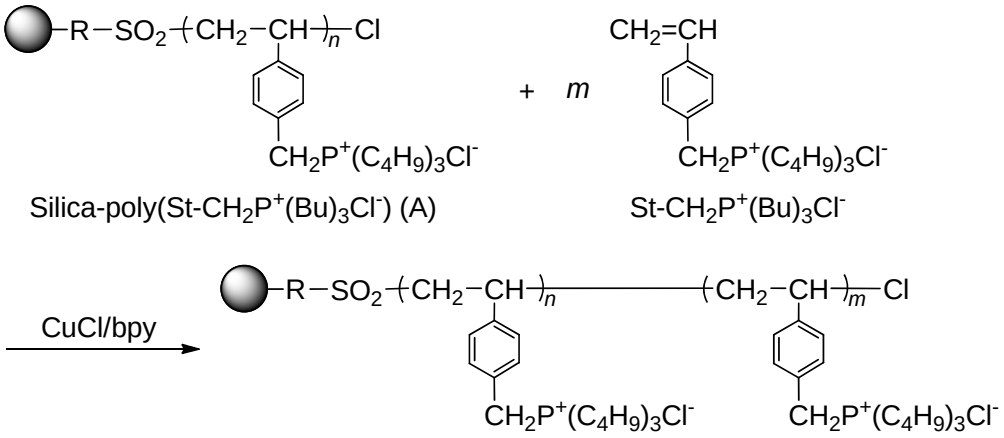

Scheme 3-6. Chain-extension graft polymerization of Silica-poly(St-$CH_2P^+(Bu)_3Cl^-$) (A) in a solvent-free dry-system.

Figure 3-13 shows result of chain-extension graft polymerization of Silica-poly(St-$CH_2P^+(Bu)_3Cl^-$) (A) by ATRP in solvent-free dry-system. It was found that the grafting of poly(St-$CH_2P^+(Bu)_3Cl^-$) was no longer increased with additional monomer at the each reaction conditions.

The result of Figure 3-12 and Figure 3-13 may be suggest that the grafting percentage of poly(St-$CH_2P^+(Bu)_3Cl^-$) by use of the initiating system consisting of Silica-SO_2Cl and CuCl/bpy in solvent-free dry-system was reached upper value. This may be due to the fact that antibacterial monomer, St-$CH_2P^+(Bu)_3Cl^-$, has bulky side group.

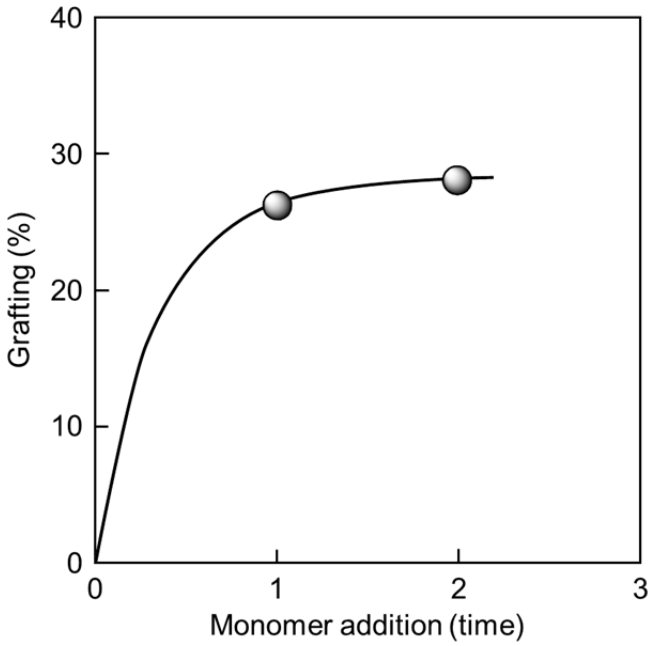

Figure 3-13. Relationship between number of monomer addition and the grafting of antibacterial polymer onto silica nanoparticle surface.
Silica, 3.0 g; St-$CH_2P^+(Bu)_3Cl^-$, 1.5 g; 2-butanone, 3.0 mL;
[SO_2Cl group]:[CuCl]:[bpy] = 1:1:3; 50 °C, 1 cycle, 20 h.

3.3.4 Estimation of antibacterial activity of silicone rubber composite filled with antibacterial polymer-grafted silica

The effect of silicone rubber composite filled with antibacterial polymer-grafted silica on the antibacterial activity against various bacteria was investigated.

Figure 3-14 and Figure 3-15 show the antibacterial activity of silicone rubber composites surface filled with 1.0 wt% of Silica-poly(St-$CH_2P^+(Bu)_3Cl^-$) (R) (Grafting = 26%) against *Staphylococcus aureus* and *Escherichia coli*, respectively.

It was found that cells of *Staphylococcus aureus* on unfilled silicone rubber (control) shows decreased from 9.7×10^5 to 1.5×10^5 CFU/mL after 24 h incubation. On the contrary, cells of *Staphylococcus aureus* on silicone rubber filled with 1.0 wt% of Silica-poly(St-$CH_2P^+(Bu)_3Cl^-$) (R) decreased from 9.7×10^5 to 70 CFU/mL after 24 h incubation (Figure 3-14). Even the surface of silicone rubber filled with 1.0 wt% of Silica-poly(St-$CH_2P^+(Bu)_3Cl^-$) (R) shows antibacterial activity. Figure 3-15 clearly

shows that the surface of silicone rubber filled with 1.0 wt% of Silica-poly(St-$CH_2P^+(Bu)_3Cl^-$) (R) also shows antibacterial activity to *Escherichia coli*.

The result suggests that the silicone rubber composite surface filled with 1.0 wt% of Silica-poly(St-$CH_2P^+(Bu)_3Cl^-$) prepared by azo-initiated radical polymerization in a solvent-free dry-system showed antibacterial activity against *Staphylococcus aureus* and *Escherichia coli*.

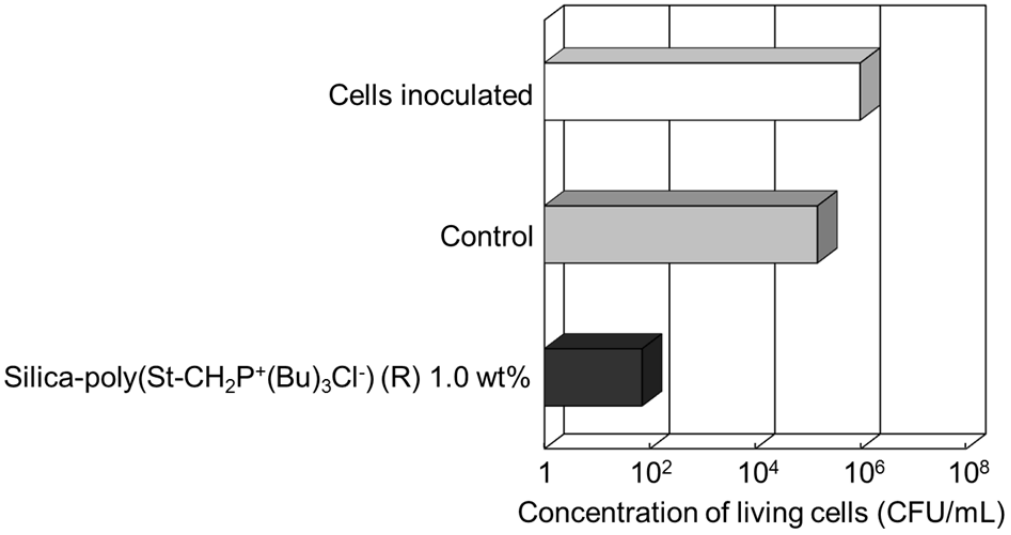

Figure 3-14. Antibacterial activity of silicone rubber composites surface filled with Silica-poly(St-$CH_2P^+(Bu)_3Cl^-$) (R) against *Staphylococcus aureus*.

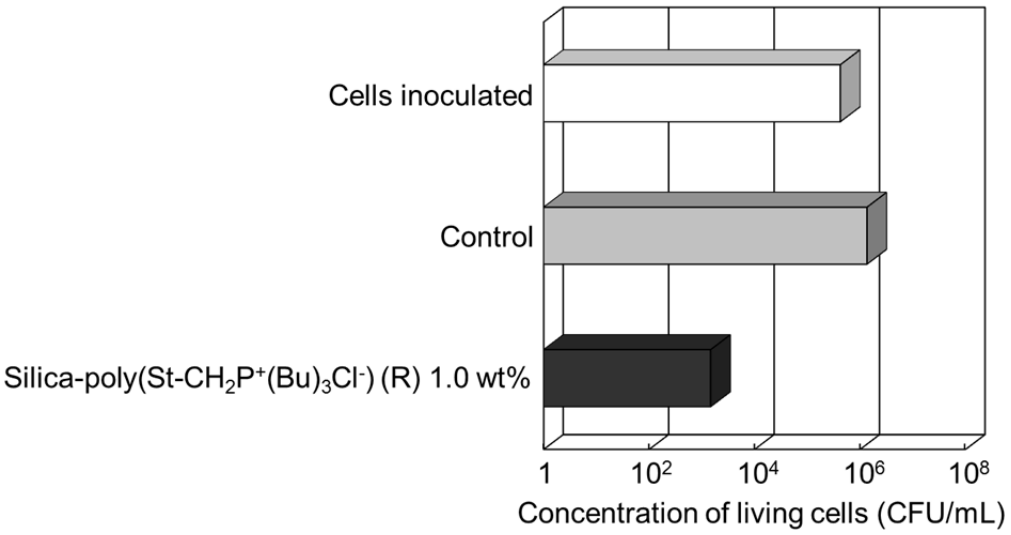

Figure 3-15. Antibacterial activity of silicone rubber composites surface filled with Silica-poly(St-$CH_2P^+(Bu)_3Cl^-$) (R) against *Escherichia coli*.

Figure 3-16 and Figure 3-17 show the antibacterial activity of silicone rubber composites surface filled with 1.0 wt% of Silica-poly(St-$CH_2P^+(Bu)_3Cl^-$) (A) (Grafting = 26%) against *Staphylococcus aureus* and *Escherichia coli*, respectively.

It was found that cells of *Staphylococcus aureus* on unfilled silicone rubber (control) shows decreased from 9.7×10^5 to 1.5×10^5 CFU/mL after 24 h incubation. On the contrary, cells of *Staphylococcus aureus* on silicone rubber filled with 1.0 wt% of Silica-poly(St-$CH_2P^+(Bu)_3Cl^-$) (A) decreased from 9.7×10^5 to 30 CFU/mL after 24 h incubation (Figure 3-16). Even the surface of silicone rubber filled with 1.0 wt% of Silica-poly(St-$CH_2P^+(Bu)_3Cl^-$) (A) shows antibacterial activity. Figure 3-17 shows that the surface of silicone rubber filled with 1.0 wt% of Silica-poly(St-$CH_2P^+(Bu)_3Cl^-$) (A) inhibited the proliferation of *Escherichia coli*.

The result suggests that the silicone rubber composite surface filled with 1.0 wt% of Silica-poly(St-$CH_2P^+(Bu)_3Cl^-$) prepared by ATRP in a solvent-free dry-system showed antibacterial activity against *Staphylococcus aureus*. However, the antibacterial activity against *Escherichia coli* was somewhat weak.

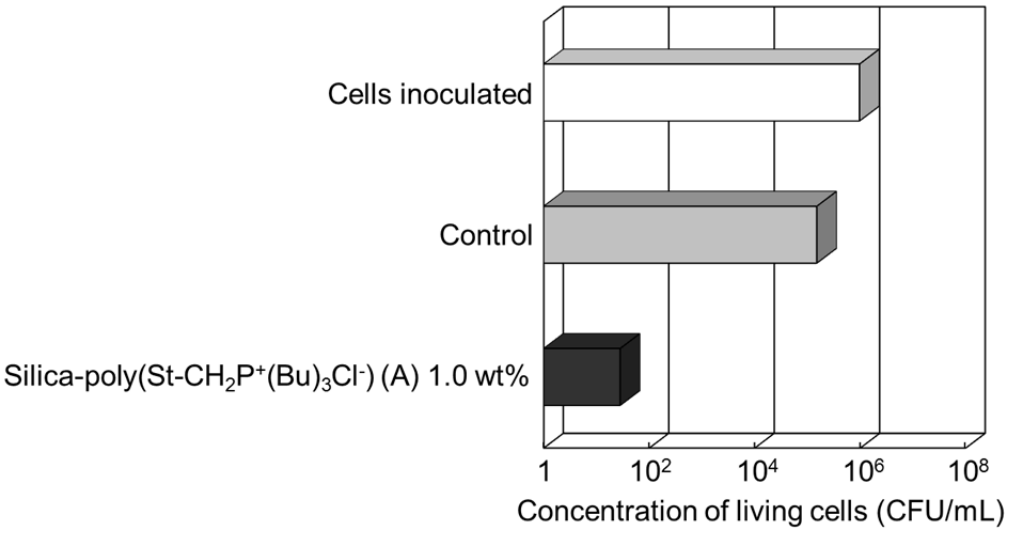

Figure 3-16. Antibacterial activity of silicone rubber composites surface filled with Silica-poly(St-$CH_2P^+(Bu)_3Cl^-$) (A) against *Staphylococcus aureus*.

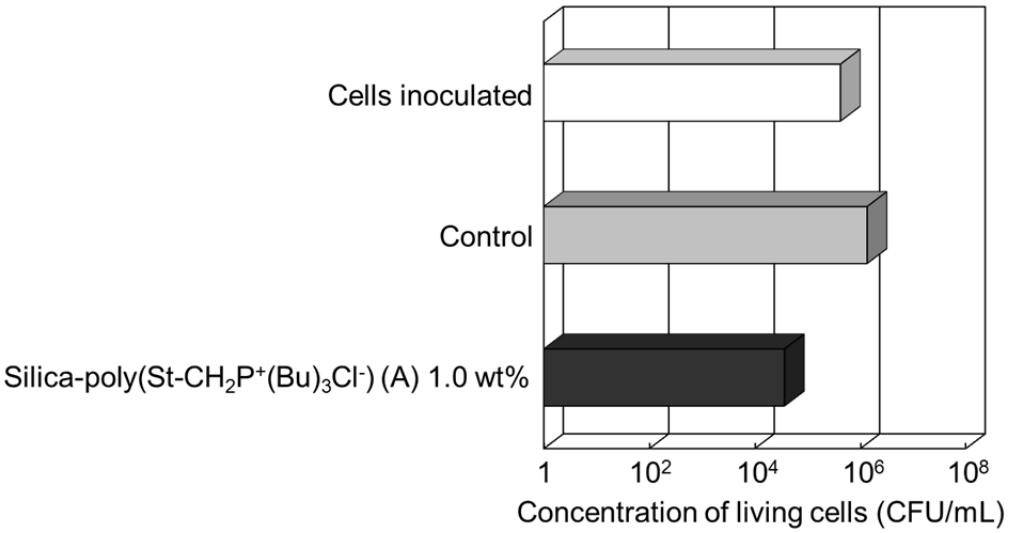

Figure 3-17. Antibacterial activity of silicone rubber composites surface filled with Silica-poly(St-$CH_2P^+(Bu)_3Cl^-$) (A) against *Escherichia coli*.

3.4 Conclusions

1. Introduction of azo groups onto silica nanoparticle surface as initiating sites for radical graft polymerization was successfully achieved by the reaction of ACVA with isocyanate groups introduced silica in a solvent-free dry-system.

2. Graft polymerization of antibacterial monomer, St-$CH_2P^+(Bu)_3Cl^-$, onto silica nanoparticle surface was successfully initiated by azo groups introduced onto the silica surface in a solvent-free dry-system.

3. Introduction of chlorosulfonyl groups onto silica nanoparticle surface as initiating sites for ATRP was successfully achieved by the treatment of CTCS with silanol groups on the silica surface in a solvent-free dry-system.

4. Graft polymerization of antibacterial monomer, St-$CH_2P^+(Bu)_3Cl^-$, onto silica nanoparticle surface was successfully achieved by ATRP in a solvent-free dry-system.

5. In azo-initiated radical polymerization and ATRP, it was found that the nearly equal amounts of antibacterial polymers were grafted onto silica nanoparticle surface in solvent-free dry-system and solvent system.

6. It was indicated that silicone rubber composites surface filled with poly(St-$CH_2P^+(Bu)_3Cl^-$)-grafted silica prepared in a solvent-free dry-system had antibacterial activity against *Staphylococcus aureus* and *Escherichia coli*.

References

[1] R. Yamashita, Y. Takeuchi, H. Kikuchi, K. Shirai, T. Yamauchi, and N. Tsubokawa, *Polym. J.* **38**, 844-851 (2006).

[2] T. Kawahara, Y. Takeuchi, G. Wei, K. Shirai, T. Yamauchi, and N. Tsubokawa, *Polym. J.* **41**, 744-751 (2009).

[3] M. Murota, S. Sato, and N. Tsubokawa, *Polym. Adv. Technol.* **13**, 144 (2002).

[4] J. Ueda, S. Sato, A. Tsunokawa, T. Yamauchi, and N. Tsubokawa, *Eur. Polym. J.* **41**, 193-200 (2005).

[5] S. B .Lee, R. R. Koepsel, S. W. Morley, K. Matyjaszewski, Y. Sun, and A. J. Russell, *Biomacromolecules* **5**, 877 (2004).

[6] H. Murota, R. R. Koepsel, K. Matyjaszewski, and A. J. Russell, *Biomacromolecules* **28**, 4870 (2007).

[7] Y. Sun, X. Ding, Z. Zheng, X. Cheng, and X. Hu, *Eur. Polym. J.* **43**, 762 (2007).

[8] E. Marutani, S. Yamamoto, T. Ninjbadgar, Y. Tsujii, T. Fukuda, and M. Takano, *Polymer* **45**, 2231 (2004).

[9] K. Ohno, T. Morinaga, K. Koh, Y. Tsujii, and T. Fukuda, *Macromolecules* **38**, 2137 (2005).

[10] L. Zhang, Z. Cheng, S. Shi, Q. Li, and X. Zhu, *Polymer* **49**, 3054 (2008).

[11] Z. Cheng, X. Zhu, Z. L. Shi, K. G. Neoh, and E. T. Kang, *Ind. Eng. Chem. Res.* **44**, 7098 (2005).

[12] C. H. Liu and C. Y. Pan, *Polymer* **48**, 3679 (2007).

[13] D. Hua, J. Tang, J. Jiang, Z. Gu, L. Dai, and X. Zhu, *Mater. Chem. Phys.* **114**, 402 (2009).

[14] R. Wang and A. B. Lowe, *J. Polym. Sci., A: Polym. Chem.* **45**, 2468 (2007).

[15] B. S. Sumerlin, A. B. Lowe, P. A. Stroud, P. Zhang, M. W. Urban, and C. L. McCormick, *Langmuir* **19**, 5559 (2003).

[16] Y. Mitsukami, M. S. Donovan, A. B. Lowe, and C. L. McCormick, *Macromolecules* **34**, 2248 (2001).

[17] V. Ladmiral, T. Morinaga, K. Ohno, T. Fukuda, and Y. Tsujii, *Eur. Polym. J.* **45**, 2788 (2009).

[18] K. Matyjaszewski and J. Xia, *Chem. Rev.* **101**, 2921 (2001).

[19] W. Jakubowski and K. Matyjaszewski, *Macromolecules* **38**, 4139-4146 (2005).

[20] J. Pyun and K. Matyjaszewski, *Chem. Matter* **13**, 3436 (2001).

[21] K. Ohno, K. Koh, Y. Tsuji, and T. Fukuda, *Macromolecules* **35**, 8989 (2002).

[22] T. Lui, S. Jia, T. Kowalewski, K. Matyjaszewski, R. Casadio-Portilla, and J. Belmont, *Langmuir* **19**, 6342 (2003).

[23] A. E. Harrak, G. Carrot, J. Oberdisse, J. Jestin, and F. Bou, *Polymer* **46**, 1095 (2005).

[24] T. Lui, R. Casadio-Portilla, J. Belmont, and K. Matyjaszewski, *J. Polym. Sci.: Part A: Polym. Chem.* **43**, 4695 (2005).

[25] T. E. Patten and K. Matyjaszewski, *Adv. Mater.* **10**, 901 (1998).

[26] K. Matyjaszewski, P. J. Miller, J. Pyun, G. Kickelbick, and S. Diamanti, *Macromolecules* **32**, 6526-6535 (1999).

[27] S. Matsuda and S. Okazaki, *Nippon Kagaku Kaishi* 1287 (1986).

[28] E. H. Brown and C. A. Krans, *J. Am. Chem. Soc.* **51**, 2690-2696 (1929).

[29] A. Kanazawa, T. Ikeda, and T. Endo, *J. Polm. Sci., Part A: Polym. Chem.* **31**, 335-343, 1441-1447, 1467-1472, 2873-2876, 3003-3011, 3031-3038 (1993).

[30] Japanese Industrial Standards (JIS), Antibacterial products - Test for antibacterial activity and efficacy, JIS Z 2801.

[31] A. Akelah, A. Rehab, T. Agag, and M. Betiha, *J. Appl. Polym. Sci.* **103**, 3739-3750 (2007).

Chapter 4

Preparation and Properties of Flame Retardant-immobilized Silica Nanoparticles

Abstract

To prepare silica nanoparticle having flame retardant activity, immobilization of flame retardant onto the surface was investigated. The immobilization of phosphorous flame retardant was achieved by two-step reactions: (1) introduction of cyclotriphosphazene (PH) groups onto silica nanoparticle by the reaction of terminal amino groups of the surface with hexachlorocyclotriphosphazene and (2) immobilization of bis(4-aminophenoxy)phenyl phosphine oxide (BAPPO) onto silica having PH groups by the reaction of PH groups on the surface with BAPPO. The immobilization of BAPPO was confirmed by FT-IR and thermal decomposition GC-MS. The composite of epoxy resin filled with BAPPO-immobilized silica (Silica-PH-BAPPO) was successfully prepared by heating in the presence of curing agents. Thermal decomposition temperature and glass transition temperature of the epoxy resin filled with Silica-PH-BAPPO was higher than that of epoxy resin filled with untreated silica, free HCTP and BAPPO. Moreover, flame retardant property of epoxy resin filled with Silica-PH-BAPPO was estimated by limiting oxygen index (LOI). The LOI value of epoxy resin filled with Silica-PH-BAPPO was higher than that of epoxy resin filled with untreated silica, free HCTP and BAPPO. This may be due the fact that char yield of the epoxy resin filled with Silica-PH-BAPPO was higher than that filled with free flame retardant. In addition, elution of flame retardant from epoxy resin was inhibited by the immobilization of flame retardant onto silica surface.

4.1 Introduction

Tsubokawa and his co-workers have reported that surface grafting of various polymers onto a silica nanoparticle by using previously introduced initiating groups on the nanoparticle surface, such as peroxyester, azo, acylium perchlorate, and potassium carboxylate groups [1-3]. In addition, they have succeeded in the grafting of functional polymers, such as biocompatible [4] and antibacterial polymers [5, 6], onto silica surface; composite surfaces prepared from the antibacterial polymer-grafted silica and conventional polymers show strong antibacterial activity [5, 6]. Tsubokawa and his co-workers have also reported immobilization of capsaicin onto hyperbranched poly(amidoamine)-grafted silica (Silica-PAMAM) surface and their properties [7].

On the other hand, most of organic polymers are combustible, because they contain hydrogen and carbon atoms. For their various applications in the building, electrical, transportation, mining and other industries, they have to fulfill flame retardant requirements. Thus main objectives in development of flame retarding polymers are to improve an ignition resistance and a reduction of flame spread when flame retardants were incorporated into flammable polymers [8]. Several types of flame retardant additives are used to improve flame retardant properties of polymer materials. These flame retardants can be divided into halogen, inorganic, phosphorous, nitrogen and nitrogen-phosphorous flame retardant [9-12].

Yuuki et al. have reported immobilization of halogen flame retardant onto Silica-PAMAM and flame retardant properties of epoxy resin filled with the flame retardant-immobilized silica [13].

However, along with this undoubted advantage, halogen containing compounds could produce corrosive and obscuring smoke and might give toxic gases with deleterious effects on environmental impact and human health, when they burned [14]. In this respect, environmentally friendly halogen-free flame retardant systems are currently being developed to substitute halogen based flame retardant systems.

In this chapter, immobilization of phosphorous flame retardant, bis(4-aminophenoxy) phenyl phosphine oxide (BAPPO), was investigated as shown in

Schemes 4-1 and 4-2. In addition, thermal property, glass-transition temperature and flame retardant property of epoxy resin filled with the BAPPO-immobilized silica will be discussed.

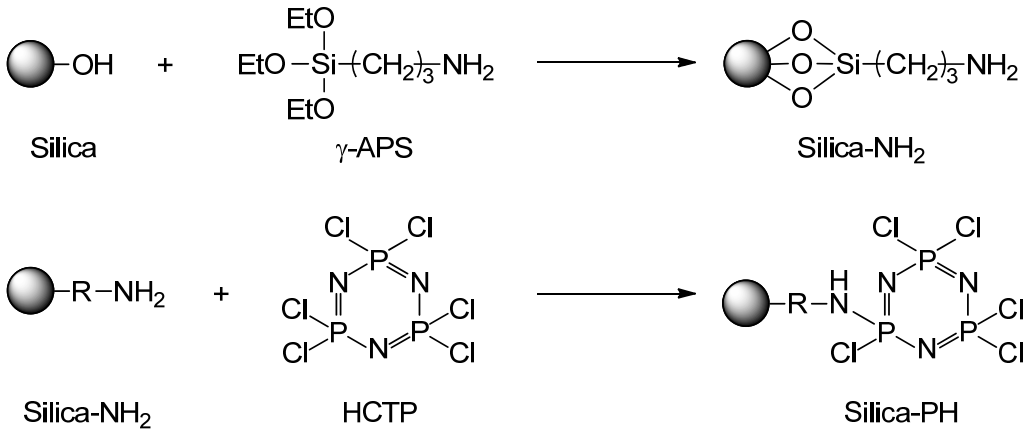

Scheme 4-1. Immobilization of chlorocyclophosphazene (PH) moieties onto Silica-NH_2 by the reaction with HCTP.

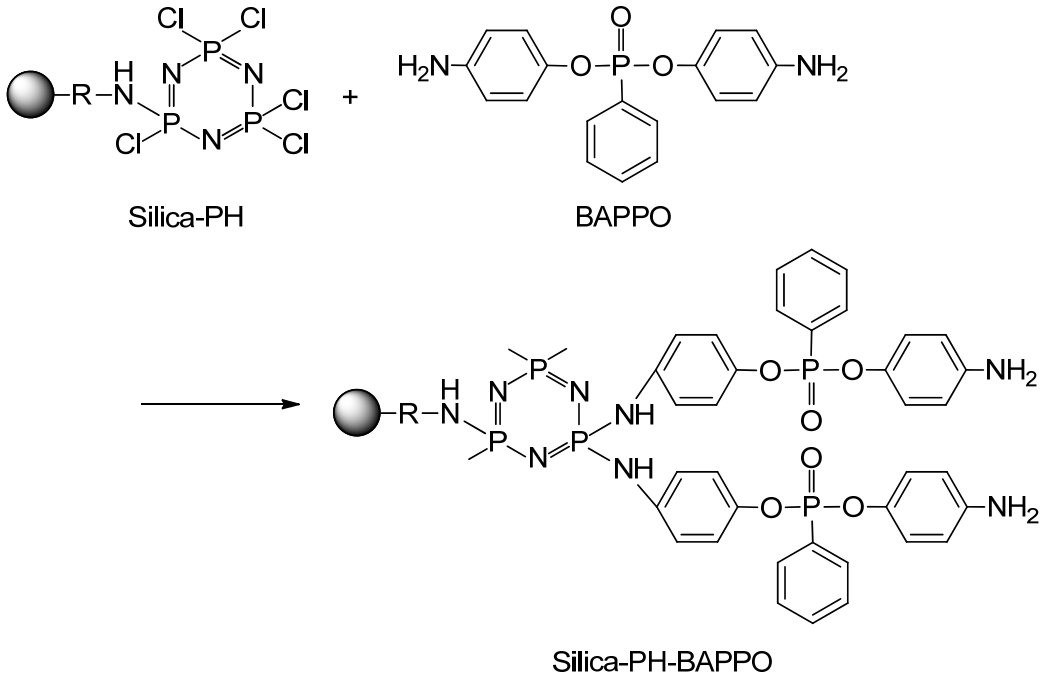

Scheme 4-2. Immobilization of flame retardant onto Silica-PH by the reaction with BAPPO.

4.2 Experimental

4.2.1 Materials and reagents

Silica nanoparticle used was Aerosil 200 and it was obtained from Nippon Aerosil Co., Ltd. Japan. The particle size, specific surface area, and silanol group content were 12 nm, 200 m^2/g, and 1.37 mmol/g, respectively. The content of silanol groups was determined by measuring volumetrically the amount of ethane evolved by the reaction with triethylaluminum [15, 16]. The silica nanoparticle was dried *in vacuo* at room temperature before use.

Hexachlorocyclotriphosphazene (HCTP) obtained from Otsuka Chemical Co., Ltd., was used without further purification. *p*-Nitrophenol, phenyl phosphonic dichloride, γ-aminopropyltriethoxysilane (γ-APS), hexamethylenediamine (HMDA), and 4,4'-diaminodiphenylmethane (DDM) were also used without further purification. Triethylamine obtained from Kanto Chemical Co., Inc., was dried over sodium hydroxide and distilled.

Bisphenol-A type epoxy resin (Araldite AER 260) was obtained from Asahi-Chiba Ltd. Japan. Epoxy equivalent and viscosity of the epoxy resin were 180-200 g/eq and 1.2-1.6 × 10^4 mPa•s, respectively. The epoxy resin was dried *in vacuo* at room temperature before use.

4.2.2 Synthesis of bis(4-aminophenoxy) phenyl phosphine oxide (BAPPO)

Bis(4-aminophenoxy) phenyl phosphine oxide (BAPPO) was synthesized by two steps according to the method of literature as shown in Scheme 4-3 [17]. The first is synthesis of bis(4-nitrophenoxy) phenyl phosphine oxide (BNPPO) was achieved by the reaction of *p*-nitrophenol with phenyl phosphonic dichloride. The second is hydrogenation of BNPPO.

4.2.2.1 Synthesis of bis(4-nitrophenoxy) phenyl phosphine oxide (BNPPO)

Synthesis of bis(4-nitrophenoxy) phenyl phosphine oxide (BNPPO) was achieved by the reaction of *p*-nitrophenol with phenyl phosphonic dichloride according to the method of literature [17]. A typical procedure was as follows. Into a flask was placed 57.0 g of *p*-nitrophenol, 240 mL of THF. 34.2 g of triethylamine and 0.6 g of Cu_2Cl_2 was added into the solution and then the solution was cooled to 0 °C in an ice bath. A solution, 30 g of phenyl phosphonic dichloride and 120 mL THF, was added to the reaction solution dropwise over a period of 30 min. The solution became thick due to the precipitation of the amine hydrochloride. After maintaining at 0 °C for 2 h, the solution was kept at room temperature for another 48 h. The precipitant was filtered and washed with THF. The filtrate was concentrated, washed with an ice-cold aqueous solution of NaOH (2% by weight) and with distilled water, and finally extracted with ethyl acetate three times. The extract was dried over $MgSO_4$ and then concentrated. The product was purified by recrystallization from ethanol and then dried *in vacuo* at room temperature.

The structure of BNPPO was confirmed by FT-IR.

4.2.2.2 Synthesis of bis(4-aminophenoxy) phenyl phosphine oxide (BAPPO)

Synthesis of bis(4-aminophenoxy)phenyl phosphine oxide (BAPPO) was achieved by the hydrogenation of BNPPO [17]. A typical procedure was as follows. Into a flask was placed 25 g of BNPPO and 180 g of powder tin(II) chloride dehydrate. A solution of 200 mL fuming hydrochloric acid in 400 mL ethanol was introduced into the flask. The reaction mixture was stirred at room temperature for 5 h. The solution was concentrated and then was neutralized by 25% NaOH aqueous solution. The obtained solution was extracted with chloroform. The organic layer was collected and concentrated under a reduced pressure. The obtained solid was recrystallized from dichloromethane and then dried *in vacuo* at room temperature.

The structure of BAPPO was confirmed by FT-IR.

4.2.3 Immobilization of HCTP onto Silica-NH_2

Introduction of amino groups onto the silica was also achieved by the treatment of surface silanol groups with γ-APS in a solvent-free dry-system according to the methods of the literature [18]. The silica having amino groups was abbreviated as Silica-NH_2.

Immobilization of HCTP onto Silica-NH_2 was achieved by the reaction of Silica-NH_2 with HCTP as shown in Scheme 4-1. A typical procedure was as follows. Into a flask was placed 2.0 g of Silica-NH_2, 0.5 g of HCTP, 60 mL of diethyl ether, and 0.2 mL of triethylamine as hydrogen chloride scavenger were added, and the mixture was stirred with a magnetic stirrer at 0 °C under nitrogen. After 18 h, the products were stirred with a large excess of heptane at 0 °C for 6 h. After the reaction, the resulting silica was centrifuged and the supernatant solution containing unreacted HCTP was removed. The precipitated silica was dispersed in THF and centrifuged again, and the procedure was repeated until no more HCTP could be detected in the supernatant solution by use of UV-Vis spectra. The resulting silica was stored *in vacuo* at room temperature. The silica was abbreviated as Silica-PH.

4.2.4 Immobilization of BAPPO onto Silica-PH

Immobilization of BAPPO onto Silica-PH was achieved by the reaction of terminal P-Cl groups on the Silica-PH with BAPPO as shown in Scheme 4-2. A typical procedure was as follows. Into a flask was placed 2.0 g Silica-PH, 0.6 g BAPPO, 150 mL of toluene, and 1.0 mL of triethylamine as hydrogen chloride scavenger were added, and the mixture was stirred with a magnetic stirrer at 60 °C for 24 h under nitrogen. After the reaction, the resulting silica was centrifuged and the supernatant solution containing unreacted BAPPO was removed. The precipitated silica was dispersed in THF and centrifuged again, and the procedure was repeated until no more BAPPO could be detected in the supernatant solution by use of UV-Vis spectra. The resulting

silica was stored *in vacuo* at room temperature. The silica was abbreviated as Silica-PH-BAPPO.

4.2.5 Determination of PH group content on Silica-PH and BAPPO content on Silica-PH-BAPPO

Immobilized PH group content on Silica-PH and BAPPO content on Silica-PH-BAPPO were determined by the following equations:

$$\text{Immobilized PH (\%)} = (A / B) \times 100$$
$$\text{Immobilized BAPPO (\%)} = [(C - A) / B] \times 100$$

where *A*, *B*, and *C* are weight of HCTP, silica, HCTP and BAPPO immobilized onto the silica, respectively. The *A* and *C* were determined by measuring the weight loss when Silica-PH and Silica-PH-BAPPO, respectively, were heated at 800 °C using a thermogravimetric analyzer (TGA) (Shimadzu Co., TGA-50) in nitrogen.

4.2.6 Measurements

Characterizations of Silica-PH and Silica-PH-BAPPO were carried out by FT-IR spectra. Difference FT-IR spectra of silica between after and before treatment was recorded on a FT-IR Spectrophotometer (Shimadzu Co., FTIR-8200A) using KBr pellet. Thermal decomposition gas chromatograms and mass spectra were recorded on a gas chromatograph mass spectrometer, Shimadzu Co., GCMS-QP2010 equipped with a double shot pyrolyzer, Frontier Laboratories Ltd., PY-2020D. The column was programmed from 70 to 320 °C at a heating rate of 20 °C/min and then held at 320 °C for 5 min.

4.2.7 Preparation of epoxy resin filled with Silica-PH-BAPPO

Silica-PH-BAPPO was dispersed in a mixture of epoxy resin and HMDA (or DDM) by use of a planetary centrifugal mixer (Thinky Co., AR-100). The mixture was poured into a Teflon mold, which was coated with a fluorine-releasing agent. The curing reaction was carried out at 100 °C for 1 h and then at 120 °C for 2 h. Size of sample was 80 mm × 6.5 mm × 3.0 mm. The composition of epoxy resin composites and the sample code was shown in Table 4-1.

Table 4-1. Compositions of the epoxy resin filled with flame retardant-immobilized silica.

Sample code	Curing agent (phr*)		Composition (phr*)			
	HMDA	DDM	Silica-PH-BAPPO	Silica-NH_2	HCTP	BAPPO
A	20	-	-	-	-	-
B	20	-	-	-	0.4	1.3
C	20	-	-	8.3	0.4	1.3
D	20	-	10	-	-	-
E	-	26.5	-	-	-	-
F	-	26.5	5	-	-	-

*phr : Parts per hundred parts of epoxy resin.

4.2.8 Glass-transition temperature of epoxy resin filled with Silica-PH-BAPPO

Glass-transition temperature (T_g) of epoxy resin filled with Silica-PH-BAPPO was measure by differential thermogravimetric analyzer (Shimadzu Co., DTG-60). The temperature range of the DTG was programmed from room temperature to 200 °C at a heating rate of 10 °C/min. The composition of epoxy resin composites and the sample code was shown in Table 4-1.

4.2.9 Evaluation of thermal stability of epoxy resin filled with Silica-PH-BAPPO

Thermal stability of epoxy resin filled with Silica-PH-BAPPO was estimated by 5% and 10% weight loss temperature determined by using a thermogravimetric analyzer (TGA) (Shimadzu Co., TGA-50) under air. The composition of epoxy resin composites and the sample code was shown in Table 4-1.

4.2.10 Estimation of Limited Oxygen Index (LOI) of the epoxy resin filled with Silica-PH-BAPPO

Flame retardant property of the epoxy resin filled with Silica-PH-BAPPO was estimated by limited oxygen index (LOI) according to the method of JIS K 7201 [19]. In the LOI test, a vertical strip of material is burned within a glass chimney containing a vertically moving column of mixture of oxygen and nitrogen. LOI is defined as the minimum percent of oxygen, in a mixture of oxygen and nitrogen, which will just support combustion of a material initially at room temperature. The composition of epoxy resin composites and the sample code was shown in Table 4-1.

4.2.11 Elution of flame retardant from epoxy resin composites

The elution of flame retardant from epoxy resin was carried out as follows. The epoxy resin composite (size of sample was 40 mm × 20 mm × 1.0 mm) was stirred in 50 g of methanol or heated to reflux in 50 g water. At specified time intervals, the absorbance of the supernatant solution was measured by UV-Vis spectrophotometer (Shimadzu Co., UV-1800) at 293 nm and the amount of eluted BAPPO was calculated from a calibration curve of BAPPO as mention above. The composition of using epoxy resin composites and the sample code was shown in Table 4-1.

The amount of eluted BAPPO was determined by the following equations.

Amount of eluted BAPPO (mg/(cm^2·dL)) = W / (S × V)

W: Weight (mg) of eluted BAPPO by calibration curve

S: Total surface area (cm^2) of sample used

V: Volume (dL) of solvent used

4.3 Results and Discussion

4.3.1 Synthesis of bis(4-aminophenoxy) phenyl phosphine oxide (BAPPO)

BAPPO was synthesized by two steps according to the method of the literature (Scheme 4-3) [17]. BNPPO was obtained as an intermediate by the reaction of *p*-nitrophenol with phenyl phosphonic dichloride. The dinitro compound, BNPPO was then hydrogenated to result in the diamine compound BAPPO.

Figure 4-1 shows FT-IR spectra of (a) BAPPO and (b) BNPPO. The formation of amino groups of BAPPO was confirmed by FT-IR. FT-IR spectra of BNPPO show absorption at 1345cm^{-1}, which is characteristic of nitro group. After the reduction of BNPPO, FT-IR spectra of BAPPO show the absorptions at 3455cm^{-1} and 3365cm^{-1} corresponds to aromatic primary amine. In addition, the characteristic absorption of nitro group of BNPPO also disappeared. The absorptions at 1190cm^{-1} and 1270cm^{-1} in FT-IR spectra of BAPPO were assigned as P-O-arom. and P=O bands, respectively.

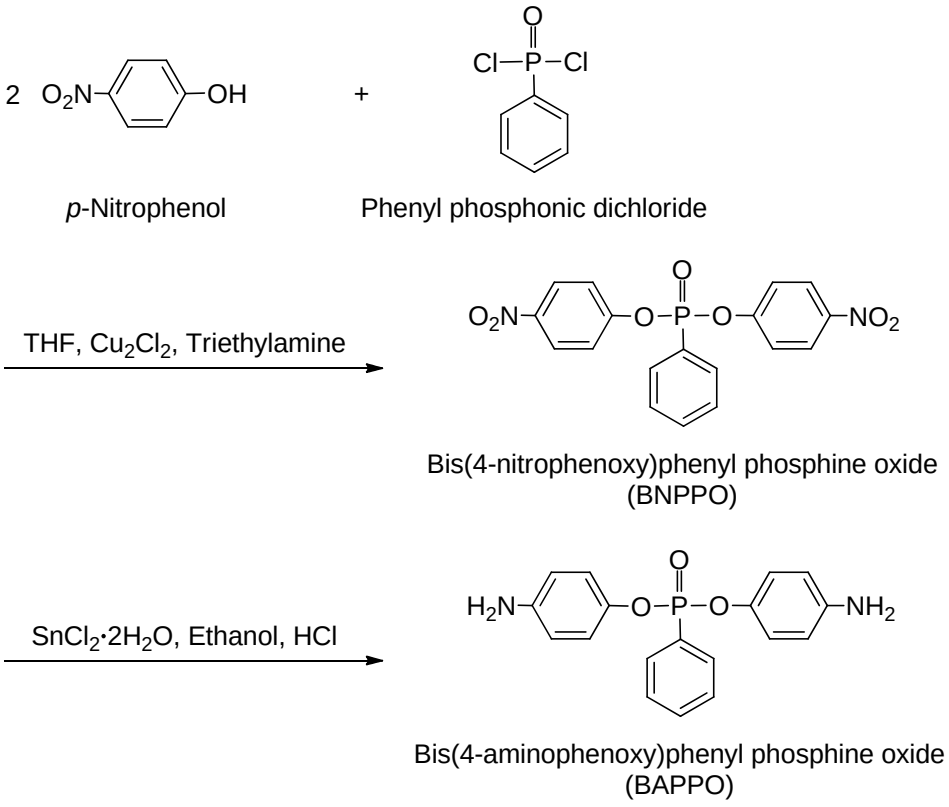

Scheme 4-3. Synthesis of BAPPO.

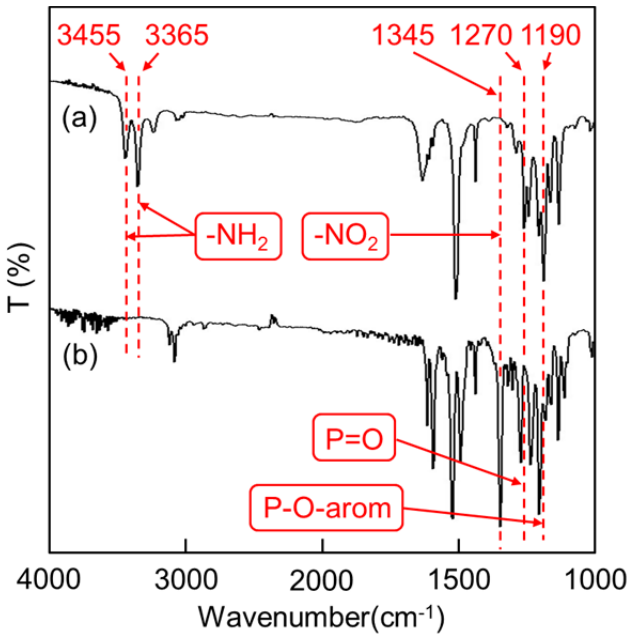

Figure 4-1. FT-IR spectra of (a) BAPPO and (b) BNPPO.

4.3.2 Immobilization of HCTP onto Silica-NH_2

Introduction of amino groups onto the silica surface as immobilizing sites for HCTP was achieved by the treatment of the silica surface with γ-APS in the solvent-free dry-system (Scheme 4-1) [18]. The amino group content introduced onto the silica surface was determined by titration to be 0.42 mmol/g.

Immobilization of PH group onto Silica-NH_2 was achieved by the reaction of terminal amino groups on the Silica-NH_2 surface with HCTP. It was found that the amount of PH groups immobilized onto the silica surface was determined by TGA to be 0.34 mmol/g (Scheme 4-1).

Figure 4-2 shows FT-IR spectra of (a) difference spectrum between Silica-PH and Silica-NH_2 (Silica-PH minus Silica-NH_2), and (b) hexachlorocyclotriphosphazene (HCTP). The difference spectrum show characteristic absorptions of HCTP. The absorption at 1245 cm^{-1} corresponds to the backbone of phosphazene. The absorptions at 528 cm^{-1} and 600 cm^{-1} correspond to P-Cl and -P=N- vibrations. Therefore, it is confirmed that HCTP was immobilized onto Silica-NH_2 to give Silica-PH.

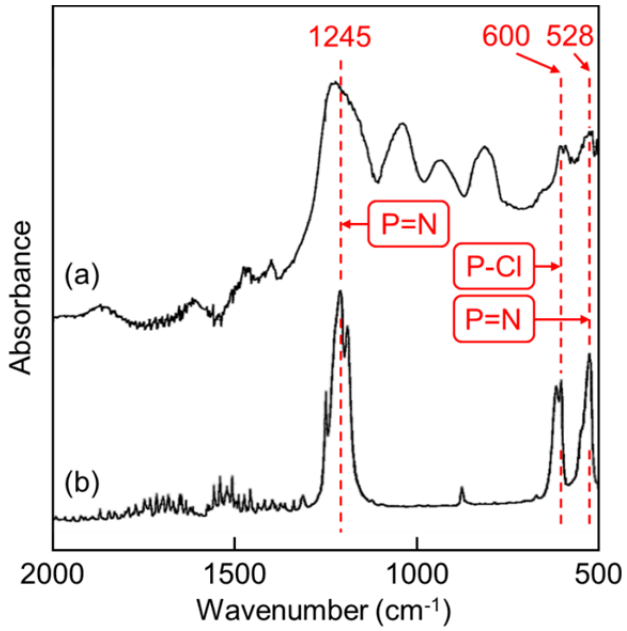

Figure 4-2. (a) FT-IR difference spectrum between Silica-PH and Silica-NH_2, and (b) FT-IR spectrum of HCTP.

Thermal decomposition GC-MS was commonly used for the identification of organic materials [20, 21]. Gas chromatograms of thermal decomposed gas of (a) Silica-NH_2, (b) Silica-PH, and (c) HCTP are shown in Figure 4-3. In comparison with these chromatograms, the thermal decomposition gas of Silica-PH at retention time 5.6 min was similar to that of HCTP. In addition, the mass spectrum of the decomposed gas of Silica-PH at retention time 5.6 min was in agreement with that of HCTP as shown in Figure 4-4. Figure 4-4 also shows that Silica-PH was decomposed to produce fragments of HCTP moieties. These results clearly show that HCTP was successfully immobilized onto Silica-NH_2 to give Silica-PH.

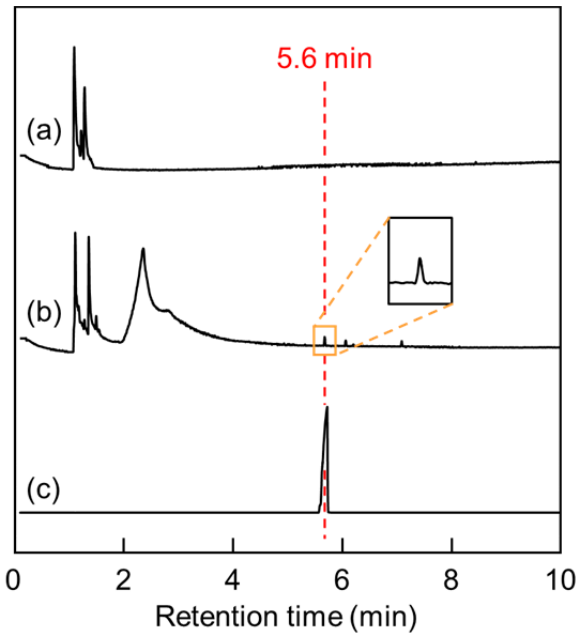

Figure 4-3. Gas chromatograms of thermal decomposed gas of (a) Silica-NH_2, (b) Silica-PH, and (c) HCTP.

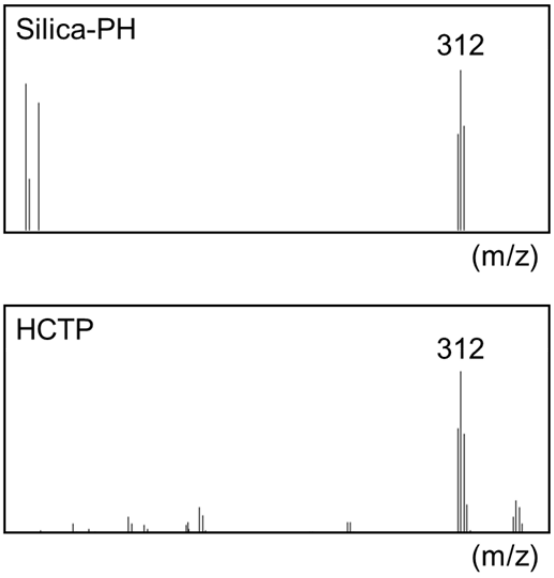

Figure 4-4. Mass spectra of thermal decomposed gas of Silica-PH and HCTP of retention time at 5.6 min.

4.3.3 Immobilization of BAPPO onto Silica-PH

Figure 4-5 shows the relationship between reaction time and the amount of BAPPO immobilized onto Silica-PH by the reaction of Silica-PH with BAPPO. The amount of BAPPO immobilized onto the Silica-PH was increased with increasing reaction time. The amount of immobilized BAPPO was reached to 8.5% after 24 h. But immobilized BAPPO was no longer increased after 48 h, because P-Cl groups of Silica-PH were blocked by immobilized BAPPO.

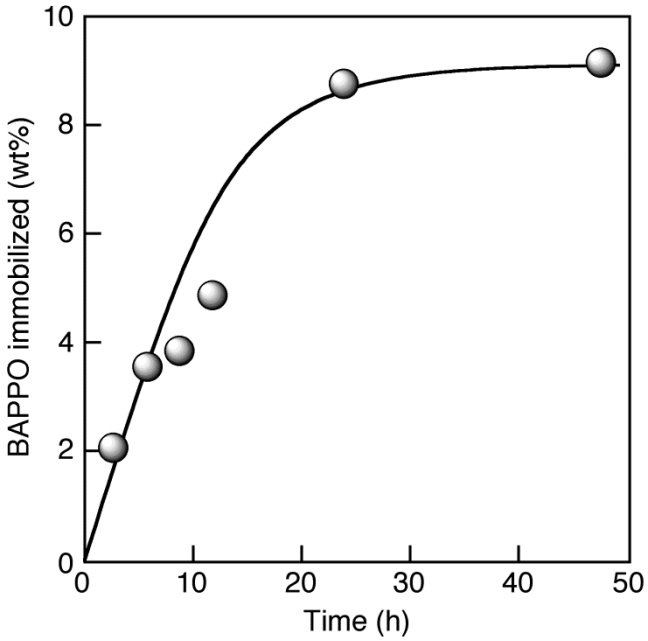

Figure 4-5. Relationship between reaction time and the amount of immobilized BAPPO onto Silica-PH.
Silica-PH, 2.0 g; BAPPO, 0.60 g; triethylamine, 1.0 mL; toluene, 150 mL, 60 °C.

Figure 4-6 shows FT-IR spectra of (a) difference spectrum between Silica-PH-BAPPO and Silica-PH (Silica-PH-BAPPO minus Silica-PH), and (b) BAPPO. The difference spectrum show characteristic absorptions of BAPPO. The absorptions at 1505 cm^{-1} and 950 cm^{-1} are characteristic of aromatic rings and P-O-C bond, respectively [17]. Therefore, it is confirmed that BAPPO was successfully immobilized onto Silica-PH.

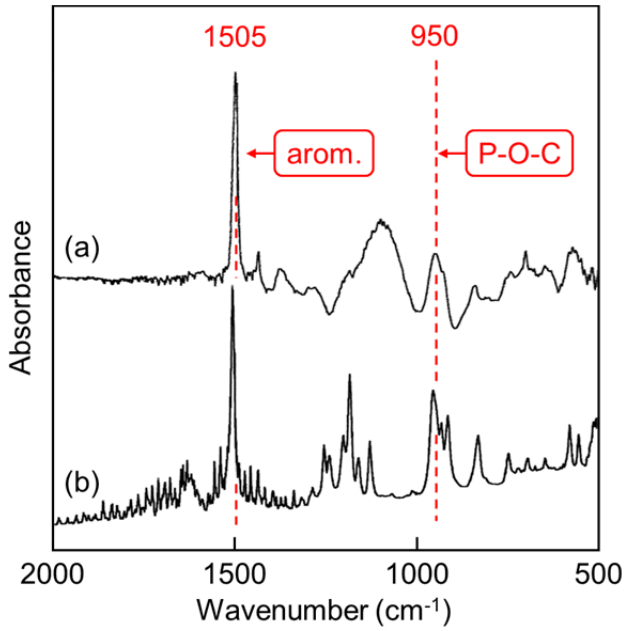

Figure 4-6. (a) FT-IR difference spectrum between Silica-PH-BAPPO and Silica-PH, and (b) FT-IR spectrum of BAPPO.

Gas chromatograms of thermal decomposed gas of (a) Silica-PH, (b) Silica-PH-BAPPO, and (c) BAPPO are shown in Figure 4-7. In comparison with these chromatograms, the thermal decomposition gas of Silica-PH-BAPPO at retention time 4.9 min was similar to that of BAPPO. In addition, as shown in Figure 4-8, the mass spectrum of decomposed gas of Silica-PH-BAPPO at retention time 4.9 min was in agreement with that of BAPPO. Figure 4-8 also shows that Silica-PH-BAPPO was decomposed to produce fragments of BAPPO. These results clearly show that BAPPO was immobilized onto Silica-PH to give Silica-PH-BAPPO.

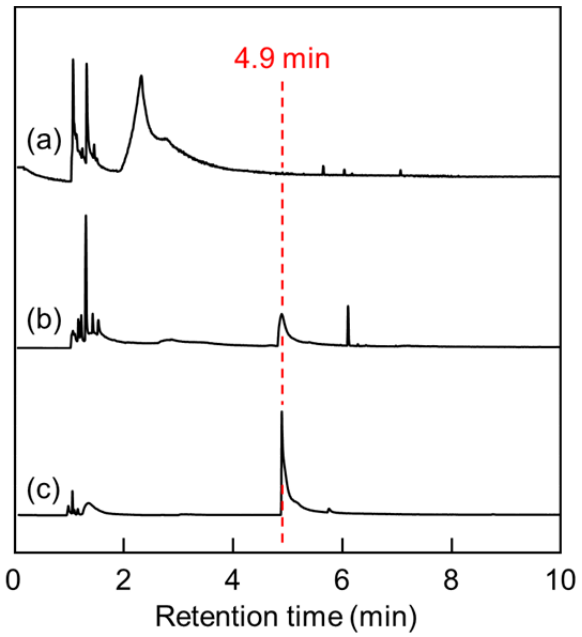

Figure 4-7. Gas chromatograms of thermal decomposed gas of (a) Silica-PH, (b) Silica-PH-BAPPO, and (c) BAPPO.

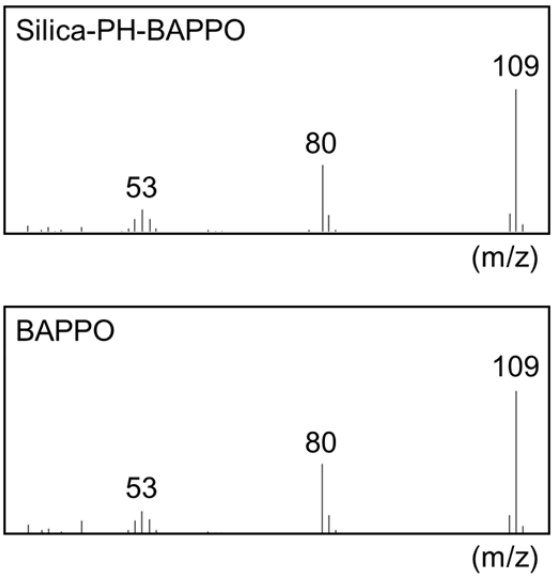

Figure 4-8. Mass spectra of thermal decomposed gas of Silica-PH-BAPPO and BAPPO of retention time at 4.9 min.

4.3.4 Glass-transition temperature of epoxy resin filled with Silica-PH-BAPPO

Epoxy resin filled with Silica-PH-BAPPO was prepared by use of two type of curing agents, HMDA and DDM. The composition of epoxy resin composites and the sample code was shown in Table 4-1.

Table 4-2 shows T_g of (A) unfilled epoxy resin, (B) epoxy resin filled with free HCTP and BAPPO, (C) epoxy resin filled with Silica-NH_2, free HCTP and BAPPO, and (D) epoxy resin filled with Silica-PH-BAPPO, which were cured by HMDA. T_g of (B) epoxy resin filled with free HCTP and BAPPO, and (C) epoxy resin filled with Silica-NH_2, free HCTP, and BAPPO were decreased about 15 °C in comparison to (A) unfilled epoxy resin. The results suggest that these additives act as plasticizer. It is interesting that the decrease of T_g of (D) epoxy resin filled with Silica-PH-BAPPO was only 7 °C. These results suggested that decrease of T_g of epoxy resin based on the addition of flame-retardants was prevented by use of Silica-PH-BAPPO.

Table 4-2. Glass-transition temperature (T_g) of the epoxy resin filled with flame retardant-immobilized silica.

Sample code	T_g (°C)
A	106
B	91.7
C	92.9
D	98.6

4.3.5 Thermal properties of epoxy resin filled with Silica-PH-BAPPO

Thermal stability of epoxy resin filled with Silica-PH-BAPPO was estimated by TGA under air. Figure 4-9 shows the thermal degradation behaviors of (A) unfilled epoxy resin, (B) epoxy resin filled with free HCTP and BAPPO, (C) epoxy resin filled

with Silica-NH_2, free HCTP and BAPPO, and (D) epoxy resin filled with Silica-PH-BAPPO, which were cured by HMDA.

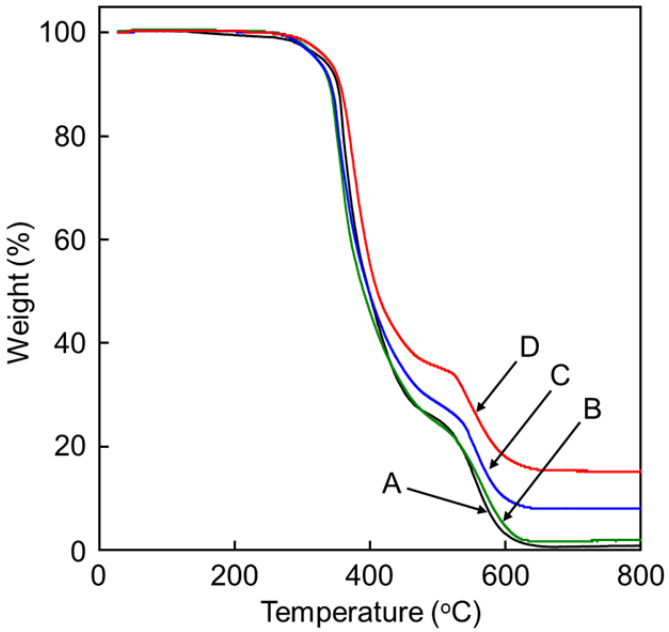

Figure 4-9. TGA curves of the epoxy resins (cured by HMDA) filled with flame retardant-immobilized silica under air.
Sample codes of epoxy resin were shown in Table 4-1.

Table 4-3 shows 5% and 10% weight loss temperature of each epoxy resins. Sample A exhibited a 5% weight loss at 329 °C and a 10% weight loss at 352 °C; Sample B exhibited a 5% weight loss at 320 °C and a 10% weight loss at 340 °C; Sample C exhibited a 5% weight loss at 321 °C and a 10% weight loss at 342 °C; Sample D exhibited a 5% weight loss at 337 °C and a 10% weight loss at 356 °C.

It was found that weight loss temperature of (D) epoxy resin filled with Silica-PH-BAPPO was higher than that of unfilled epoxy resin, in spite of that of (B) epoxy resin filled with free HCTP and BAPPO, and (C) epoxy resin filled with Silica-NH_2, free HCTP and BAPPO decreased. This may be due to the fact that elimination of flame retardants (HCTP and BAPPO) by evaporation with rising temperature was inhibited, because HCTP and BAPPO were immobilized onto silica nanoparticle surface (an anchor effect).

Table 4-3. Thermal properties and LOI of the epoxy resin filled with flame retardant-immobilized silica.

Sample code	Temperature of weight loss (°C)		Char yield at 800 °C (%)		LOI
	5%	10%	Char	Char + Silica	
A	329	352	0.9	-	19.9
B	320	340	2.0	-	23.4
C	321	342	1.6	8.0	22.4
D	337	356	8.8	15.2	25.9
E	366	373	1.8	-	23.3
F	373	380	4.2	7.4	27.5

Figure 4-10 shows thermal degradation behaviors of (E) unfilled epoxy resin and (F) epoxy resin filled with Silica-PH-BAPPO, which were cured by DDM. Table 4-3 also shows 5% and 10% weight loss temperature of each composite. Sample E exhibited a 5% weight loss at 366 °C and a 10% weight loss at 373 °C; Sample F exhibited a 5% weight loss at 373 °C and a 10% weight loss at 380 °C. These weight loss temperatures of epoxy resins cured by DDM were higher than that of epoxy resin cured by HMDA, because DDM has aromatic structures. The result suggested that the thermal stability of the epoxy resin was improved by use of Silica-PH-BAPPO.

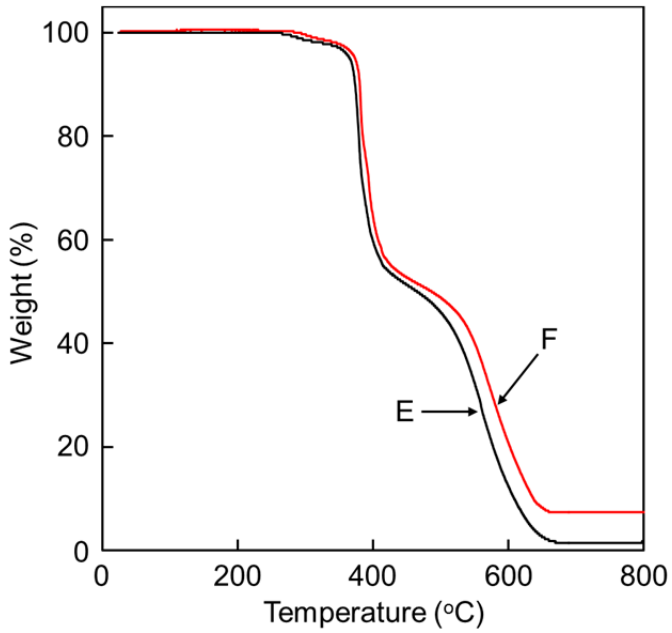

Figure 4-10. TGA curves of the epoxy resins (cured by DDM) filled with flame retardant-immobilized silica under air.
Sample codes of epoxy resin were shown in Table 4-1.

4.3.6 Flame retardant properties of epoxy resin filled with Silica-PH-BAPPO

In order to estimate the effect of Silica-PH-BAPPO on the flame retardant properties of epoxy resin, char yield and LOI value of epoxy resin filled with Silica-PH-BAPPO were investigated. Table 4-3 shows char yields at 800 °C and LOI values of (A) unfilled epoxy resin, (B) epoxy resin filled with free HCTP and BAPPO, (C) epoxy resin filled with Silica-NH_2, free HCTP and BAPPO, and (D) epoxy resin filled with Silica-PH-BAPPO, which were cured by HMDA. The value of char yields were obtained by subtracting the amount of silica, which were calculated from the amount of silica added to epoxy resin.

The char yield of Samples A, B, C and D was 0.9%, 2.0%, 1.6% and 8.8%, respectively. The char yield of epoxy resin filled with Silica-PH-BAPPO shows the highest value. The char yield was important to flame retardancy of polymers, since high char yields always lead to high flame-retardant activity of the phosphorous flame retardants [22-24]. Moreover, LOI value of the epoxy resin filled with

Silica-PH-BAPPO shows also the highest value, in spite of that of (B) epoxy resin filled with free HCTP and BAPPO, and that of (C) epoxy resin filled with Silica-NH_2, free HCTP and BAPPO, which were contained same amount of phosphorous flame retardants. On the other hand, char yield and LOI of (B) epoxy resin filled with free HCTP and BAPPO, and that of (C) epoxy resin filled with Silica-NH_2, free HCTP and BAPPO were almost the same value. Therefore, it was found that the flame retardant properties hardly changes even with the addition of untreated silica.

These results may be due to the fact that a protective layer was effectively formed on the epoxy resin surface and the layer served as a barrier against heat and oxygen diffusion to increase flame retardant property of epoxy resins, because phosphorous flame retardant was immobilized onto silica nanoparticle surface.

In addition, char yield and LOI value of (F) epoxy resin filled with Silica-PH-BAPPO, which was cured by DDM, was higher than that of (E) unfilled epoxy resin, and LOI value of Sample F reached to 27.5. These results suggested that flame retardant property of epoxy resins was considerably improved by use of Silica-PH-BAPPO.

4.3.7 Elution of flame retardant from epoxy resin composites

Figure 4-11 shows the relationship between dipping time in methanol and the amount of eluted BAPPO per unit volume in 100 mL methanol from Sample (B), epoxy resin filled with free HCTP and BAPPO, and Sample (D), epoxy resin filled with Silica-PH-BAPPO. The amount of eluted BAPPO from epoxy resin filled with free HCTP and BAPPO increased with increasing dipping time and reached to 4.0 mg/(cm^2·dL) after 2 days. On the contrary, the elution of BAPPO from epoxy resin filled with Silica-PH-BAPPO was hardly seen even after dipping for 6 days.

Figure 4-12 also shows the relationship between boiling time in water and the amount of eluted BAPPO per unit volume in 100 mL water from Samples B and D. The amount of eluted BAPPO from epoxy resin filled with free HCTP and BAPPO increased with increasing boiling time and reached to 2.0 mg/(cm^2·dL) after 1 days. On

the contrary, the elution of BAPPO from epoxy resin filled with Silica-PH-BAPPO was hardly seen even after dipping for 2 days.

These results suggested that the elution of BAPPO from epoxy resin was inhibited by the immobilization of flame retardant onto silica surface. This may be due to an anchor effect of silica nanoparticle.

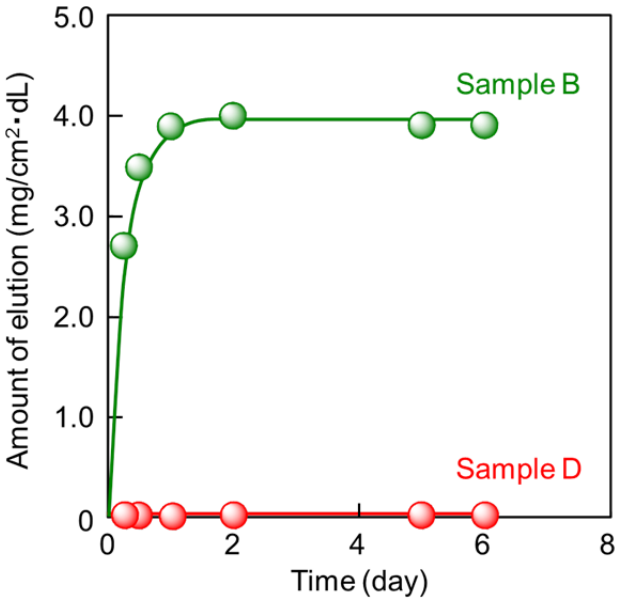

Figure 4-11. Elution of BAPPO from epoxy resin filled with flame retardant-immobilized silica in methanol.

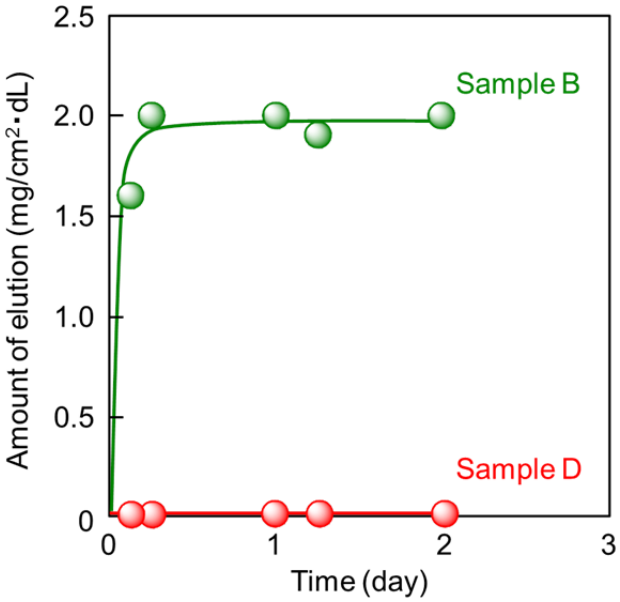

Figure 4-12. Elution of BAPPO from epoxy resin filled with flame retardant-immobilized silica in water.

4.4 Conclusions

1. Immobilization of phosphorous flame retardant, BAPPO, onto Silica-PH was successfully achieved by the reaction of amino groups of BAPPO with P-Cl groups on Silica-PH, which was prepared by the reaction of amino groups on silica with HCTP.

2. The amount of BAPPO-immobilized onto Silica-PH was increased with increasing reaction time. The amount of BAPPO immobilized onto Silica-PH was determined to be 8.5 wt%.

3. Char yield of the epoxy resin filled with Silica-PH-BAPPO was higher than that filled with free HCTP and BAPPO.

4. Flame retardant property and decrease of T_g of the epoxy resin was considerably improved by the addition of Silica-PH-BAPPO.

5. Elution of flame retardant from epoxy resin was inhibited by the immobilization of flame retardant onto silica surface.

References

[1] N. Tsubokawa, *Polym. J.* **37**, 637-655 (2005).

[2] N. Tsubokawa, *J. Jpn. Soc. Colour Mater.* **80**, 174-182, 215-226, 267-276 (2007).

[3] N. Tsubokawa, *J. Adhesion Soc. Jpn.* **45**, 63-69 (2009).

[4] R. Yokoyama, S. Suzuki, K. Shirai, T. Yamauchi, N. Tsubokawa, and M. Tsuchimochi, *Eur. Polym. J.* **42**, 3221-3229 (2006).

[5] R. Yamashita, Y. Takeuchi, H. Kikuchi, K. Shirai, T. Yamauchi, and N. Tsubokawa, *Polym. J.* **38**, 844-851 (2006).

[6] T. Kawahara, Y. Takeuchi, G. Wei, K. Shirai, T. Yamauchi, and N. Tsubokawa, *Polym. J.* **41**, 744-751 (2009).

[7] T. Yamauchi, T. Saitoh, K. Shirai, K. Fujiki, and N. Tsubokawa, *J. Polym. Sci.: Part A: Polym. Chem.* **48**, 1800-1805 (2010).

[8] H. Nishizawa, in: Flame-Retardant Technology of Polymeric Materials, CMC press, Tokyo, 2002, p. 113.

[9] H. Nishizawa, *J. Soc. Rubber Ind. Jpn.* **79**, 316-322 (2006).

[10] F. Laoutid, L. Bonnaud, M. Alexandre, J. Lopez-Cuesta, and P. Dubois, *Mater. Sci. Eng.: R* **63**, 100-125 (2009).

[11] L. Chen and Y. Z. Wang, *Polym. Adv. Technol.* **21**, 1-26 (2010).

[12] H. Lu, L. Song, and Y. Hu, *Polym. Adv. Technol.* **22**, 379-394 (2011).

[13] T. Yamauchi, A. Yuuki, G. Wei, K. Shirai, K. Fujiki, and N. Tsubokawa, *J. Polym. Sci.: Part A: Polym. Chem.* **47**, 6145-6152 (2009).

[14] A. Sen, B. Mukherjee, A. Bhattacharya, L. Sanghi, P. De, and A. Bhowmick, *J. Appl. Polym. Sci*, **43**, 1673-1684 (1991).

[15] S. Matsuda and S. Okazaki, *Nippon Kagaku Kaishi* 1287 (1986).

[16] E. H. Brown and C. A. Krans, *J. Am. Chem. Soc.* **51**, 2690-2696 (1929).

[17] Y. Liu, G. Hsiue, R. Lee, and Y. Chiu, *J. Appl. Polym. Sci.* **63**, 895-901 (1997).

[18] M. Murota, S. Sato, and N. Tsubokawa, *Polym. Adv. Technol.* **13**, 144-150 (2002).

[19] Japanese Industrial Standards (JIS), Determination of burning behaviour by oxygen index, JIS K 7201.

[20] M. Blazsó, Zs. Czégény, and Cs. Csoma, *J. Anal. Appl. Pyrolysis* **64**, 249-261 (2002).

[21] E. Jakab, M. A. Uddin, T. Bhaskar, and Y. Sakata, *J. Anal. Appl. Pyrolysis* **68-69**, 83-99 (2003).

[22] M. Shau, P. Tsai, W. Teng, and W. Hsu, *Eur. Polym. J.* **42**, 1899-1907 (2006).

[23] H. Nishizawa, in: Flame Retardant Technology of Polymeric Materials, CMC press, Tokyo, 2002, p. 190.

[24] S. S. Mahapatra and N. Karak, *Polym. Deg. Stab.* **92**, 947-955 (2007).

Chapter 5

Concluding Remarks

In this thesis, functionalization of silica nanoparticle by grafting of antibacterial polymers and immobilization of flame retardant onto the surface was investigated to improve the problems when the functional material was added to the polymer matrices and to prepare the silica having functionality. In addition, the properties of polymer composites filled with functionalized silica were also investigated. The results and conclusions are as follows.

1. Antibacterial polymer, poly(vinylbenzyl tributylphosphonium chloride) (poly(St-$CH_2P^+(Bu)_3Cl^-$)), was successfully grafted by two methods: Method 1 is treatment of poly(St-CH_2Cl)-grafted silica with tributylphosphine and Method 2 is direct grafting of poly(St-$CH_2P^+(Bu)_3Cl^-$) by radical graft polymerization of the corresponding monomer. The preparation of poly(St-CH_2Cl)-grafted silica and the direct grafting of poly(St-$CH_2P^+(Bu)_3Cl^-$) were successfully initiated by the system consisting of trichloroacetyl groups on the silica surface and $Mo(CO)_6$. The grafting of antibacterial polymers onto silica surface was confirmed by FT-IR, pyrolysis GC-MS, and ^{13}C-CP/MAS-NMR. The percentage of grafting of antibacterial polymers on the silica surface by Method 1 and 2 were determined to be 142% and 22.6%, respectively by TGA. The surfaces of silicone rubber, polystyrene film, and paints, filled with poly(St-$CH_2P^+(Bu)_3Cl^-$)-grafted silica showed strong antibacterial activity against various bacteria. In addition, the surface of silicone rubber filled with poly(St-$CH_2P^+(Bu)_3Cl^-$)-grafted silica was maintained antibacterial activity even after boiling for 24 h in water because of an anchor effect of silica nanoparticle.

2. The scale-up synthesis of grafting of antibacterial polymer-grafted silica in a solvent-free dry-system was investigated. The graft polymerization of antibacterial monomer, St-$CH_2P^+(Bu)_3Cl^-$, onto silica nanoparticle surface was successfully initiated by azo groups introduced onto the silica surface in a solvent-free dry-system. The graft polymerization of antibacterial monomer, St-$CH_2P^+(Bu)_3Cl^-$, onto silica nanoparticle surface was also successfully achieved by atom transfer radical polymerization (ATRP) in a solvent-free dry-system. In azo-initiated radical

polymerization and ATRP, it was found that the nearly equal amounts of antibacterial polymers were grafted onto silica nanoparticle surface in a solvent-free dry-system and solvent system. It was indicated that silicone rubber composites surface filled with poly(St-$CH_2P^+(Bu)_3Cl^-$)-grafted silica prepared in a solvent-free dry-system had antibacterial activity against *Staphylococcus aureus* and *Escherichia coli*.

3. The immobilization of phosphorous flame retardant was achieved by two-step reactions: the first is introduction of cyclotriphosphazene (PH) groups onto silica nanoparticle by the reaction of terminal amino groups of the surface with hexachlorocyclotriphosphazene (HCTP) and the second is immobilization of bis(4-aminophenoxy)phenyl phosphine oxide (BAPPO) onto silica having PH groups by the reaction of PH groups on the surface with BAPPO. The amount of BAPPO-immobilized onto the silica was increased with increasing reaction time. The amount of BAPPO immobilized onto the silica was determined to be 8.5 wt%. Char yield of the epoxy resin filled with flame retardant-immobilized silica was higher than that filled with free HCTP and BAPPO. Flame retardant property and decrease of glass-transition temperature of the epoxy resin was considerably improved by the addition of flame retardant-immobilized silica. Elution of flame retardant from epoxy resin was inhibited by the immobilization of flame retardant onto silica surface.

Based on the above results, it is concluded that functionalization of silica nanoparticle could be achieved by grafting of antibacterial polymers and immobilization of flame retardant onto the surface. In addition, it was found that the properties of polymer composites filled with functionalized silica were superior to free functional materials.

Therefore, it is concluded that surface modification of the nanoparticles used in this study could be applied to other functional materials to be added to the polymer matrices, such as antioxidant, light stabilizer, and antistatic agent and so on.

List of Publications

1. Takashi Kawahara, Yoko Takeuchi, Gang Wei, Kumi Shirai, Takeshi Yamauchi, and Norio Tsubokawa, “Preparation of Antibacterial Polymer-Grafted Silica Nanoparticle and Surface Properties of Composites Filled with the Silica (2)”, *Polym. J.*, **41**, 744-751 (2009).

2. Takashi Kawahara, Akira Yuuki, Kumi Hashimoto, Kazuhiro Fujiki, Takeshi Yamauchi, and Norio Tsubokawa, “Immobilization of Flame-Retardant onto Silica Nanoparticle Surface and Properties of Epoxy Resin Filled with the Flame-Retardant-Immobilized Silica (2)”, *React. Funct. Polym.*, **73**, 613-618 (2013).

3. Takashi Kawahara, Hiroshi Matsuda, Takeshi Yamauchi, and Norio Tsubokawa, “Preparation and Properties of Antibacterial Polymer-grafted Silica Nanoparticles in a Solvent-free Dry-system”, in preparation.

Acknowledgments

This dissertation has been carried out during 2009-2012 as a doctorate thesis under the direction of Professor Dr. Norio Tsubokawa at the Graduate School of Science and Technology, Niigata University.

The author wishes to express his deepest gratitude to Professor Dr. Norio Tsubokawa, Faculty of Engineering, Niigata University for his constant guidance and kind suggestions throughout this work. The author is also deeply thankful to Professor Dr. Takeshi Yamauchi, Faculty of Engineering, Niigata University for his reviewing this thesis, helpful advice, and discussions. The author would like to express his gratitude to Professor Dr. Toshiki Aoki, Faculty of Engineering, Niigata University, Professor Dr. Takashi Kaneko, Graduate School Science and Technology, Niigata University, and Professor Dr. Masayuki Taniguchi, Faculty of Engineering, Niigata University, for their reviewing this thesis. The author is deeply indebted to Professor Dr. Kazuhiro Fujiki, Department of Environmental Science, Niigata Institute of Technology, for the many useful suggestions and comments.

The author wishes to thank Mrs. Kumi Sato, Mr. Takeshi Fukuda, Mr. Hiroshi Saito, Mr. Akira Yuuki, Ms. Yoko Takeuchi, Mr. Hiroshi Matsuda, Mr. Keita Konno, and all current and former colleagues of Tsubokawa laboratory, Niigata University for their help, discussion, and useful suggestions. Without them, many experimental results in this thesis would not be obtained. The author also wishes to thank all current and former colleagues of Yamauchi laboratory, Niigata University for their help and discussion. The author wishes to thank Dr. Akihito Ochiai, and all current and former colleagues of Taniguchi laboratory, Niigata University for supports of antibacterial test.

Finally, the author wishes to express his grateful thank to his parents, Mr. Kenji Kawahara and Mrs. Yuko Kawahara, and his family, for their encouragement and support during this work.

Takashi Kawahara

Doctoral Program in Advanced Materials Science and Technology,

Graduate School of Science and Technology,

Niigata University,

February, 2013.